THE UNIVERSITY OF
SYDNEY

THE UNIVERSITY OF SYDNEY

BIOACTIVE GLASS MICROSPHERES WITH CONTROLLED DRUG ELUTING CAPABILITIES FOR USE IN SYNTHETIC SKIN SCAFFOLDS

Benjamin Yew Loong Chow

2014

This thesis is submitted for the completion of the

Master degree of Philosophy

School of Aerospace, Mechanical and Mechatronic Engineering,

Faculty of Engineering & Information Technologies

The University of Sydney

Supervised by:

Professor Andrew Ruys

Dr Philip Boughton

Abstract

Chronic skin wounds are a significant health condition caused by a wide range of factors. In Australia, it is estimated that over 200,000 people each year suffer from a chronic skin wound condition costing up to $285 million annually in treatments. Currently, severe cases of chronic skin wounds are treated using skin grafts and tissue engineered skin constructs. These devices are expensive and are unable to prevent infections. Without proper monitoring and replacement, these grafts and constructs can act as reservoir for pathogens to proliferate protected from the patient's immune system. Infected wounds are often polymicrobial and the microbes able to produce biofilm which acts as a barrier between the microbe and antibiotic molecules.

Currently, research is focused on the development of synthetic scaffolds with antimicrobial capabilities. Scaffolds created by other researchers either focuses on biocompatibility and mimicking of the extracellular matrix or delivery of drugs in a sustained release. Rarely both are combined due to problems of maintaining sustained drug release lasting the entire wound healing period. A two-part device consisting of a biocompatible biodegradable scaffold and bioactive glass microspheres to act as a delivery vector for antibiotics has been proposed in this thesis. This thesis will explore the methods of producing bioactive glass microspheres of various forms, attachment of the microspheres to the scaffold in a non-destructive method and the drug loading and release profile of the device when combined together.

Results from this thesis show that wholly formed and hollow microspheres can be produced using a flame spray technique. Attachment of these microspheres to the scaffolds can be achieved by taking advantage of the low glass transition phase of the scaffold material while minimising scaffold damage. Microspheres attached using these methods are mechanically stable. Drug released from microspheres attached to the scaffold are significant but not sustained. In conclusion, a two-part wound healing device can be used to treat infected chronic wounds.

Acknowledgements

I wish to acknowledge the following people for their contributions to this thesis.

I would like to thank my supervisors, Prof. Andrew Ruys and Dr. Philip Boughton, for their support and direction in completing this thesis.

I would also like to thank Dr. Giang Tran from the Australian Technology Park for his assistance and for lending the use of his spectrophotometer and laboratory.

I thank Mr. Abdul Khalil for his assistance in the production of bioactive glass microspheres. Without his help and resources, major parts of this thesis could not be completed.

I would also like to thank Alex Jia for his assistance in taking SEM images of scaffolds and microspheres. I wish the very best for him as he completes his PhD.

Finally, I would like to thank my friends and family who have supported me and have waited patiently.

Declaration of Contribution

I, Benjamin Yew Loong Chow, declare that:

- The literature review was conducted by myself and ideas and concepts are referenced properly
- I designed and developed all experiments in this thesis with help from Dr Philip Boughton, Abdul Khalil and Alex Jia.
- I performed all microsphere production experiments with the help of Dr. Philip Boughton and Abdul Khalil
- I performed all microsphere attachment studies on my own with help from Alex Jia for SEM images.
- I performed drug release studies with the help of Dr. Giang Tran
- I collected and analyzed all experiment data on my own.

The above represents an accurate statement of the contributions to this thesis.

X

Andrew Ruys
Professor

X

Benjamin Yew Loong Chow

Table of Contents

Figures, Tables and Equations

Figures

Tables

Equations

Abbreviations

FDA - Food and Drug Administration

MRSA - Methicillin resistant *Staphylococcus aureus*

MS - Microsphere

PCL - Polycaprolactone

PDLLA - Poly-DL-lactic acid

PEO - Polyethylene oxide

PLA - Polylactic acid

PLGA - Poly(lacto-co-glycolic acid)

SEM - Scanning Electron Microscopy

TEC - Tetracycline

UIN - Unique Identifying Number

VRE - Vancomycin-resistant *enterococci*

Glossary

Q-cell: Sodium borosilicate microspheres.

Bioglass 45S5: Bioactive glass composite with biocompatible and biodegradable properties.

Iaxsys: In-vitro Actuation System. Device able to perform actuation studies on small materials and tissue within a 6 well culture plate.

1 Introduction

Chronic skin wounds are defined as skin wounds which do not heal in the normal manner or time due to complications. Chronic wounds are in a constant state of inflammation as the body attempts to recover [1–4]. During this period, there is a high risk of infection of the wound which are known to increase the severity of the wound and lead to other health issues [4–6]. In Australia, it is estimated that over 200,000 people each year suffer from a chronic skin wound condition [7]. This amounts up to $285 million annually in treatments [7].

Currently, severe cases of chronic skin wounds are treated using skin grafts and tissue engineered skin constructs. These grafts are generally expensive costing up to $33/cm^2 and often require multiple replacements to maintain the biological benefits [8]. In large chronic wound cases, there is also the issue of vascularisation of the graft. Poor vascularisation will lead to graft failure and tissue necrosis of the graft [9, 10]. Grafts are susceptible to infections by microorganisms, especially during the initial stage post implantation. The graft can act as a reservoir for infectious microorganisms to proliferate where they are protected from the body's immune system due to poor vascularisation [11]. In addition, antibiotics administered intravenously are unable to penetrate deep within the graft if there is poor vascularisation [6, 12].

In response to these issues facing biological grafts, research is focused on the development of synthetic scaffolds with antimicrobial capabilities [13]. Scaffolds created by other researches either focuses on biocompatibility and mimicking of the extracellular matrix or delivery of drugs in a sustained release. Rarely both are combined due to problems of maintaining sustained drug release lasting the entire wound healing period [14, 15].

In this thesis, a two-part device consisting of a biocompatible biodegradable scaffold and bioactive glass microspheres to act as a delivery vector for antibiotics will be developed. Chapters within will explore methods of producing bioactive glass microspheres of various forms, attachment of the microspheres to the scaffold in a non-destructive method and the drug loading and release profile of the device when combined together.

2 Literature Review

2.1 Anatomy and Physiology of the Skin

The skin is the largest organ of the body acting as a multifunctional barrier between the internal components of the body and the external environment. It has an average surface area of 1.75m^2 and weighs approximately 15% of the body mass [1, 16]. Average thickness of the skin lies between 0.5 – 5 mm depending on the skin location on the body [17, 18]. Skin thicknesses can also vary significantly between individuals, and the age of the individual [19, 20]. It is typically thinner in infants and elderly persons [21]. Other features of the skin that may differ between individuals include skin colour, texture, thickness and appendages such as hair [20, 22, 23].

Compared to other organs of the body, the structure and physiological role of the skin may appear relatively simpler. Nevertheless, the skin is a complex structure consisting of many different types of specialized cells and tissue structures which serve the broad purpose of providing and maintaining a barrier to the external environment.

2.1.1 Anatomy

The skin can be classified into three distinct layers as seen in Figure 2-1. Going from external to internal, these layers are the epidermis, the dermis and the hypodermis or subcutaneous layer.

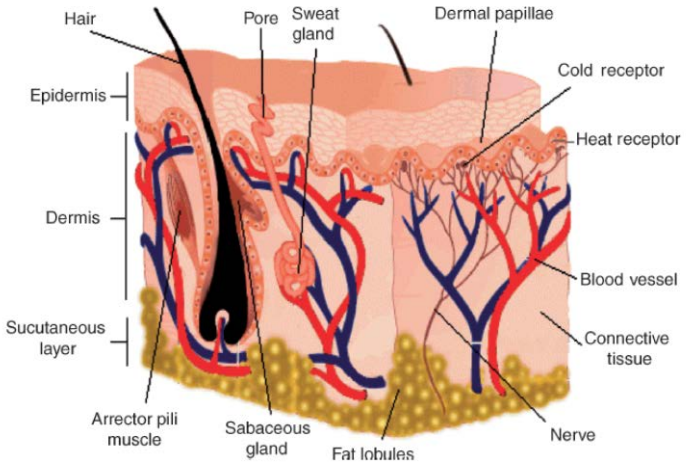

Figure 2-1: Anatomy of the skin showing the main structures of the skin [1].

2.1.1.1 The Epidermis

The epidermis refers to the external layer of skin exposed to the environment. The layer is approximately 0.1 – 1.5mm thick depending on body location [1, 19]. The majority of cells in the epidermis are keratinocytes which make up to 90% of the epidermal cellular composition [21].

Keratinocytes form a stratified squamous layer of cells which forms a watertight layer and prevents foreign objects from invading the body [1]. These cells are formed from an internal cell layer known as the basement membrane. As new cells form, older cells are pushed towards the surface of the skin. In the process, the cells differentiate and change morphology due to the internal cell production of keratin [20]. Keratinocytes eventually die and become a hydrophobic layer of cells which continuously slough of the skin [24]. It can take approximately 40 to 50 days for new keratinocytes to reach the surface and slough off depending on the thickness of the skin [25].

Other cells present include melanocytes, Langerhans cells and Merkel cells. Melanocytes are irregular-shaped cells which produce melanin, a group of pigments which gives colour to the skin and provides some protection against ultraviolet light [26]. Langerhans cells are a group of dendritic cells or antigen presenting cells (APCs) which function as part of the immune system gathering extracellular antigens [22, 27]. Langerhans cells are able to leave the skin and migrate to lymphatic nodes via the lymphatic vessels where they help initiate immune responses to the antigen [27]. Merkel cells are specialised epidermal cells which are associated with mechanoreceptors in the skin [19, 28].

2.1.1.2 Dermis

The dermis lies anatomically deep to the epidermis and superficial to the hypodermis [1, 17, 20]. The cell population of this layer consists of fibroblasts, adipose cells and macrophages [1, 17, 20]. A key characteristic of the dermis is the fibrous network which consists mostly of two proteins that are secreted by fibroblasts; collagen and elastin [29]. Collagen provides mechanical strength while elastin provides the elasticity component of the skin. In addition, there are reticular fibres and glycosaminoglycans in the fibrous network [30]. Also present in

the dermis are a number of other structures which include blood vessels, nerve endings and receptors, lymphatic vessels, sebaceous glands and hair follicles [1, 18].

The dermis can be divided into two layers; the papillary layer and the reticular layer. The papillary layer forms a junction with the epidermis and is characterised by appendages known as dermal papillae which extends into the epidermis. It consists of loose connective tissue and blood vessels which supply the epidermis with nutrients, remove waste products and aid in regulating body temperature [17]. The reticular layer lies beneath the papillary layer and forms a continuous layer with the underlying hypodermis. This layer is composed of dense irregular connective tissue which is able to resist stretching in many directions [19].

2.1.1.3 Hypodermis

The hypodermis is the most internal layer of the skin and is comprised of fibroblasts, adipose cells and macrophages in a loose connective tissue network comprising of collagen and elastin fibres [1]. The layer separates the dermis from the underlying structures of deep fascia, muscle and bone. It is mostly comprised of adipose tissue with approximately half of the body's fat stored here [22]. The adipose tissues function as a source of energy, insulation and padding to absorb mechanical loads [1].

2.1.2 Physiology

Despite its relatively simplistic structure compared to other organs of the body, the skin is able to perform a number of important functions. These include:

- Protection of our internal body from the physical, chemical and biological substances in the environment
- The sensations of touch and thermal detection
- The regulation of body temperature through the secretion of sweat and exposed surface areas
- The synthesis of vitamin D
- Water resistance to prevent essential nutrients being removed from the body.
- Excretion of waste products such as salts and certain organic compounds.

- Detection and immunity to foreign pathogens.
- Acting as a reservoir for up to 10% of the total blood flow in an adult which aids in temperature regulation and blood supply for active muscles during strenuous exercise [1, 20, 31].

Of particular interest are the skin's defences to pathogenic microorganisms. This is important as infections in chronic wounds and skin grafts are common [32, 33].

2.1.2.1 Defence mechanisms of the skin

The skin has a number of mechanisms to prevent infection and pathogenesis of microorganisms [34–37]. These include:

- Chemical environment of the skin
- Desquamation of the skin
- Endogenous microflora of the skin
- Innate immune cells

Of particular interest is the role of endogenous microflora and the innate immune system. These aspects of the skins defence mechanisms have a significant role in wound healing and infection control. For chronic wounds, microbial flora and innate immune cells are often critical factors which have a role in prolonging wound healing.

2.1.2.1.1 Endogenous microflora of the skin

Despite the harsh chemical and physical environment of the skin, there are certain types of microorganisms which are found naturally on our skin. These microorganisms, termed endogenous microflora, are generally non-pathogenic whilst residing on the skin. The microflora of the skin helps prevent attachment and colonisation of pathogenic microorganisms though competition of colonisation sites limiting regions where foreign microorganisms can attach and limited nutrients which are necessary for proliferation. Common microorganism species which are native to the skin include *Staphylococcus*, *Micrococcus*, *Corynebacterium*, *Propionibacterium*, *Malassezi*, *Brevibacterium*, *Acinetobacter* and *Dermabacter* [16, 38, 39]. Whilst these microorganisms pose no harm residing on the

skin surface, they can become pathogenic and pose serious health risks if they infect and colonise an open wound [5, 16].

2.1.2.1.2 Underlying immune cells

In the event that the skin barrier is disrupted and broken, there are a number of immune functions which are capable of suppressing and removing infectious microorganisms. As mentioned before in section 2.1.1.1 The Epidermis, one of the key immune cells in the epidermis are Langerhans cells, a type of APC. Langerhans cells are able to detect and phagocytose exogenous antigens, process the antigens and migrate to lymph nodes where they present the antigens to CD4 T helper cells. CD4 T helper cells respond by initiating the appropriate immune response whether it is activation of CD8 cytotoxic cells or activation of B cells to produce immunoglobulins [40–42].

In addition, neutrophils also play a large role in the immunity of the skin, particularly where there has been a physical breach of the skin resulting from physical trauma and burns. Neutrophils are able to reach the wound site through the blood vessels and are attracted by chemoattractants released by cells at the wound site. At the wound site, they are involved in the eradication of bacteria through phagocytosis and are able to activate and attract more immune cells through the secretion of cytokines and chemoattractants [41–44].

2.2 Physiology of Wound Healing

Wound healing is a complex process in which multiple cells and extracellular pathways are activated in a tightly regulated and coordinated manner. Factors which cause skin wounds can be defined in three broad categories [1].

- Physical wounds caused by mechanical forces or physical trauma to the skin.
- Chemical wounds where corrosive reactions occurring at the skin damage surrounding cells.
- Biological wounds whereby cells of the skin die due to lack of nutrients or infection.

2.2.1 Acute Wound Healing

There are a number of methods which can be used to describe acute wound healing. The process of wound healing can be classified into four main stages [1, 40, 41, 43, 45]. These stages in chronological order are:

- Haemostasis
- Inflammation
- Proliferation
- Maturation and Remodelling

These stages do not operate in isolation as there is considerable overlap between adjacent stages. Relationships between the wound healing stages as depicted in Figure 2-2 and described in detail in the following sections.

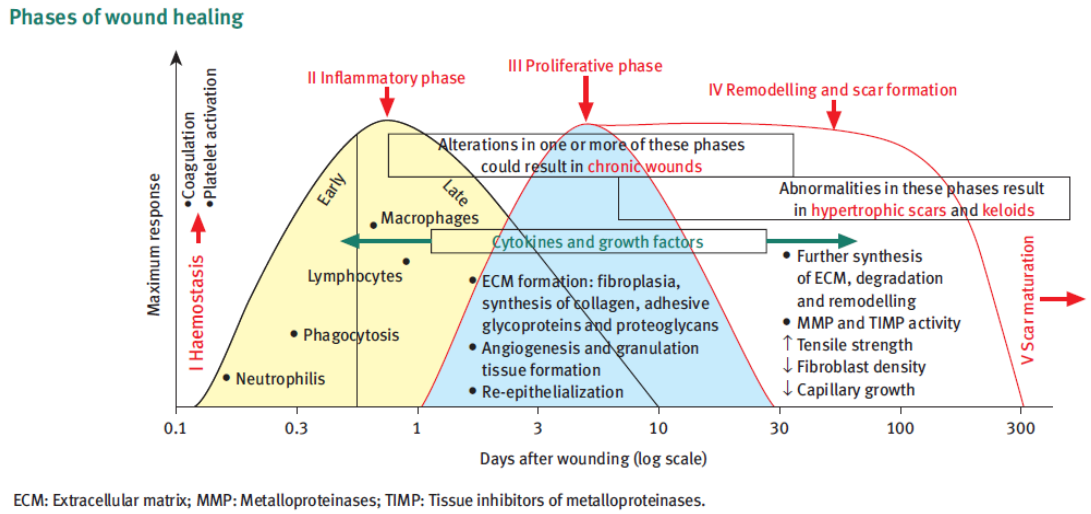

Figure 2-2: Phases of wound healing and associated events [43]**.**

2.2.1.1 Haemostasis

At the time of injury where the skin has been breached and underlying blood vessels have been damaged, the body immediately responds to prevent exsanguination and promote haemostasis. Damaged arterial vessels rapidly constrict leading to reduced blood flow [41]. This in turn leads to tissue hypoxia and acidosis. While in this state, there is an increased production of nitric oxide, adenosine and other vasoactive metabolites which promote

vasodilation and arterial relaxation [41]. Injured skin cells release clotting factors which activate the extrinsic clotting cascade[5]. In addition, platelets are recruited to the wound site by cytokines such as serotonin and platelet factors.

A fibrin clot forms over the injury site preventing the influx of microorganisms [41]. The clot, made of platelets, fibrin and fibronectin, also plays a role in wound healing acting as a scaffold matrix that guides and supports the infiltration of fibroblasts and keratinocytes [41]. The fibronectin protein acts as a chemoattractants for wound repair cells, acts as a template for collagen fibre deposition, and participates in wound debridement by degrading extracellular matrix (ECM) debris and activating phagocytic characteristics in macrophages [46]. When the clot is no longer useful, it is degraded by the enzyme plasmin which breaks down the fibrin matrix [47].

Cytokines play an important role in wound healing. Cytokines released during the process are highly potent and specific in their action in the microenvironment of the wound site. One group of cytokines, platelet-mediated growth factors, are responsible for fibroblast and keratinocyte migration, synthesis of collagen and other extracellular matrix products, regulation of cell movement, direction of new capillary growth and synthesis of enzymes used in remodelling newly formed connective tissue [48].

2.2.1.2 Inflammatory response

The inflammatory response begins within minutes of the initial damage and is characterized by the influx and actions of many types of leukocytes (colloquially known as white blood cells) at the wound site to arrest any infections and remove wound debris and dead tissue [40, 41, 43].

One of the most prominent leukocytes involved in this phase are neutrophils. Neutrophils are the most abundant leukocyte in the body accounting for 50-70% of all leukocytes in the body. These cells are recruited from blood vessels near the wound site through the action of chemokines secreted by cells in trauma near the wound site [49]. Once present at the wound site, the primary function of neutrophils is to phagocytose bacteria cells and break them

down through to release of reactive oxygen species and hydrolytic enzymes. Neutrophils will continue to migrate to the wound site until the infection has been arrested. In addition, they are also involved in the breakdown of extracellular matrix and secretion of cytokines in preparation for proliferation and maturation stages. In time, neutrophils are removed by either apoptosis or macrophage phagocytosis [49–51].

Macrophages are another important type of leukocyte. Macrophages are the derivation of monocyte cells which had been recruited from the blood and matured upon receiving of appropriate cytokine stimulus. Macrophages remove wound debris and bacteria much like neutrophils. In addition, macrophages secrete nitric oxides and cytokines to help regulate wound repair [52]. They also produce a key type of enzyme called matrix metalloproteinases or metalloproteases (MMPs). One such type, collagenase, is required for the degradation of the extracellular matrix in preparation for new matrix deposition [53].

Some other key cells important to this phase are T lymphocytes, mast cells and dendritic cells [40–42]. These cells function as a component of the immune response to foreign bodies.

2.2.1.3 Proliferation

Proliferation is characterized by the development of new skin over the wound site and the restoration of vascular integrity to the region. The tensile strength of the wounded area begins to redevelop [1]. The key cells during this process are fibroblasts and keratinocytes. There are three key events which occur during proliferation: reepithelialization, angiogenesis and granulation.

2.2.1.3.1 Reepithelialization

Reepithelialization is the process where keratinocyte cells reform skin over the wound re-establishing an external barrier that minimizes fluid loss and pathogen invasion [41]. Keratinocytes are stimulated by locally released growth factors and begin to rapidly proliferate and migrate across the wound bed within 12 to 24 hours of injury. Migration of keratinocytes relies on a number of factors. It requires a fluid environment and involves a series of complex steps controlled by chemokines and growth factors [31, 40, 41].

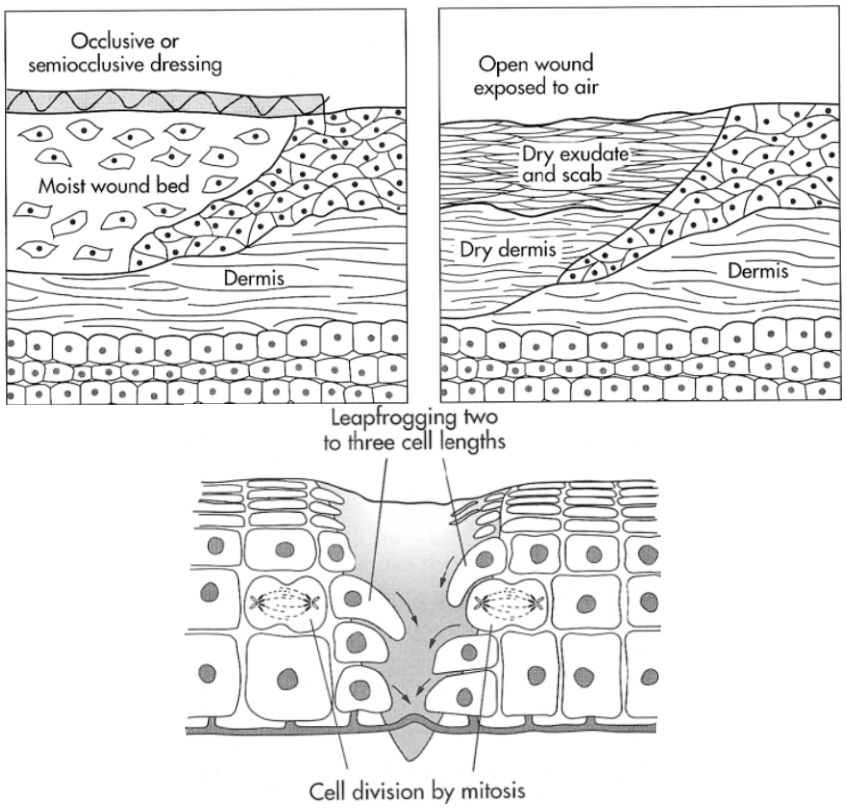

Figure 2-3: Diagram of migration of epidermal cells in (a) moist environment and (B) dry environment. Bottom diagram shows epidermal cell migration via cell proliferation and leapfrogging [41]**.**

As seen in Figure 2-3, newly formed keratinocytes enter the moist fluid environment by detaching themselves from neighbouring keratinocytes and the basement membrane. The migrating keratinocyte elongates itself in the direction of the required growth. The leading edge of the elongated cell attaches to a new spot on the wound bed and the cell contracts, pulling itself across the wound. When migrating cells from opposite sides of the wound touch each other, the migration process ceases in a process known as contact inhibition. Another process used in reepithelialization is leapfrogging. As shown in Figure 2-3, leapfrogging is the process where a single cell moves only 2 or 3 cell lengths before stopping and allowing following cells to climb over [41].

In addition, keratinocytes also play a role in reshaping the extracellular matrix through the degradation of supporting structures which are replaced by temporary anchors during keratinocyte migration. Once migration is complete, the keratinocytes stabilize themselves by forming strong attachments to neighbouring cells [54].

2.2.1.3.2 Angiogenesis

Angiogenesis (also known as neovascularization) is the process of restoring a vascular network to the repairing wound site [41, 55]. It is a critical component of wound healing as newly formed blood vessels provide a steady supply of nutrients and oxygen to the reforming skin. Angiogenesis is stimulated by growth factors and tissue hypoxia [56, 57].

Before new blood vessels can be formed, there are a number of events which occur. Firstly, a hypoxic gradient forms between damaged tissue and well vascularized tissue. This is compounded when a fibrin clot forms to act as a temporary barrier to the environment. Once the clot is formed and the wound is sealed, angiogenesis can proceed. The hypoxic environment stimulates macrophages to produce angiogenic growth factors. A number of other growth factors secreted by platelets, fibroblasts and endothelial cells are also released. New blood vessel formation begins from intact blood vessels in the underlying dermis. New capillary buds form capillary loops which slowly extend into the wound environment [55, 57, 58].

2.2.1.3.3 Granulation

Granulation refers to the development of a transitional substance which replaces the fibrin/fibronectin matrix known as granulation tissue. The tissue is metabolically active, supports proliferation and is highly vascular [1, 40, 41].

Fibroblasts are the prominent cell type found in granulation tissue [29]. These cells produce collagen and numerous other proteins which build an ECM. In addition, the influx of fibroblasts helps degrade the provisional matrix and replace it with a new matrix rich in hyaluronan, fibronectin and other compounds. The new extracellular matrix allows for cell migration and organization [41]. The structure and composition of the granulation tissue undergoes constant remodelling until the skin tissue matures [40].

2.2.1.4 Maturation and remodelling

The last stage of wound healing involves processes involved in restoring the strength of the skin tissue. Granulation tissue matures into connective tissue. The key cells involves in this stage are macrophages and fibroblasts. The extracellular matrix reshapes through the cross-

linking collagens, cell maturation and cell apoptosis. Collagen synthesis peaks around 5 days after injury and may last for months afterwards [45].

Although the wounded skin region recovers some strength, it never achieves more than 80% of the pre-injury strength [41]. This ends the wound healing process for the skin under normal conditions.

2.2.2 Chronic Wounds

There are a number of varying criteria which can be used to describe chronic wounds. Chronic wounds are generally defined as wounds which do not heal in a normal and timely manner [1–4]. The normal wound healing process is interrupted and the wound enters a state of pathologic inflammation. This results in a delayed, incomplete wound healing scenario with poor anatomical and functional outcomes [46, 59].

There are a number of factors which can lead to a chronic wound state. As listed in Table 2-1, these factors can generally be split into two categories. Local factors generally describe factors which directly influence the characteristics of the wound itself while systemic factors refer to the overall health and condition of the individual and his/her ability to heal [60]. It is important to note that many of these factors are related [60].

Table 2-1: Factors contributing to chronic wounds[1, 60]

Local Factors	Systemic Factors
Infection	Age and Gender
Oxygenation	Poor nutrition
Foreign Body	Underlying Chronic Disease
Venous insufficiency	Medication
Necrotic Tissue	Compromised Perfusion
Local Pressure/shear and friction	Alcohol and Smoking
	Obesity
	Ischemia
	Immunodeficiency

There are a number of differences between acute and chronic wound states. In the broadest sense, cellular and molecular abnormalities in the chronic wound prevent acute wound healing processes from occurring. In the majority of chronic wounds, there is excessive recruitment of inflammatory cells, such as neutrophils, to the wound site. This is most often due to the presence of an infection [4, 5]. Excessive recruitment of inflammatory cells which fail to harness the infection can also impair wound healing through the production of various reactive oxygen species which damage extracellular matrix and cell membranes [61]. In addition, they can also increase the production of proteases and MMPs. Overproduction of proteases and MMPs can accelerate extracellular matrix degradation and inactivate components of the extracellular matrix and growth factors leading to an impaired wound healing process. This process explains why there is a limited quantity and bioavailability of growth factors in chronic wounds [62].

2.2.2.1 Epidemiology

Chronic wounds are a global issue and are thought to affect a significant portion of the population in developed countries [63]. For the elderly, defined as persons aged over 65 years, the rate increases due to poorer health and healing outcomes [64].Between 1998 and 2008, there was a rise in the number of patients admitted with a skin and soft tissue infection in Australia [65].

Chronic wounds are a significant burden to the individual and the public. Studies indicate that the cost of treatment and care for chronic wounds is around 3% of the total healthcare expenditure in developed countries. For Australia, this equates to approximately $2.6 billion in direct healthcare costs [66]. It is estimated that the cost of treating a chronic wound can reach up to $27,493 per wound [67]. The primary factor for the high cost arises from the prolonged length of time required for the wound to heal. Reported healing times for chronic wounds indicate that 69% heal in 12 weeks, 83% heal within 24 weeks and 17% remain unhealed after 52 weeks [67]. Other factors include treatment options and infrastructure costs [68].

Complications from chronic wounds are exacerbated in rural areas where there is a lower quality of healthcare due to less infrastructure and medical staff [69]. In addition, there is a higher incidence of chronic diseases in rural regions which can lead to the formation of chronic wounds [69, 70]. In particular, diabetes mellitus can lead to diabetic foot ulcers, a condition that affects 12-25% of all diabetic patients [71].

Rural regions in Australia are significantly disadvantaged in healthcare compared to urban populations. This is due to numerous factors, in particular the lack of medical professionals and staff, inadequate infrastructure to service a sparsely populated region, lower healthcare expenditure for rural regions, lower education outcomes and income disparities [66, 69, 70, 72].

2.2.2.2 Infection

One of the major complications associated with chronic wounds is infections. Infections of chronic wounds are the result of pathogenic organisms reaching a population threshold or producing toxins which overwhelm the patient's immune system. A number of articles have defined infection of wounds as the presence of more than 10^5 organisms per gram of tissue or the presence of beta-haemolytic streptococci [4, 16, 73]. This definition however does not take into account other factors such as chronic illnesses and immunocompromisation.

An infection is enough in itself to cause a wound to enter a chronic state. Pathogens such as bacteria, fungi and viruses have a number of virulence factors which help it colonise the wound. Some of the main factors include adhesion, colonisation, invasion, immune response inhibitors and toxins. Briefly summarising each point, adhesion refers to the aspect of a pathogen to attach itself to a surface which is a prerequisite for proliferation. Colonisation refers to the production of special enzymes or proteins which allow the pathogen to survive in particular areas of the body. Invasion describes the ability to produce enzymes to breakdown tissue or cell membranes allowing penetration. Immune response inhibitors are a variety of strategies a pathogen can use to evade or inhibit the host's immune system. Finally toxins produced by pathogens can cause poisoning and cause tissue damage [74].

Another issue regarding infected chronic wounds is that the majority of chronic wounds are colonised by more than one type of microorganisms. A study by Hansson et al on leg and foot ulcer found that in 86% of wounds with no clinical sign of infection there was more than one type of bacterial species present [39]. Fungal pathogens are also present in some chronic wounds which can complicate treatment since antibiotics do not treat fungal infections [39, 75].

Table 2-2: Frequency of common microorganisms found in chronic wounds.

Study	**Hansson et al (1995)** [39]	**Gjodsbol et al (2006)** [76]	**Davies et al (2007)** [77]
Number of patients involved	58	43	66
Test site	Venous leg ulcers	Venous leg ulcers	Venous leg ulcers
Microorganism		**Frequency (%)**	
Staphylococcus aureus	88	93.5	71.2
Pseudomonas aeruginosa		52.2	71.2
Coagulase-negative *Staphylococcus* species	-	45.7	62.1
***Enterococcus* species**	74	71.7	-
Escherichia coli	-	32.6	-
***Enterobacter* species**	29	-	-
***Enterobacteriaceae* and nonfermentive gram-negative bacilli**	-	37	-
***Corynebacterium* species**	-	30.4	-
***Bacillus* species**	-	4.3	-
***Peptostretococcus* species**	29	-	-
Other anaerobes	-	39.1	-
Fungi	11	-	12.1

A list of common microorganisms found in chronic wounds is presented in Table 2-2. *Staphylococcus aureas* is the most common bacteria found in wounds. This is primarily due to the fact that is it is found on the skin of around 35-60% of the human population allowing it to access the wound site with relative ease [78]. In addition, *Staphylococcus aureus* is also capable of producing a wide range of enterotoxins and cytotoxins which can overwhelm the patient's immune system [16].

2.2.2.2.1 Biofilm

Biofilms are a community of bacteria which have formed an attachment to a surface and produce an extracellular polysaccharides matrix [79–81]. The extracellular polysaccharide matrix covers the bacterial community and helps protect the microorganisms from the host immune defence and antibiotics. Protection from the hosts immune system is conferred by masking the surface markers of the bacteria from immune cells whilst protection from antibiotics is thought to be due to interfering with antibiotic diffusion into bacterial cells or by direct binding of antibiotics to the extracellular polysaccharide matrix[82]. It is estimated that the presence of biofilm reduces the effectiveness of antibiotic treatment by as much as 1000 fold [83].

Biofilms can be created by a number of pathogenic organisms include common species such as *Staphylococcus aureus* [84, 85]. Up to 80% of human infections are estimated to involve pathogenic biofilms [86]. In addition, most biofilms consist of multiple species of bacteria [82]. It is estimated that volume of biofilms consist of 80-85% extracellular polysaccharide matrix and only 10-15% cells [87].

2.2.2.2.2 Antibiotic Resistance

One of the major emerging concerns of infections is the rise of antibiotic resistance in pathogens. Patients with chronic wounds are considered to be a high-risk group for the acquisition, carriage and dissemination of antibiotic resistant pathogens. Also, due to the polymicrobial nature of chronic wounds as mentioned in section 2.2.2.2 Infection, there is a higher chance of genetic exchange between bacteria which could lead to an increase of antibiotic resistance of multiple strains. The presence of antibiotic resistant pathogens in chronic wounds can significantly complicate treatment. Compared to non-resistant pathogen strains, the cost of treating antibiotic resistant pathogens can be between 1.3 to 2 fold higher [88].

One of the most well-known antibiotic resistant bacteria is methicillin resistant *Staphylococcus* aureus (MRSA). In a study by Colsky *et al* [89] on hospitalised patients with leg ulcers, half of all the *Staphylococcus aureus* isolates found were methicillin resistant and

more than a third of *Pseudomonas aeruginosa* isolates were resistant to ciprofloxacin. MRSA infections are generally nosocomial meaning that they are most commonly acquired in a hospital setting. However, there has been a steady rise of MRSA infections picked up from the community leading to increased strain on treatment methods [90].

Due to the rise of antibiotic resistance, there are many issues which need to be addressed regarding antibiotic loaded biomaterials. Devices which use antibiotics as a form of sterilisation or prophylactic inhibitory mechanism need to be carefully evaluated. The risks of antibiotics used in a preventative manner has been well documented, particularly in the case where antibiotics were added to animal feed [91]. For bioengineering, there is a need for strict guidelines and further clinical proof of the efficacy of antibiotic releasing devices, particularly if the device is designed as a first-line treatment for infections [92].

2.3 Overview of Treatment Methods for Chronic Wounds

Wound dressings have a long history dating back to the ancient Egyptians around 3000-2500 BC. Since then, wound dressings have changed significantly as more knowledge of the wound is discovered. There is now a large range of wound management products for use in different scenarios.

When designing a wound dressing product, some desirable characteristics include:

- Maintaining a warm moist environment
- Protection from microbial infection and foreign material
- Easy to apply
- Comfortable to wear
- Ease of removal
- Minimisation of frequent dressing changes [93, 94]

2.3.1 Traditional Wound Care

Traditional wound care is primarily aimed at maintaining an ideal environment that allows natural wound healing events to occur without disruption. These dressings typically include cotton, wool, natural or synthetic bandages and gauzes. These dressings are typically used in

non-chronic wound cases where the wound is clean and dry or as a secondary dressing to absorb exudates and protect the wound [95].

Gauze dressings can provide some protection against bacterial invasion [96]. However, this protection is lost when the gauze becomes moistened from wound exudate or external fluids. In addition, gauzes become adhered to the wound over a period of time and are painful to remove. Gauze dressings also do not prevent moisture loss by evaporation leading to dehydration of the wound [95].

Another traditional technique commonly associated with wound care is debridement. Necrotic tissue cannot be revived and functions as a source of nutrients for pathogens. Necrotic tissue also encourages the overproduction of degradation enzymes which has negative impacts on wound healing. Surgical debridement can include cleaning the wound with saline or dilute antiseptic solution, using a curette to scape biofilms and, for extreme cases, surgical removal of dead tissue [97].

Traditional wound products are generally not used in chronic wound cases and burns. They have been replaced by more recent and advanced dressings which are more suited to treat the complex issues of chronic wounds.

2.3.2 Modern Wound Care

Modern wound dressings refer to a large range of products developed to retain moisture and create the ideal wound healing environment. They are generally made from materials designed to provide or maintain moisture in the wound.

Table 2-3: List and descriptions of some products used in the treatment of wounds [93, 94, 98, 99]**.**

Category	Type	Description	Examples
Dressings	Low adherent dressings	• Dressing with low adherence to the wound rather than non-adherent. • Typically used in conjunction with a secondary dressing • Unable to absorb exudate	• Melolin™ • N-A Ultra™ • Release™ • Telfa™ • Tricotex™
	Semipermeable films	• Allows transmission of air and water vapour whilst being impermeable to fluids and bacteria. • Flexibility allows use in difficult anatomical sites • Unable to handle large amounts of exudate	• Bioclusive™ • Mefilm™ • Tegaderm™ • OpSite Flexigrid™ • OpSite Plus™
	Hydrocolloids	• Interactive dressing made of hydrocolloid base made from cellulose, gelatin or pectins with a polyurethane or foam backing • Forms a gel that promotes a moist wound environment • No secondary dressing required	• Comfeel Plus™ • Cutinova Hydro™ • Granuflex™ • Tegasorb™ • Alione™

	Hydrogels	• Consists of insoluble polymer matrix with up to 96% water content • Able to absorb exudate or hydrate dry wounds • Requires secondary dressings	• Granuge™l • Intrasite Gel™ • Nu-Gel™ • Sterigel™ • Aquaform™ • Purilon™
	Alginates	• Dressings which contain calcium or sodium alginate • Interacts with the wound to reshape and absorb exudate • Typically used on high exuding wounds	• Algisite™ • Algosteril™ • Curasorb™ • Kaltostat™ • Sorbalgorn™ • Sorbsan™ • Tegagen™
	Foam	• Typically made from polyurethane or silicone foam • Transmit water vapour and oxygen and provides thermal insulation • Contains exudate	• Allevyn™ • Biatain™ • Cutinova Hydro™ • Lyofoam™ • Tielle™
	Antimicrobial	• Generally refers to dressings with an antimicrobial compound • Used to treat and prevent further infections	• Silver • Iodine • Copper • Metronidazole gel • Chlorhexidine • Hydrogen Peroxide

Antibiotics	Topical	• Typically administered as a cream, gel or ointment. • Generally not used due to poor penetration through tissue to infected site	• Gentamicin • Metranidazole • Neomycin sulfate • Nitrofurazone • Bacitracin • Fusidic acid
	Systemic	• Typically used to treat infected wounds • Requires administration via intravenous catheter	• Penicillins • Cephalosporins • Aminoglycosides • Quinolones • Clindamycin • Metronidazole • Trimethoprim
Other	Honey	• Used since ancient times in wound care • Has a number of useful wound healing properties • Insufficient studies to conclude effectiveness.	• Medihoney™

As depicted in Table 2-3, there are a number of product categories for modern wound dressings. They are typically used in conjunction with a secondary dressing to maintain their position and provide a protective barrier. As mentioned before, these modern wound dressings are primarily focused on maintaining wound moisture. In addition, gel-type dressings (hydrocolloids, alginates and hydrogels) are able to absorb wound exudate which can help maintain moisture and reduce wound pressure.

To maintain moisture levels in the wound, the majority of modern wound dressings are occlusive in nature. Occlusive dressings limit the transmission of fluids, water vapour and gases from the wound bed to the environment. A moisture vapour transmission rate of less than 35g of water vapour per square meter of dressing per hour is generally considered to be able to maintain moisture in the wound [94]. A moist wound environment also helps maintain a mildly acidic pH and relatively low oxygen tension creating an optimal condition for fibroblast proliferation and granulation tissue formation [94]. In addition, moisture helps prevent wound desiccation and facilitates epidermal migration, angiogenesis and connective tissue synthesis [100]. Occlusive dressings are also capable of limiting the pain of partial-thickness wounds to a much greater degree than non-occlusive dressings [101].

Another feature of modern wound care is the use of antimicrobial and antibiotic compounds. Antimicrobials refer to a group of chemical agents that can be used against microbes such as bacteria, fungi, viruses and parasites. Antibiotics refer to a subset of antimicrobials which have inhibitory or lethal effect on bacteria.

2.3.2.1 Antimicrobials

Antimicrobial compounds are being increasingly used in wound healing products particularly as an anti-infection mechanism. In Table 2-3, a number of antimicrobial substances were listed. Of particular interest are the use of silver and iodine in wound management.

2.3.2.1.1 Silver

Silver has been used for medicinal purposes and water purification since ancient Greece. It has broad antimicrobial properties, particularly against MRSA and vancomycin-resistant *enterococci* (VRE), as well as moderate anti-inflammatory properties. Silver needs to be presented in an ionic or nanocrystalline form to be antimicrobial [94, 102]. It also requires fluid within the wound bed for it to access all areas of the wounds [102]. Silver has several mechanisms of antimicrobial action. These include blocking nutrient transport through bacterial cell walls, denaturing proteins involved in microbial respiration and inactivation of protein translation and replication of DNA [94].

Silver is known to be cytotoxic as it cannot differentiate between healthy cells and pathogenic bacteria. A study by Poon found that 0.5% silver nitrate solution, first used in 1965 on extensive burns, is cytotoxic to keratinocytes and fibroblasts [103]. However, silver toxicity is less prominent in a clinical setting where tissue cells are arranged in a complex manner. Studies have found silver to have toxic effects in acute donor site wounds reducing healing rates [104]. However, in chronic wound cases, the benefits may outweigh the risks, especially in high risk cases where antimicrobial activity must be maintained [105].

2.3.2.1.2 Iodine

Iodine is a broad-spectrum antiseptic commonly used to disinfect skin or clean grossly infected wounds. It is typically used in alcohol solution at 1% to 10% concentration. Povidone-iodine is a common antibacterial formulation and is available in solution, cream, ointments and scrub. One of the major advantages of povidone-iodine is the seemingly zero microbial resistance to the compound [106]. Another iodine compound is cadexomer iodine in which iodine is contained in spherical hydrophilic beads of cadexomer starch. Cadexomer iodine is able to absorb wound exudate and release iodine into the wound bed [93].

There are a number of conflicting studies which question the effect of iodine in wounds. Povidone iodine is cytotoxic to fibroblasts and can interfere with epithelisation. However, the exact concentration varies between studies [93, 107].

2.3.2.2 Antibiotics

Antibiotics are the primary choice when dealing with infections. Approximately a quarter of all patients with chronic wounds are receiving antibiotics at any given time and 60% of those have received systemic antibiotics within the previous 6 months [107]. Patients receiving antibiotic treatment are generally given broad spectrum antibiotics due to the polymicrobial nature of infected wounds and lack of identification of the bacteria initially [108].

Application of antibiotics can be either topical or systemic. Generally for infected wounds, antibiotics are administered systemically as topical applications may not penetrate the tissue to reach deep infections. In addition, topical antibiotics side effects include host sensitisation, contact dermatitis and promotion of antimicrobial resistance [107]. It should

also be noted that systemic antibiotics should not be used in topical application products due to the risks of negative side effects and promotion of antibiotic resistance [93]. Systemic antibiotics are able to treat infections which are accessible to blood vessels. The use of systemic antibiotics include the risk of secondary infection sites at the cannula insertion, and liver and renal complications [6, 12, 108].

Use of antibiotics as a prophylactic/prevention mechanism is under increasing scrutinisation due to the rise of antibiotic resistant organisms. As mentioned in section 2.2.2.2.2 Antibiotic Resistance, there is a need to develop strict guidelines into the proper usage of antibiotics in order to reduce the risk and prevalence of antibiotic resistant microorganisms.

2.3.3 Tissue Engineered Skin Constructs

Tissue engineered skin constructs refer to a range of products which contain a biologically derived component. These skin constructs have a long history with developing tissue engineering technology which has resulted in a number of commercial. Tissue engineered constructs are generally used in severe cases of burns, chronic wound developments and where large areas of skin need replacement and no suitable donor site can be identified. The key concept behind tissue engineered skin construct which differentiates them from traditional and modern wound care products is the ability to encourage regrowth of skin by filling wound defects, and delivering and activating growth factors and other cytokines that promote healing [8, 109, 110].

Table 2-4: List of tissue engineered skin constructs. Table adapted from Böttcher-Haberzeth (2009) [8]**.**

	Commercial Product	Company	Layers
Cellular epidermal replacement	Epicel ®	Genzyme Corp.	Cultured epidermal autograft
	Epidex™	Euroderm GmbH	Cultured epidermal autograft
	ReCell®	Clinical Cell Culture (C3), Ltd.	Autologous epidermal cell suspension
Engineered dermal substitute	Alloderm®	LifeCell Corp.	Acellular donated allograft human dermis
	Integra®	Integra LifeSciences Corp.	Thin polysiloxane (silicone) layer; cross-linked bovine tendon
Engineered dermo-epidermal substitutes	Aplifgraf®	Organogenesis Inc.	Human allogenic neonatal keratinocytes; bovine collagen type 1 containing human allogenic neonatal fibroblasts
	OrCel®	Forticell Bioscience, Inc	Human allogenic neonatal keratinocytes on gel-coated non-porous side of sponge containing human allogenic neonatal fibroblasts

Tissue engineered skin constructs can generally be sorted into three categories based on what layers of the skin they are designed to replace as seen in

Table 2-4. They include cellular epidermal replacements, engineered dermal substitutes and engineered dermo-epidermal substitutes. Cellular epidermal replacements generally consist of keratinocyte sheets cultured on a membrane. The keratinocyte sheet is applied to the patient's dermis using a synthetic or biomaterial dressing and can take up to 10 days for suitable attachment of keratinocytes to the dermis [111, 112]. Engineered dermal substitutes are typically decellularized organic scaffolds designed to mimic the extracellular matrix of the dermis. They can be sourced from cadavers, animals or synthetic biocompatible polymers and treated to remove immunogenic compounds [113, 114]. Dermal substitutes tend to have a silicone membrane to act as a temporary epidermis [113]. Engineered dermo-epidermal substitutes combine both epidermal and dermal biomaterials creating a bi-layered skin construct. They have been shown to have good uptakes with a clinical trial conducted using Apligraf® showing a 80% graft uptake [115].

There are a number of advantages and benefits of bioengineered skin constructs. They can be used to address serious cases of burns and chronic wounds, particularly where the defect exceeds 50-60% of the total body surface [8]. These products address the issues surrounding skin donors and can promote the wound healing processes of the patients own body through the secretion of growth factors found in the tissue engineered skin construct.

Whilst tissue engineered skin constructs are advantageous in certain situations, there are a number of limitations to their use. These include costs, infrastructure required, poor vascularisation through the graft and the inability to resist infections. From a commercial point of view, these skin constructs are extremely expensive ranging from \$10/cm^2 to \$33/cm^2. The average cost to heal a chronic wound defect can add up to approximately \$2,300 [116]. The high cost can be attributed to the highly specialised infrastructure required to source the biomaterials [117, 118], treatment and processing of the materials [109, 117], storage facilities [119] and poor shelf life [112]. Whilst clinical trials report high graft uptake and wound closure using tissue engineered skin constructs, the vascularisation through the graft implant remains quite low. This results in multiple surgeries being required to replace old graft with new ones to maintain healing and remove necrotic tissue [9, 10]. Finally, tissue

engineered skin constructs are unable to resist infections. In fact, they often act as a container for pathogens to proliferate without any interference by the host immune system [11].

2.3.4 Synthetic Skin Scaffolds

Synthetic skin scaffolds refer to a range of constructs which contain biocompatible polyesters and are typically shaped into a 3D porous structure. There has been a significant amount of research into the development of synthetic skin scaffolds over the past decade. The ideal synthetic skin scaffold would have the following properties [13]:

- Able to resist infection
- Able to prevent water loss
- Able to withstand the shear forces
- Cost effective
- Widely available
- Long shelf life and easy to store
- Lack of antigenicity
- Flexible in thickness
- Durable with long-term wound stability
- Can be conformed to irregular wound surfaces and
- Easy to be secured and applied

Whilst no wound management product, modern, tissue engineered or synthetic, is able to meet all these criteria, synthetic skin scaffolds meet a number of these properties better than other counterparts. These include cost effectiveness, ability to withstand shear forces, availability, long shelf life and easy storage, lack of antigenicity, flexibility in thickness, durable, conformation and ease of application. In addition, antimicrobial characteristics can be added to synthetic scaffolds through the loading of antimicrobial compounds into the scaffold [14, 120]. Other further criteria synthetic scaffolds should fulfil include facilitation of tissue ingrowth and biodegradation allowing for full tissue regeneration of the wound [121, 122]. There are a large number of published articles on the development of synthetic skin scaffolds. More recent articles are summarised in

Table 2-5.

Table 2-5: List of recent publications of synthetic skin scaffolds.

Author/s	Scaffold	Characteristics	References
Raghavendra et al (2013)	Cellulose-silver nanocomposite fibres	Demonstrates antibacterial activity against *E. Coli*	[123]
Veleirinho et al (2012)	Hybrid poly(3-hydroxybutyrate-*co*-3-hydroxyvalerate) (PHBV)/chitosan nanofibers	Biocompatible	[124]
Unnithan et al (2012)	Polyurethane and emu oil electrospun fibres	Biocompatible and demonstrates minor antibacterial activity	[125]
Garric et al (2012)	PLA-PEO-PLA type scaffolds	Biocompatible and suitable to undergo gamma sterilisation	[126]
Rnjak-Kovacina (2012)	Tropoelastin and collagen blend electrospun scaffolds	Mimics the physical, mechanical and biological components of the skin dermis	[127]
Franco et al (2011)	Bilayer scaffold consisting of electrospun PCL and poly(lacto-co-glycolic acid) (PCL/PLGA) membrane and gluteraldehyde (3.5% v/v) cross-linked chitosan/gelatin hydrogel	Overall improved mechanical strength, slower biodegradation rates and minimal swelling compared to gels. Biocompatible.	[128]
Ahn et al (2010)	Collagen scaffold produced by a 3D dispensing system supplemented with a cryogenic system	Biocompatible	[129]
Chang et al (2008)	Gravity spun PCL fibers	PCL fibers loaded with gentamicin which released over a number of days	[130]
Zhu et al (2008)	Highly porous electrospun mats made of collagen	Biocompatible	[131]
Zhang et al (2005)	Hollow PCL nanofibers with therapeutics core	Able to contain drugs within hollow PCL fibres	[132]

2.3.4.1 Production processes

From

Table 2-5, it is apparent that synthetic skin scaffolds can be produced using a number of methods. These include electrospinning, solvent casting, phase inversion, laser excimer and thermally induced phase separation [122]. Of these methods, electrospinning appears to be the most popular technique. Electrospinning produces fine polymer fibres with a thickness as small as 100nm [132]. The process is simple, cost-effective and able to produce fibres with various polymers, drugs and other therapeutics. In addition, there is a reasonable potential for the process to be upscaled to industrial production. The downside of this process is that structures produced by electrospinning tend to be fibrous mats with low porosity and pore sizes.

Another popular technique used is solvent leaching. This process involves using a porogen material to act as a mould that can be removed using solvents. Solvent leaching can be used to easily create 3D porous structures with high porosity up to 95% [14]. The process takes more time compared to electrospinning and requires more technological infrastructure to upscale.

2.3.4.2 Materials

Table 2-5 also shows a wide range of biocompatible polymers that have been investigated for use in these scaffolds. Some prominent biocompatible polyesters include poly(lactic-co-glycolic acid) (PLGA) [128], polylactic acid (PLA) [133], polycaprolactone (PCL) [134, 135], collagen [136, 137], and chitosan [138]. Of these materials, PCL is a popular choice as it is a FDA approved biocompatible polymer with good chemical, mechanical and degradation properties [134].

2.3.4.3 Therapeutic loading

Compared to tissue engineered skin constructs, synthetic skin scaffolds naturally lack bioactive compounds to encourage wound healing. Drug loading and elution profiling is an important topic in synthetic skin scaffold research, especially studies which load scaffolds with antibiotics. The key premise behind antibiotic-loaded scaffolds is the concept of locally delivering larger doses of antibiotics to an infection site while avoiding side effects commonly associated with systemic antibiotic use as mentioned in 2.3.2.2 Antibiotics [12].

The simplest method of loading therapeutics onto scaffolds is by soaking the scaffold in a solution containing the therapeutic of choice. The therapeutic is adsorbed onto the scaffold and is held there by weak electrostatic forces such as hydrogen bonding and Van der Waal interactions. The amount of therapeutic loaded onto the scaffold is related to the concentration of the therapeutic solution, the time length of soaking, and the available surface area. This method is suitable for all therapeutics, especially growth factor proteins which may be damaged if loaded using other methods. The limitation of this method lies in the poor consistent drug release [14].

Another popular method is the incorporation of the therapeutic of choice directly into the polymer solution prior to scaffold formation. This technique is popular amongst researchers who use electrospinning techniques as it involves little change to the method and equipment setup. The therapeutic is trapped evenly throughout the scaffold and has a long term drug release period spanning multiple weeks [125, 130, 139].

One of the more interesting methods of therapeutic loading was described by Zhang et al (2005) whereby a bilayer electrospun fibre was produced with an inner core of antibiotic and an outer core of PCL [132].The result was high drug loading of the fibres. However, the drug release profile suggests that the majority of the antibiotic was released in a very short period of time. This would be useful for local delivery of antibiotics to chronic wound infection sites but requires another mechanism to prevent reinfection of the wound.

2.4 Drug Delivery Systems for Chronic Wounds

A major component of synthetic skin scaffold development is the loading and delivery of therapeutics such as antibiotics and growth factors. There are a large number of drug delivery systems developed to address the deficiencies of conventional administration of drugs [140]. Over 30% of drugs are delivered using some form of a controlled-release technology [141]. Advantages of developing new drug delivery technologies include consistent drug delivery to the site of action, prevention of fluctuations in drug concentration, reduction in drug dosage, avoidance of side effects, reduced dosage frequency and improved patient compliance [142].

2.4.1 Drug Elution Profiles

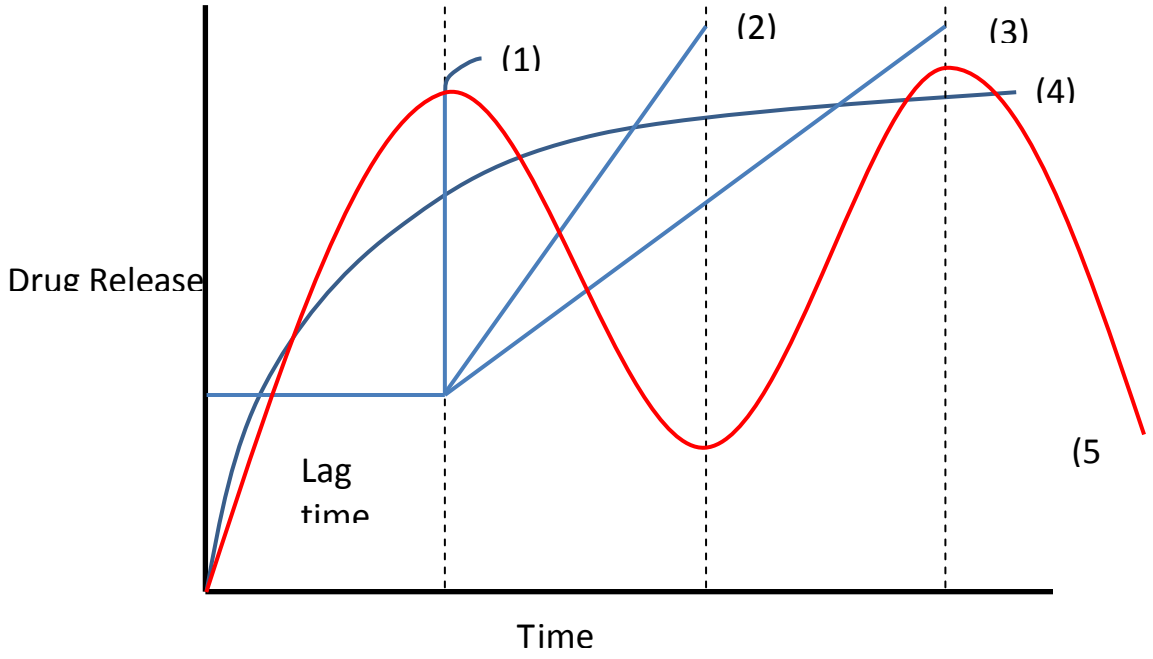

Figure 2-4: Schematic representation of different drug delivery systems where (1) sigmoidal release after lag time (2) delayed release after lag time (3) sustained release after lag time, (4) extended release without lag time and (5) generic pulsatile release. Adapted from Chaudri (2011) [142].

Figure 2-4 represents a few drug release profiles. Of particular interest is the extended release without lag time as seen in Figure 2-4 (4) which is commonly seen in many drug releasing devices, especially drug eluting microspheres [141]. Key features of this logarithmic release profile include the burst phase and the sustained phase. . In the burst phase, drug

molecules attached to the surface are quickly released into solution typically in a matter of hours. Following this, the sustained phase, drug further entrapped in the polymer matrix slowly gets released through the gradual degradation of the polymer matrix [141–143].

With regards to treatment and prevention of microbial infection in wounds, there are a number of factors that need to be considered. It is important to ensure that enough antibiotic is delivered to the site of action to treat or prevent the infection. This, however, does not necessarily mean that every single microbe in the wound must be treated with antibiotic. The aim of antibiotic delivery is to reduce bacterial burden in the wound to a level that the patient's immune system can handle. Failure to do so can lead to recurring infections and increase the risk of the development of antibiotic resistance [6, 12, 108]. It is important to also consider excessively large doses of antibiotics can have a cytotoxic effect on the host cells killing them [6, 73].

2.4.2 Drug Loading Efficiency

The method of loading drugs onto a delivery vector is just as important as the release kinetics, especially when attempting to commercialize the device. Drug loading efficiency is one of the main factors to consider. Drug loading efficiency is typically less than 30% depending on type of delivery vector, the material used and the concentration of antibiotic solution. Hao et al (2011) managed to load the antibiotic chloramphenicol onto lipid nanoparticles with a maximum antibiotic loading efficiency of 10.29% [144]. Chang et al (2008) achieved a loading efficiency of 18.5% using gentamycin sulphate loaded onto PCL nanofibers while Schienders et al (2006) was able to load gentamycin in PLGA microspheres in mixture with bone cement with a drug loading of 30% [145]. Another factor to consider is whether it the method of loading drugs onto the delivery vector. Typically, loading drugs onto vector using a soaking method produces poor loading efficiency and short release kinetics. However, incorporating the drug into the vector during its production can reduce the rate of release minimizing the effectiveness of the burst phase of the release kinetics. In addition, loading drugs using this method limits the type of drug to ones which are

compatible with the vector production methods. In general, this rules out most bioactive protein molecules [143].

An ideal drug release profile would treat an infection and prevent further infection until the wound heals. Currently, the trend for a burst phase followed by a long sustained phase of drug release is adequate. In the burst phase, a large dose of antibiotic can be delivered quickly to arrest the growth of bacteria and kill them. It has been determined that bacteria must be prevented from colonizing and proliferating before 6 hours past implantation of the device [146]. Following this, a long sustained release of antibiotic is useful in preventing further infection without interfering with wound healing processes [147, 148].

2.5 Bioglass

Bioglass (also known as bioactive glasses) refers to biocompatible and bioresorbable ceramics developed by Prof. Larry Hench in 1969 [149]. The material contains SiO_2, CaO, Na_2O, CaF_2, and P_2O_5 in certain ratios. Figure 2-5 shows the potential formulations of Bioglass and their respective interaction with hard and soft tissue.

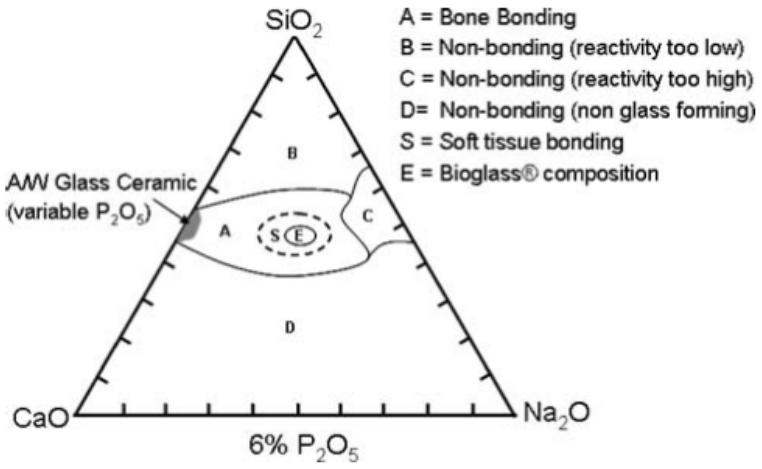

Figure 2-5: Diagram demonstrating how different concentrations of Bioglass components affect the bioactivity. The zone marked by the dashed lines denotes the region where Bioglass supports soft tissue attachment [150]**.**

Bioglass is able to form bonds with tissues through the result of a sequence of chemical reactions when inserted into living tissues. Briefly, a series of reactions leads to the release of soluble ions leading to a formation of a high surface area hydrated silica and

polycrystalline hydroxyl carbonate apatite (HCA) bilayer on the surface. This layer enhances adsorption and desorption of growth factors which promotes cell compatibility and tissue attachment [149, 151].

Of particular interest is the formulation of Bioglass 45S5 which has been shown to have a positive interaction with soft tissues. The name 45S5 signifies the glass composition of 45 wt. % of SiO_2 and a 5:1 ratio of CaO to P_2O_5 [150]. In 1981, Wilson et al reported that Bioglass 45S5 is able to form connections with soft tissue if the interface was immobile. In addition, the paper established the safety of using the ceramic in particulate form as well as bulk implants [152]. A more recent study by Gillette found that Bioglass 45S5 can increase tissue strength which could be beneficial in the treatment of wounds [153]. Another benefit of Bioglass 45S5 is its ability to stimulate angiogenesis leading to new blood vessel formation [154].

2.5.1 Bioglass 45S5 Scaffolds

Bioglass 45S5 has been used in the creation of synthetic skin scaffolds in a number of ways. Most recently, Bioglass 45S5 nanofibers have been created using an electrospinning process. The resulting material is pliable and has a rapid degradation rate making it useful for soft tissue regeneration such as that of chronic wounds [96, 155]. Other scaffolds involving the use of Bioglass 45S5 include a PDLLA/Bioglass 45S5 foam composite shown to be compatible with human lung epithelial type II cells [156], and a Bioglass 45S5/PCL composite scaffold primarily for bone regeneration [157].

2.5.2 Bioglass 45S5 Antimicrobial Properties

Bioglass 45S5 is capable of exhibiting some antimicrobial activity as mentioned in a number of articles [158–160]. The mechanism for the antimicrobial effect comes from the release of basic products during degradation which increases the pH of the local environment. It should be noted that the antimicrobial properties have only been demonstrated *in vitro* where there is a high concentration of bioglass 45S5. A study by Xie et al found that particulate bioglass 45S5 did not prevent *Staphylococcus aureus* infections in open tibial fractures on rabbits [161].

Antimicrobial properties of Bioglass 45S5 can be enhanced through the doping of antimicrobial ions such as silver, zinc and copper. Silver, whose antimicrobial properties are mentioned in 2.3.2.1.1 Silver, can be added to Bioglass 45S5 in nanoparticles of AgO_2. A study of surgical sutures coated with Bioglass 45S5 doped with 3 wt% AgO_2 demonstrated reduced bacterial attachment under flowing conditions [162].

2.6 Drug Eluting Bioglass 45S5 Microspheres

Bioglass 45S5 has numerous properties which make it ideal to use as a carrier for drugs. It is biocompatible, bioresorbable with controllable degradation and offers suitable surface chemistry for cell attachment, proliferation and differentiation. In addition, Bioglass 45S5 is able to withstand a certain amount of mechanical force making it ideal for bone tissue engineering [163]. Bioglass 45S5 can also be combined with polymers to create a composite system that provides more mechanical flexibility and easier processing capabilities [156]. Whilst Bioglass 45S5 has been demonstrated to also have antibacterial effect [158, 160, 164, 165], further investigation has found that this is generally only the case where there is a high weight percentage of bioglass 45S5 particles to bacterial broth volume. The mechanism of the antibacterial effect is due to the increase in pH from the leaching of ions from the Bioglass 45S5 [158, 160]. This can have a negative effect on host cells. Bioglass 45S5 activity against biofilm forming bacteria has also been investigated, but further research is required to link lab experimental results to clinical results [159].

Bioglass 45S5 microspheres are one of the many forms that have been investigated for delivering drugs, particularly antibiotics. For soft tissue purposes, it is beneficial to have Bioglass 45S5 in the form of microspheres for a number of reasons. Bioglass 45S5 microspheres are easier to manufacture when compared to making Bioglass 45S5 scaffolds which are more suited for hard tissue engineering. Secondly, microspheres loaded with drugs are easier to incorporate into polymer scaffolds which can be done using thermal adhesion or direct addition of microspheres to the polymer scaffold processing. Finally, microspheres have a greater surface area compared to other structures allowing for greater drug loading.

Drug loading onto Bioglass 45S5 microspheres can be accomplished in a number of ways. Sol-gel technology allows drugs, proteins and other biologically active molecules to be incorporated into the bioglass 45S5 in a room temperature process [166]. Radin et al [166] demonstrated how the antibiotic vancomycin can be loaded onto silica discs. Issues with this process include long processing time up to 3 days, extremely low pH (pH 2.5 – 3) involved which may exclude the ability to load proteins and the large amounts of monitoring required [166]. Another approach is to soak the bioglass 45S5 in a solution of the desired loading molecule allowing the molecule to attach to the surface [167]. This results in low drug loading efficiencies, even with surface modifications such as mesopores to increase total surface area [167]. Finally, chemical bonding can be achieved through the interaction of hydroxyl and amino groups of molecules with the Si-OH and P-OH groups present on bioactive glasses [168]. However, it should be noted that antibiotics only work when they are taken up by bacteria cells meaning that the chemical bond must be cleaved or the molecule released in some mechanism [6]. Incorporating antibiotics during traditional bioglass 45S5 production is generally dismissed due to the high temperature involved which can incinerate antibiotics [166].

Another method of loading drugs onto bioglass 45S5 microspheres is through the use of hollow mesoporous microspheres. A hollow mesoporous microsphere significantly increases the total surface area of the microsphere allowing for greater drug loading. In addition, it can be combined with a polymeric or gel –like filler to decrease the initial mass and rate of drug eluted allowing for longer sustained release. An optimal configuration of the microsphere would be to have antibiotic solution trapped inside a hollow microsphere. The size and number of mesopores could theoretically be used to control the release of antibiotic solution until the Bioglass 45S5 degrades allowing for the remaining antibiotic to be released. Combined with antibiotic attachment to the surface and mesopores channels, this design setup could potentially create a double burst profile of antibiotic release which would be useful in treating infected chronic wounds.

There are few articles which investigate this setup. Most bioglass 45S5 microspheres represented in literature are mesoporous but not mesoporous and hollow. Also, there are no articles on loading antibiotics or drugs as a solution inside hollow Bioglass 45S5 microspheres. An article by Fu et al in 2011 [169] developed hollow hydroxyapatite microspheres which were loaded with bovine serum albumin in a similar setup as described previous paragraph and depicted in Figure 2-6. The antibiotic solution was loaded using a soaking procedure assisted with a vacuum chamber. The setup used by Fu cannot be exactly copied using Bioglass 45S5 as hydroxyapatite ceramic is naturally porous as opposed to Bioglass 45S5 which is solid [169].

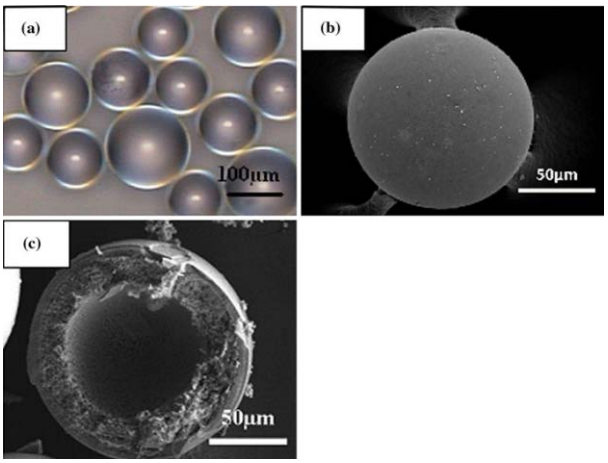

Figure 2-6: (a) Optical image of starting glass (CaLB3-15) microspheres, and SEM images of (b) external surface of hollow HA microsphere prepared by converting the glass microspheres for 48 h in 0.02 M K2HPO4 solution at 37°C and pH = 9, (c) cross section of hollow HA microsphere [169]**.**

2.7 Commercial Products of Microsphere Drug Delivery Systems

The commercial market for drug delivery systems was $47 billion in 2002 has been growing ever since. There are a number of devices on the market for controlled release drug delivery ranging from insulin pumps to biodegradable polymeric microspheres. There are over 30 companies involved with polymeric drug delivery systems. Examples of commercial microsphere products include Lupron Depot® and Nutropin Depot®. Lupron Depot® delivers luprolide acetate in PLG microspheres to treat prostate cancer, endometriosis, fibroids and central precocious puberty [170, 171]. Nutropin Depot® delivered recombinant human

growth hormone (rhGH) encapsulated in PLG microspheres to treat growth hormone deficiencies [172, 173].

The major concern of biodegradable polymeric microspheres is the highly complicated and technical manufacturing and production requirements which incur significant costs. Nutropin Depot® was removed from the market because of the high costs and poor uptake of the device [174].

Future markets that controlled release biodegradable microspheres have been tapped into include controlled-release vaccines [175], stabilisation of encapsulated protein therapeutics [176, 177]and DNA encapsulation for gene therapy [178]. In addition, these microspheres have been investigated for developing new delivery vectors for therapeutics through the respiratory tract [179, 180].

2.8 Summary of Literature Review

Chronic skin wounds are a serious health issue which affect a significant proportion of society in developed countries, particularly amongst the elderly, indigenous and rural communities. The major complication associated with chronic wounds is infections. Currently, there is a large spread of medical products used to treat chronic wounds from traditional wound dressings to modern tissue engineered skin constructs. These forms of treatment are generally conducted with the addition of antimicrobial agents or administration of systemic antibiotics. There are no commercial products in which the dressing itself is capable of long term antibiotic release. Emerging research in this area focuses on the development of synthetic skin constructs which can be loaded with drugs, growth factors or other biological compounds. One method of drug loading and delivery involves the use of bioactive resorbable glass microspheres which could be tailored to hold high quantities of drugs. Drugs can be attached to the surface and pores of the microsphere, or encapsulated within the microsphere within a hermetic seal. Currently, polymeric microspheres have been used in treatments of cancer, diabetes, and growth hormone deficiencies. Furthermore, other potential markets include vaccine therapy, protein

therapeutics and DNA gene therapy. There are no commercial bioactive glass ceramic microspheres on the market.

3 Design Process

3.1 Introduction

As outlined in the literature review, there is a need for effective chronic wound treatments which addresses device uptake, combats infections and reduces overall wound healing time. Synthetic skin substitutes have the potential to address all these issues in a single product. For this thesis, an investigation will be carried out to the development of a synthetic skin scaffold containing antibiotic-loaded bioactive glass microspheres.

In order to develop a device which sufficiently treats chronic wounds, it is important to identify the user requirements and design risks involved in synthetic skin scaffolds which contain antibiotic-loaded bioglass 45S5 microspheres. There are a number of user requirements related to the device which includes clinical and mechanical needs. It is also important to identify potential design risks which could pose hazards to users of the device.

The synthetic skin scaffold to be developed in this thesis combines the technology of synthetic polycaprolactone scaffolds and bioglass 45S5. These scaffolds are three dimensional, porous polyester scaffolds which promote vascularization and tissue regrowth [181]. Its high surface area and low glass transition temperature make it an ideal carrier of bioglass 45S5 microspheres which can be attached to the surface of the scaffold.

Bioglass 45S5 microspheres enhance cell attachment to the scaffold and can be modified to load drugs such as antibiotics to create a long-term antimicrobial environment. A number of bioglass 45S5 microsphere design iterations will be explored in this chapter. In addition, similarities and differences between bioglass 45S5 and sodium borosilicate glass will be addressed to show that sodium borosilicate microspheres can be used as an analogue for bioglass 45S5 microspheres in experiments.

This thesis aims to explore design modifications to bioglass 45S5 microspheres, methods of attaching bioglass 45S5 microspheres to the scaffold and how these modifications can be used to load and release antibiotics. From the results, enough information should be

available to verify the ability of a synthetic skin scaffold with antibiotic-loaded microspheres to be used to treat chronic skin wound conditions.

3.2 User Requirements and Design Risk Assessment

3.2.1 User Requirements

A user requirement table outlines the specifications a product should meet as part of its functionality. These specifications can come from a wide range of sources which includes users and regulatory standards. Since the device to be developed in this thesis is within early development stages, user requirements will be focused on specifications required for the device to act primarily as a wound healing device, secondly as a wound healing device capable of treating infections and thirdly as a wound healing device capable of sustained antimicrobial activity.

Table 3-1 lists the clinical and mechanical requirements for a synthetic skin scaffold with antibiotic-loaded microspheres. Each user requirement is given a unique identifying number (UIN) and assigned a priority ranking of I, II or III. Priority ranking of I describes requirements needed to ensure the device is able to be used in chronic wound healing. Priority ranking of II addresses functions of the device which would allow it to additionally treat and maintain a level of antimicrobial activity. Priority ranking of III refers to requirements which are not necessary but would enhance the effectiveness of the device.

Chronic wounds sizes vary significantly in width, depth and contour. It is important that the scaffold is able to fit into the majority of major chronic wounds. In addition, for each individual wound, there should be minimal modifications required to make the scaffold fit in the wound.

A major issue with the wound healing of chronic wounds is the vascularization of the device replacing the degraded skin. Vascularization, as explained in 2.2.1.3.2 Angiogenesis, is necessary for tissue growth and host antimicrobial activity.

Table 3-1: User requirement table

Unique Identifying Number (UIN)	User requirement	Priority Ranking: I, II or III
	Clinical	
UR1	Able to fit a wide range of wounds	I
UR2	Encourages vascularization and tissue regrowth	I
UR3	Deliver antibiotics locally to the wound site	II
UR4	Maintain a sustained antimicrobial environment	II
UR5	Seal the wound from the external environment	III
	Mechanical	
UR6	Stiffness of entire assembly is less than the modulus of skin tissue	I
UR7	Scaffold must not fragment or degrade during wound healing	I
UR8	Biodegrade upon wound closure	I
	Other	
UR9	Low Production Time	III

In the early stages of wound healing using skin devices, there is a significant risk of infection. Currently, antibiotics are administered intravenously. However, if there is low vascularization of the wound, there may be a diminished antibiotic effect. For a synthetic scaffold, it would be ideal if the antibiotic was locally delivered with the scaffold using an appropriate delivery vector such as microspheres.

It is ideal if the wound maintains an antimicrobial environment whilst tissue regeneration occurs. This can be achieved by having a sustained antibiotic delivery system capable of week-long antibiotic delivery. Simultaneously, the solution needs to support granular tissue formulations.

To help maintain sterility and prevent further infection, an external seal should also be applied to protect the wound from the external environment. This can be done in a number of ways which may or may not be coupled with the scaffold device.

The scaffold should have a similar elasticity to the surrounding skin. Large differences in elasticity can promote pain, wound erosion and increase wound healing time.

The scaffold should also maintain structural integrity whilst wound healing is occurring. Degradation in structure could hinder vascularization and tissue regrowth.

Once tissue growth and wound closure is achieved, the scaffold will be integrated with the skin and become irremovable. The scaffold should biodegrade allowing full restoration of skin tissue.

Another user requirement would be low production time and costs to allow the device to be a cost-efficient competitive product amongst all the other wound healing products on the market.

3.2.2 Design Risk Assessment

A design risk assessment helps to identify factors or events which could impede the function of the device to act as a chronic wound healing product. As seen in Table 3-2, each risk is given a likelihood and severity number ranging from one to five where one is minimum and 5 is maximum. The likelihood and severity ratings are multiplied to give an importance rating out of a maximum of 25. The higher the importance rating, the more significant the risk is.

Table 3-2: Importance rating system

		Severity				
		1	**2**	**3**	**4**	**5**
Likelihood	**1**	Acceptable	Acceptable	Acceptable	Moderate	Moderate
	2	Acceptable	Acceptable	Moderate	Moderate	Moderate
	3	Acceptable	Moderate	Moderate	Moderate	Severe
	4	Moderate	Moderate	Moderate	Severe	Severe
	5	Moderate	Moderate	Severe	Severe	Severe

Table 3-3 lists design risks associated with using a synthetic skin scaffold with antibiotic-loaded microspheres. These include biological risks the device may induce once used and design risks which affect the functionality and effectiveness of the device to perform its use.

Table 3-3: Design Risk table

Unique Identifying Number (U.I.N)	Risk Assessment	Likelihood (1-5)	Severity (1-5)	Importance (Likelihood x Severity)
Biological risks				
RA1	Biological rejection of scaffold	2	5	Moderate
RA2	Adverse reactions to antibiotics	2	5	Moderate
RA3	Microbial infections and colonization of the scaffold	4	5	Severe
Design Risks				
RA4	Unable to make bioglass 45S5 microspheres	2	4	Moderate
RA5	Scaffold destruction during microsphere attachment	3	4	Moderate
RA6	Unsecure microspheres attached to scaffold	4	2	Moderate
RA7	Unable to load antibiotics onto microspheres	1	5	Moderate
RA8	Unable to deliver sustained antibiotic release (< 1 week)	4	3	Moderate
RA9	Unable to maintain scaffold integrity during cyclic loading tests	3	4	Moderate

Biological rejection of the scaffold could arise from a number of issues. In graft constructs, this is due to the incompatibility of the major histocompatibility complex cell surface receptors between the host and graft leading to immune rejection. For synthetic scaffolds,

where there are no surface receptors involved, rejection can occur due to non-biocompatible materials used and infections present in the wound.

Adverse reactions to antibiotics present in the microspheres are an issue which needs to be considered. Ideally, a patient with allergies to certain antibiotics would be known beforehand. However, careful monitoring of the patient would be required as standard practice. As the antibiotic is loaded onto the microspheres as opposed to the scaffold, a change of antibiotics is possible and would only be limited to the time it takes to load antibiotics and attach microspheres to the scaffold.

Microbial infections are a major source of concern. Untreated infections can result in scaffold rejection, worsening condition of the chronic wound and decline in patient health. Antibiotics loaded with the scaffold need to be able to release a sufficient amount of drug to treat the infection and prevent further infection during wound healing.

A key part of this thesis is the production of bioglass 45S5 microspheres. Currently, the most popular method of making bioglass 45S5 microsphere is using the sol-gel technique which requires up to 3 days. An alternative method is to flame spray the microspheres and collect them. This method would only require a few minutes to complete.

Microspheres would ideally be adhered to the scaffold by taking advantage of the low glass transition phase of the scaffold. However, due to the micron size struts, the scaffold can easily undergo heat damage reducing porosity. This would in turn reduce the capability of vascularization throughout the scaffold.

On the contrary, poor microsphere attachment could lead to migration of microspheres through the skin tissue away from the wound site through muscle contractions. This could lead to issues regarding localized treatment of infections.

Another key part of this thesis is the loading and release of antibiotics from bioglass 45S5 microspheres. Ideally bioactive glass microspheres and any modifications to the microspheres would be able to have a high drug loading efficiency and sustained release.

Regarding sustained release, the ideal time length of the sustained release period is equal to the time required for the chronic wound to heal. However, due to the varying size and conditions of chronic wounds, there will always be a discrepancy between the two periods. Initial development would focus on a week-long release period.

Finally, the scaffold should maintain structural integrity during wound healing. Whilst wound dressings over the chronic wound site should minimize movement of the scaffold, it would be ideal of the scaffold itself is able to maintain form over 50% elastic deformations whilst vascularization and tissue regrowth occurs through the scaffold.

3.3 Design Rationale

Section 2.3.4 Synthetic Skin Scaffolds from the literature review outlines the ideal general properties of synthetic scaffolds, how they are produced and what materials scaffolds are made from. Scaffolds produced by solvent leaching have a greater interpenetrating network with a porosity of greater than 95%. PCL scaffolds are popular due to the well-known biocompatibility and FDA approval of the polyester. Methods of loading drugs onto scaffolds are outlined in section 2.3.4.3 Therapeutic loading. Most methods involve a single scaffold unit with antibiotics loaded directly onto the scaffold. This results in a sustained release lasting only a few days. So far, there has been no research into a two part device in which antibiotics are loaded onto a delivery vector which is attached to the scaffold.

A two-part synthetic skin construct is proposed in this thesis. It consists of a PCL scaffold utilizing a bioglass 45S5 microsphere as a delivery vector for antibiotics.

3.3.1 Scaffold

Figure 3-1: PCL scaffolds

The scaffold for the device, as seen in Figure 3-1, is made using a PCL solvent leaching technique. The scaffold has an interpenetrating network of channels creating a matrix with greater than 95% porosity. This allows proliferating cells to infiltrate throughout the scaffold, attach and proliferate. The high porosity of the scaffold is achieved using a unique porogen which the scaffold is moulded around. This interpenetrating network of channels has been shown to accelerate the revascularisation of the wound site within two weeks in animal studies [181]. In addition, the scaffold has elasticity similar to skin which is necessary to optimise skin regeneration and provide mechanical strength to the wound region.

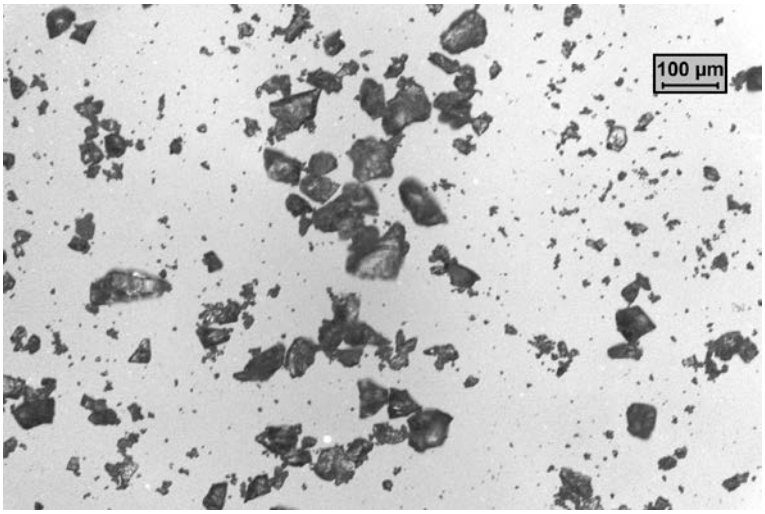

Figure 3-2: Bioactive glass powder granules

In addition to the scaffold, Bioglass 45S5 powder of less than 50 µm diameter is coated onto the surface of the scaffold. Bioglass 45S5 powder, described in detail in 2.5 Bioglass, encourages the attachment of cells to bioinert surfaces increasing the rate of uptake of the scaffold in the skin and reducing wound healing time. In addition, bioglass 45S5 dissolution products neutralize the acidic degradation products of PCL.

Previous research involving polycaprolactone scaffolds has looked at the addition of antibiotics to the scaffold as a means of treating and preventing infections. Scaffolds have been loaded with chloramphenicol and tetracycline using a soaking protocol and various scaffold modifications to delay antibiotic release and prolong the sustained release period. However, the studies found that the majority of antibiotic was released within 2 hours followed by a very low amount of antibiotic release over 24 hours. Other issues identified were poor shelf life due to the degradation of antibiotics over time, and large losses of antibiotic during manufacturing [14, 182].

Following on from these studies, a change in the design was made to separate the antibiotic delivery vector from the scaffold creating a two-part product. Antibiotics would be loaded onto bioactive glass microspheres which in turn would be adhered to the scaffold prior to clinical use. Adhesion of the microspheres to the scaffold would be performed using a thermal attachment process where the scaffold is heated enough to allow the microspheres to bind to the scaffold surface. Advantages of using this system include longer shelf life of scaffolds, control over dosage concentration for medical staff, and potentially more sustained antibiotic release.

3.3.2 Microspheres

3.3.2.1 Synthesis

Bioactive glass microspheres can be made from various methods. One of the more popular methods is through sol-gel techniques. Briefly summarizing the technique, metal organic and metal salt precursors undergo hydrolysis and poly-condensation reactions to form a gel over a period of several days. The gel is then dried at 600-700°C to form the glass. Bioglass 45S5 microspheres can be designed using through the addition of polymer molecules capable of

self-assembling into microspheres such as chitosan [183]. Problems associated with this technique include the long processing time [166] and the fragile nature of the chemical reactions which can be interfered by slight changes in pH and precursor concentrations [184].

Instead of using sol-gel techniques, bioglass 45S5 powder will be transformed into microspheres through the use of an oxy-acetylene flame gun [185, 186]. This significantly speeds up the process allowing the creation of microspheres from raw materials to be processed within a day. Particle size of bioglass 45S5 microspheres can be easily controlled through the input of controlled sized powder. In addition, this process can be easily upscaled to mass manufacturing [187].

3.3.2.2 Microsphere configurations

Ceramic microspheres have been investigated as potential delivery vectors for antibiotics and were reviewed in length in section 2.6 Drug Eluting Bioglass 45S5 Microspheres. There are a number of design considerations which need to be taken into consideration. They include:

- High surface area for antibiotic loading via electrostatic and weak intermolecular bonding
- Ease of manufacturing
- Capability for long term antibiotic release

Table 3-4 lists a number of microsphere design iterations that could be used for antibiotic loading. Microsphere designs are listed from simple to complex iterations listing the advantages and disadvantages of each iteration.

Table 3-4: Bioglass 45S5 microsphere configurations.

#	Microsphere design	Image cross-section depiction	Advantages	Disadvantages
1	**Normal**	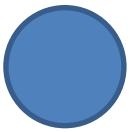	Low technology requirements to produce	Low surface area for antibiotics to attach to compared with other design iterations
2	**Porous**		Increased surface area compared to normal microspheres	Requires further treatment to create pores Longer production time
3	**Hollow (intact)**		Potential to load antibiotic solution within a hermetically sealed bioglass 45S5 microsphere	Getting antibiotic solution inside hollow microsphere is extremely difficult
4	**Hollow (porous)**		Greater surface area	Requires further treatment to create porosity
5	**Hollow (porous) with gel center**		Prolongs antibiotic release period Capable of loading more antibiotic through gel center	Increases production time significantly Gel core may cause bioglass 45S5 to undergo degradation reactions, especially if it holds water
6	**Coated**	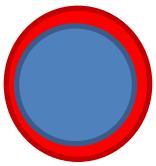	Polymer coating prolongs antibiotic release and delays bioglass 45S5 degradation	Bioglass 45S5 surface not available for interaction with cells until polymer coating degrades. Antibiotic may be lost during polymer coating process

The first design iteration is normal spherical microspheres. It should be possible to manufacture these microspheres from bioglass 45S5 powder using a flame-spray gun. Whilst microspheres have high surface area to volume ratios, other design iterations offer more surface area which allows for greater antibiotic loading.

Design iteration 2 builds on the first design iteration by increasing the surface area of the microsphere by introducing pores into the surface. Pores can be etched into the microsphere using highly basic solutions such as hydroxide solutions. At high temperature, alkali solutions can etch bioglass 45S5 through the following chemical reaction.

Equation 1: Chemical Etching reactions of Bioglass 45S5 with potassium hydroxide (KOH) solution.

$$SiO_2 + 2KOH \xrightarrow{\Delta} K_2SiO_3 + H_2O$$

$$P_2O_5 + 4KOH \xrightarrow{\Delta} K_2HPO_4 + H_2O$$

Chemical etching is time and heat intensive process requiring up to a day for processing depending on the strength of the alkali solution. Focused ion beam techniques could also be used to create pores on the surface of microspheres although the technique is highly technical and not easily upscaled.

Hollow microspheres are a byproduct of flame-spray. It is believed that certain compounds within the bioglass 45S5 powder react to produce gas at high temperatures. If the microsphere is cooled fast enough, the gas remains trapped within microsphere. It is theorized that with a modification to the process, liquid solutions of antibiotics could potentially also be trapped within the microspheres creating a ceramic hermetically sealed antibiotic solution delivery vector.

Design iteration 4 combines iterations 2 and 3 to create a hollow porous microsphere. This greatly increases the surface area available for antibiotic loading. However, producing these microspheres would require a balance between chemical etching technique and size of the inner diameter of the microsphere else risking complete dissolution of the microsphere.

Design iteration 5 builds on iteration 4 with the addition of a gel to lock in antibiotic bound to the inner surfaces of the microsphere. The gel itself could be used to load more antibiotic increasing the total antibiotic load per microsphere. This would prolong antibiotic delivery as either antibiotic molecules move through the gel or remain locked until the gel degrades exposing the inner surfaces. Other factors which would affect antibiotic release is the viscosity of the gel, the degradation rate and water solubility of the gel.

Design iteration 6 describes any of the previous design iterations with the addition of a polymer coating to prolong antibiotic loading and delay degradation. The polymer coating would also be useful for scaffold adhesion if the coating polymer is the same as the scaffold polymer and if the polymer is thermo-adhesive. Problems associated with polymer coatings include the restriction of bioglass 45S5 surface for cell attachment and the potential of antibiotic loss to occur during the polymer coating phase.

For this thesis, design iterations 1, 2 and 3 will be investigated. These iterations were chosen as they provide the groundwork for design iterations 4, 5 and 6. Design iterations 4, 5 and 6 and other further work could form the basis of a follow-up Masters or PhD project.

3.3.3 Bioglass 45S5 vs Sodium Borosilicate Microspheres (Q-cells)

The primary design of the synthetic wound healing device described in this thesis is to use Bioglass 45S5 microspheres as the carrier for antibiotics. However, due to difficulties in sourcing Bioglass 45S5, sodium borosilicate microspheres have been used as an analogue for bioglass 45S5 microspheres in some experiments. Hence it is important to note the differences between Bioglass 45S5 and sodium borosilicate microspheres as shown in Table 3-5.

Table 3-5: Similarities and differences between Bioglass 45S5 and sodium borosilicate microspheres.

Similarities	Differences
• Both amorphous silicate-based material • Similar mechanical, chemical and thermal properties • Antibiotic loading primarily through electrostatic/weak intermolecular forces	• Sodium Borosilicate is hydrophobic while Bioglass 45S5 is hydrophilic • Slight compositional differences leads to differences in the rates of hydration of silicate compounds.

For the purposes of microsphere attachment to scaffolds and primary method of loading antibiotics to microspheres, the two materials are quite similar in their characteristics. The biggest difference between the materials is that sodium borosilicate microspheres are hydrophobic while Bioglass 45S5 microspheres are hydrophilic. To compensate for the differences, ethanol has been used in conjunction with water in some experiments to mimic the conditions and behaviors of bioglass 45S5 microspheres in water. A minor difference between the two materials is that Bioglass 45S5 can form a gel layer if it is exposed to water for a long time. This is part of the process of bioglass 45S5 dissolution that releases bioactive compounds to attach cells to bind to surfaces. Sodium borosilicate microspheres do not dissolve in water. The scope of this thesis does not expand far enough for this difference to have a significant effect on experimental procedures and data.

3.4 Experimental Philosophy

Section 3.2 User Requirements and Design Risk Assessment identifies some key requirements and concerns regarding synthetic skin scaffolds. A combination of literature review articles and experiments will be used to adequately address these points.

Table 3-6: Assessment of user requirements and risk assessment from literature review

UIN	Requirement or Risk	Literature	References
UR1	Able to fit a wide range of wounds	Scaffolds are able to be shaped to fit wounds either through pre-forming or post-formed modifications.	[181]
UR2	Encourages vascularization and tissue regrowth	Scaffold has been shown to encourage vascularization in animal models	[181]
UR5	Seal the wound from the external environment	Separate wound dressings can be used to help seal the wound	[94, 188]
UR6	Stiffness of entire assembly is less than the modulus of skin tissue	Modulus of scaffold ranges between 20-60 kPa	[181, 182]
UR8	Biodegrade upon wound closure	PCL and Bioglass 45S5 are biocompatible and biodegradable	[134, 149, 151]
UR9	Low Production Time	Scaffold production time is 3 days when operations are conducted in serial progression	[181]
RA1	Biological rejection of scaffold	PCL and bioglass 45S5 are biocompatible, biodegradable and shown to encourage vascularization in animal models.	[134, 149, 151, 181]
RA2	Adverse reactions to antibiotics	Antibiotic sensitivity will need to be confirmed before use. Antibiotic microspheres can be left out of the device if necessary.	[189]

Table 3-6 addresses as many user requirements and risks as possible from using information from the literature review. User requirements and risk assessments listed in Table 3-6 are recognized as issues which have already been addressed in other research articles.

Scaffolds for wound healing should be able to fit a wide range of wound sizes and depth. Scaffolds are able to be produced in a wide range of shapes within a three day production phase. In addition, the scaffolds are soft to be manually cut within surgery to fit the wound.

Scaffolds have also been shown to encourage vascularization throughout the scaffold in non-apoxic wounds in animal models. Full tissue regrowth is achieved within 1 week of implantation [181].

Protecting the wound from the external environment is important for preventing further infection and maintains wound moisture levels. Whilst the device doesn't currently account for this, there are many wound dressings which are also commonly used in conjunction with skin constructs.

The Young's modulus of the device should be less than the modulus of the surrounding skin in order to prevent abrasion and pain. The modulus of the scaffold ranges between 20-60 kPa as it becomes compressed which should be lower than the modulus of the surrounding skin.

Since the scaffold will integrate fully with new tissue, it cannot be removed and must biodegrade. Multiple journal articles show that PCL scaffolds and Bioglass 45S5 microspheres are biodegradable which is necessary for synthetic wound healing devices [134, 149, 157].

The production time of the device is important in terms of manufacturing, product turnover and being commercially competitive. Scaffolds used in this thesis have a three day production time if the processes are executed in serial sequence. It is possible for the production to be greatly reduced if processes involved are performed in parallel. The production time of bioglass 45S5 microspheres will be investigated in the experiments in Chapter 4: Production and Characterisation of Microspheres.

As mentioned before, the materials used in the device are biocompatible and biodegradable. In addition they are able to promote vascularization and granular tissue formation within a week of implantation.

Adverse reactions to antibiotics are a serious issue. Antibiotic sensitivity needs to be confirmed by the clinician before use of the device. Since the device consists of two parts, it is possible for the scaffold to be kept separated from the antibiotic loaded microspheres.

While antimicrobial activity won't be present from the scaffold, infections can be treated through I.V. antibiotic administration or through other antimicrobial products.

Table 3-7: Experimental process

#	Experiments	Relevant UINs	Pass/Fail/ Incomplete
	Chapter 4 - Production and Characterisation of Microspheres		
4.1	Production of Bioglass 45S5 microspheres	UR3, UR4, UR9, RA4	
4.1a	➢ Whole		
4.1b	➢ Hollow		
4.1c	➢ Porous		
4.2	Able to load antibiotics within hollow microspheres	UR3, UR4	
4.3	Standardize particle size	UR3, UR9	
	Chapter 5 - Microsphere Attachment Studies		
5.1	Able to attach microspheres to scaffold	UR2, UR3, RA5	
5.2	Maintain scaffold integrity during attachment process	UR7, RA5, RA6	
5.3	Maintain scaffold integrity during cyclic loading test	UR7, RA9	
	Chapter 6 - Drug Release Studies		
6.1	Able to load antibiotics onto microspheres	UR3, RA7, RA8	
	➢ Able to load antibiotic-loaded microspheres onto scaffolds		
6.2	Release of antibiotic from device	UR4, RA8	
6.2a	➢ 1 day		
6.2b	➢ 1 week		
6.3	Reliable release of antibiotics from device	UR3, UR4	

Table 3-7 lists the experiments that will be performed in this thesis and the relevant user requirements and risks which will be answered by these experiments. A completed version of this table will be addressed in section 7 General Discussion.

Chapter 4 of this thesis focuses on the production of different types of microspheres. As stated in section 3.3.2.2 Microsphere configurations, whole, porous and hollow microspheres will be attempted to be produced. In addition, an attempt to load liquid into a hermetic-sealed hollow microsphere will be conducted to determine the feasibility of producing hollow microspheres with antibiotic solution within. Characterization studies of the particle sizes of the microspheres will be carried out.

Chapter 5 focuses on the attachment of microspheres to the scaffold. During microsphere attachment to the scaffold, there is a potential for the scaffold to lose structural integrity through heat damage. Experiments on how heat affects microsphere attachment and scaffold damage will be carried out. In addition, once microspheres have been attached to the scaffolds, a cyclic loading test will be carried out to determine the percentage of microspheres lost during 50% elastic compression at 1.5Hz for 24 hours.

Chapter 6 involves the study of drug release from microspheres attached to the scaffold. Chloramphenicol antibiotic will be loaded onto microspheres through a soaking technique. The loaded microspheres will then be attached to scaffolds. Drug release from the device will be monitored using a UV spectrophotometer calibrated to detect release of chloramphenicol molecules.

4 Production and Characterisation of Microspheres

4.1 Introduction

This chapter will explore the production of three types of microsphere design iterations; whole, hollow and porous. In addition, experiments will be conducted to investigate the potential of creating an antibiotic-solution filled microsphere through flame-spray techniques.

The primary production method for microspheres used in this chapter will involve the use of a flame-spray setup. Two types of flame guns, Thermospray Type 5P and SuperJet S, were used to produce bioglass 45S5 microspheres from bioglass 45S5 powder. Thermospray Type 5P is a hand-held industrial flame gun commonly used to deliver metal coatings on large surfaces. SuperJet S is a smaller hand-held flame gun that is typically used for metal coating small hard to reach surfaces with its long narrow barrel.

Characterization of microspheres produced in using flame-spray processes will involve optical microscopy, image analysis, and scanning electron microscopy (SEM).

4.2 Methodologies

4.2.1 Materials and Equipment

Bioglass 45S5 powder (<40μm) was produced in the University of Sydney. Sodium borosilicate microspheres were sourced from Barnes (Q-cell 520, Barnes). Flame spraying was performed using two types of flame guns, a Thermospray Type 5P (Metco) and a SuperJet S (Eutalloy). A paint spray gun (Metabo) was used to deliver red dye into the path of the flame for experiments to test the validity of loading antibiotic solutions inside a hermetically sealed hollow bioglass 45S5 microsphere.

Potassium hydroxide (KOH) was sourced from Sigma Aldrich. Optical microscopy and particle size analysis was performed using a Leica DMRXE upright microscope and Leica Qwin Image Analysis Software. Scanning Electron Microscopy was carried out at the Australian Centre for Microscopy and Microanalysis (ACMM).

4.2.2 Flame Spray Process

To generate bioglass 45S5 microspheres from crushed bioglass 45S5 powder, a flame spray approach was used. Flame spraying was carried out using the setup shown in Figure 4-1. Bioglass 45S5 powder was fed into the flame gun and sprayed into a collection container filled with water to cushion to impact of microspheres. The variables changed during the process include the type of gun used and the use of cooling air jets when the Thermospray Type 5P gun was used. Controlled variables include the mixture of oxygen to acetylene fuel set at 24/29 psi and the length of the gun from the collection container set at twice the length of the flame.

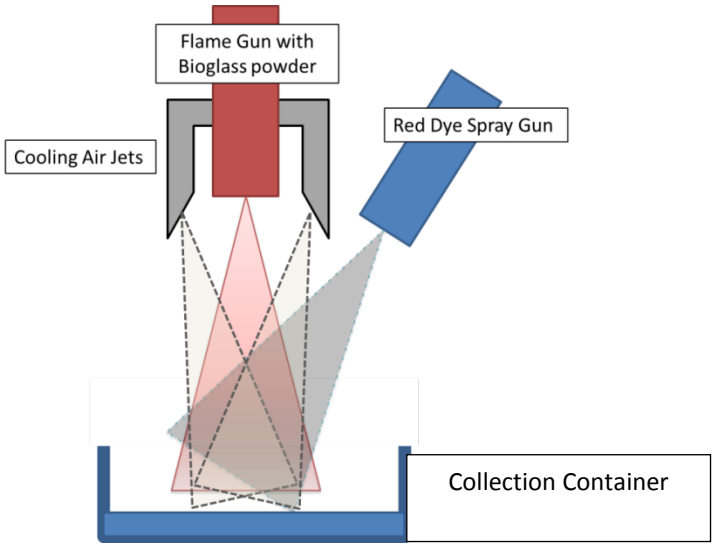

Figure 4-1: Diagram of flame spray setup.

Microspheres were collected from the collection container and filtered through a filter paper. Once filtered, the microspheres were dried and stored in a desiccator jar until microscopy analysis.

4.2.2.1 Encapsulation of red dye in MS

To determine whether it is feasible to load antibiotic solution inside hollow microspheres and create a hermetic seal around the solution, a brief experiment was conducted. Red dye was used as an analogue to antibiotic solution. Red dye would be sprayed into the path of the flame at various angles at the highest safe pressure setting available (40kPa).

Microsphere particles were collected in the same manner outline in section 4.2.2 Flame Spray Process.

4.2.3 Characterisation of Microsphere Features

Microspheres were observed under an optical microscope. Images were taken of whole, hollow and chipped microspheres. The optical microscope light setting was set on transmissive in order to identify internal features of the microsphere. Other artifacts found in the sample were taken. For the encapsulation of red dye in microspheres experiment, images of red particles were taken using a reflective optical setting to ensure the red colour can be seen. To determine if hollow microspheres were being produced, SEM images were taken with the aim of finding broken hollow microspheres.

4.2.3.1 Particle Size Analysis

Particle size analysis was conducted on images taken from the optical microscope. 0.1g of Bioglass 45S5 or Q-cell microspheres was suspended in 1 mL water or ethanol respectively. Three droplets (approximately 0.3 mL) was added to a glass slide and covered with a glass covering slip. Three separate images were taken of each sample. Images were chosen to ensure that there was at least one microsphere present. Image analysis was conducted using parameters which removed particles of less than 2.5 µm diameter. Microspheres which overlapped each other were counted as separate entities given that the minimum potential microsphere was 2.5 µm in diameter.

4.2.4 Chemical Etching

Chemical etching was conducted on Q-cells due to limited supply of Bioglass 45S5. 0.1g of Q-cell was suspended in 10ml of pure ethanol. 40mL of 0.5M KOH was added to the Q-cell suspension. The suspension was heated to 90°C and constantly stirred using a glass rod to minimize damage to the Q-cell microspheres. At time intervals 20, 40 and 60 minutes, samples of the Q-cell suspension were taken and washed 3 times in distilled water to halt any chemical etching reactions. Q-cell samples were analyzed using SEM looking for any damage to the surface of the microspheres.

4.3 Results

4.3.1 Optical Images

4.3.1.1 Flame-Sprayed Bioglass 45S5 Microspheres

Bioglass 45S5 microspheres were collected from Thermospray Type 5P and a SuperJet S flame guns and imaged under an optical microscope. No microsphere morphology differences were observed from using the two different guns.

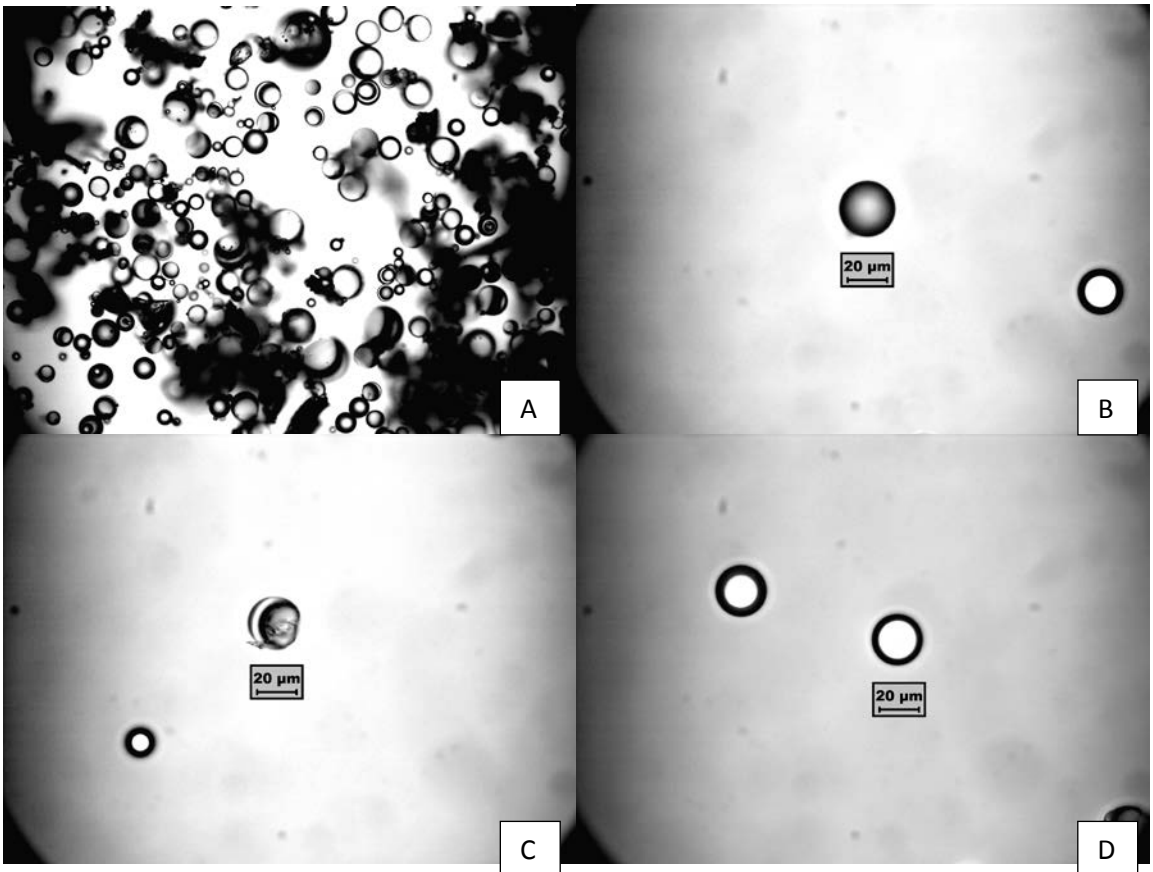

Figure 4-2: Optical images of flame sprayed bioglass 45S5 microspheres. (A) shows the 100x optical view of the microspheres collected. (B) shows an example image of whole microspheres found, (C) shows chipped microspheres found and (D) shows hollow microspheres found. (B), (C), and (D) type of microspheres were found for both types of flame-spray guns.

Figure 4-2 shows optical images of bioglass 45S5 microspheres collected from the flame spray-process. Image A shows a wide frame capture of the microspheres collected. We can see a mix of whole, hollow and chipped microspheres of various sizes present in the collection. In addition, there is a significant amount of non-microsphere debris present in the image. Image B shows an example image of a whole microsphere. Whole microspheres are

identified by the gradient grey distribution from the centre to the surface of the microsphere and the perfect circular shape of the microsphere. Image C shows an example image of chipped microspheres found. Key features of these microspheres are the imperfect non-circular shape and sharp dark edges through the middle of the microspheres. Cracks can also be seen as dark lines running through the microsphere. Image D shows an example image of hollow microspheres found. Hollow microspheres are identified by the sharp gradient change in the greyscale from the centre to the edge of the microsphere. Hollow microspheres also have a perfect circular shape.

4.3.1.2 Encapsulation of red dye in MS

Encapsulation of red dye in microspheres was attempted using the protocol listed in section 4.2.2.1. The product of the experiment was collected and imaged under an optical microscope to determine any presence of red dye encapsulated in microspheres.

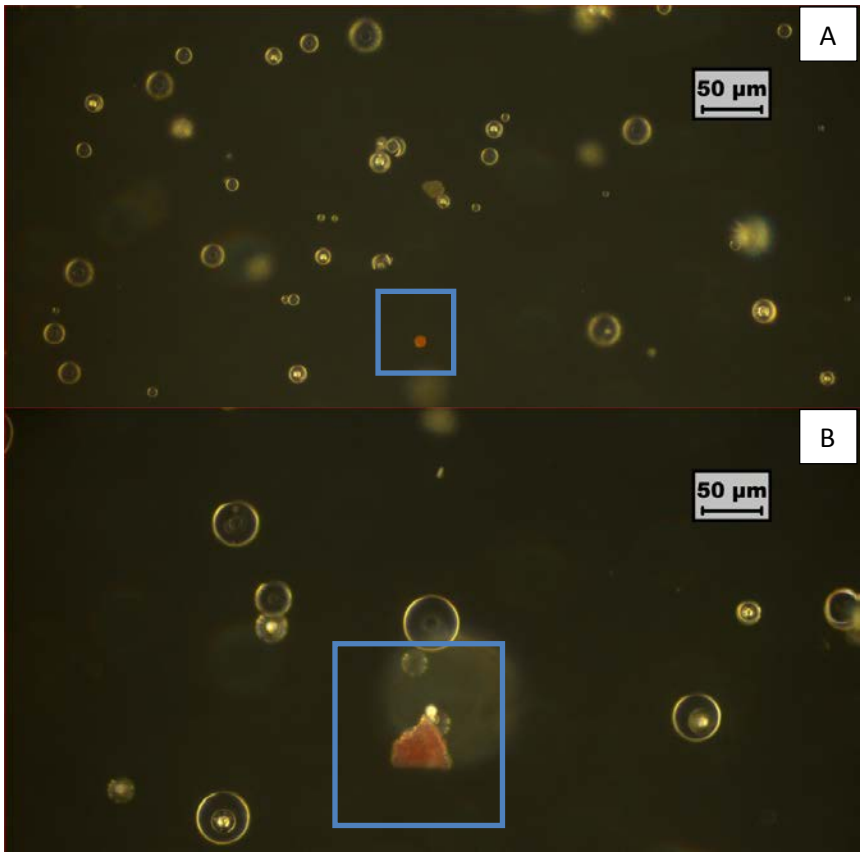

Figure 4-3: Red dye sample images of red artefacts found. No red microspheres were found.

Figure 4-3 shows images of red artefacts found in the red-dye encapsulation microsphere collection. Image A shows a red microsphere. It cannot be determined if the red colour lies inside a hollow microsphere, evenly distributed throughout a whole microsphere or coated on the surface of the microsphere. Image A also highlights the extremely low yield of red microspheres found in the collection. Image B shows a red non-microsphere artefact found in the collection. Similar other red artefacts were found in the collection at a slightly higher yield than red microspheres.

4.3.2 SEM images

Bioglass 45S5 microspheres produced by the two types of flame guns were imaged using SEM to determine if any surface texture differences were present. SEM images showed that there were no surface texture differences between microspheres produced by the two different flame guns.

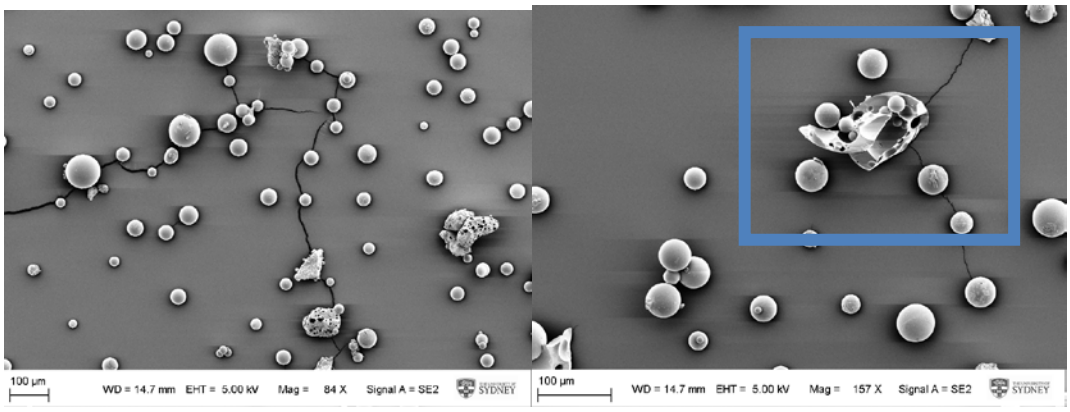

Figure 4-4: SEM images of Bioglass 45S5 microspheres. Top image shows particle size distribution while bottom image shows open hollow microsphere.

Figure 4-4 shows two SEM images of bioglass 45S5 microspheres. The images shows the surface of the bioglass 45S5 microspheres is quite smooth. The right image contains what appears to be a quarter of a broken hollow microsphere. Closer inspection of the image also reveals some hollow pockets at the top right of the broken hollow microsphere.

4.3.3 Particle Size Analysis

Figure 4-5 shows the particle size distribution of bioglass 45S5 microspheres produced from the two types of flame guns used; Thermospray Type 5P and SuperJet S. In addition, the

particle size distribution of Q-cells, which will be used as an analogue for Bioglass 45S5 in future experiments, is also compared to the Bioglass 45S5 microspheres. Particle size distribution is similar for all three categories.

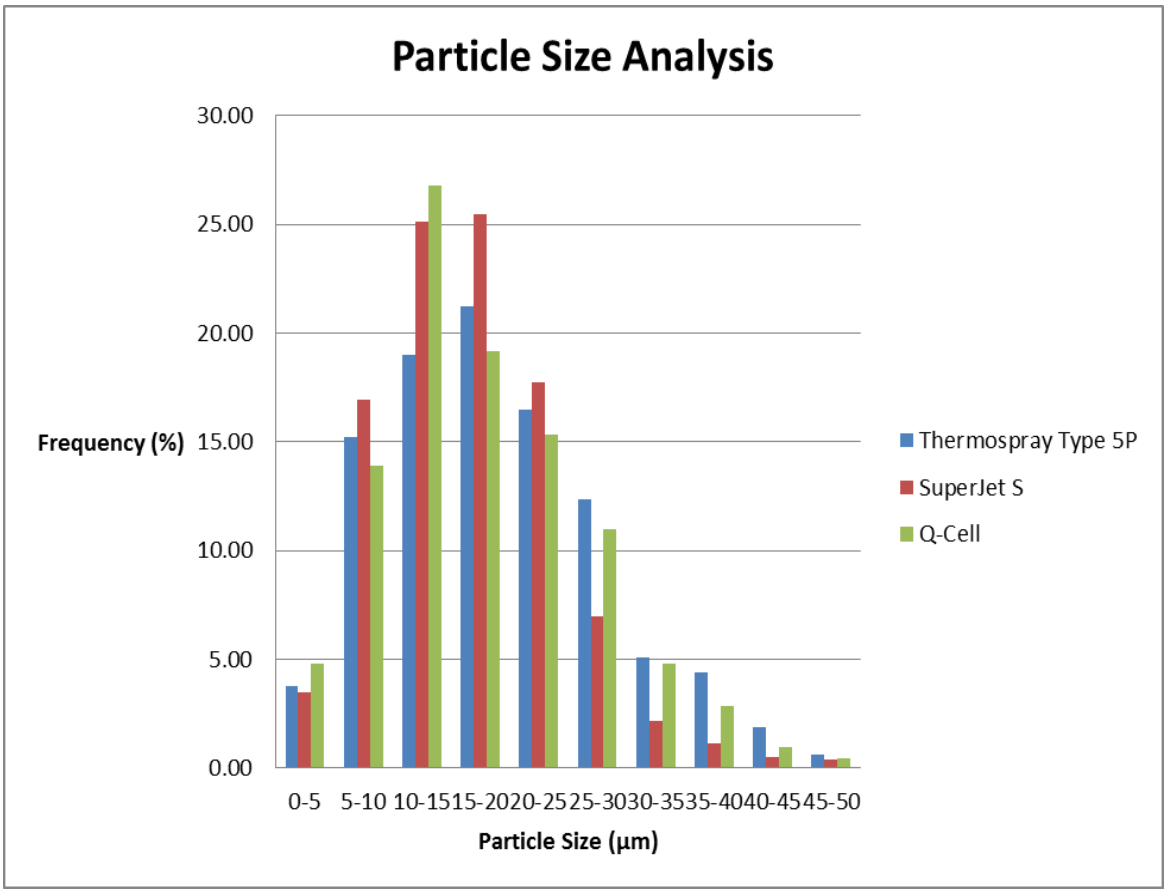

Figure 4-5: Particle size distribution of Bioglass 45S5 microspheres made from Thermospray and SuperJet flame guns and Q-cell microspheres.

Thermospray particles mostly fall in the 15-20 µm particle size bins at a frequency of 21.20%. Microspheres produced using the SuperJet S also frequently fall within the 15-20 µm range with a frequency of 25.49%. Q-cell microspheres are generally smaller with falling within the 10-15 µm range at a frequency of 26.79%.

4.3.4 Chemical Etching of Q-cells

Figure 4-6 shows SEM images of Q-cell microspheres which had undergone chemical etching treatment over 60 minutes. Comparing the three time point images, there appears to be no significant differences in microsphere surface texture over 60 minutes.

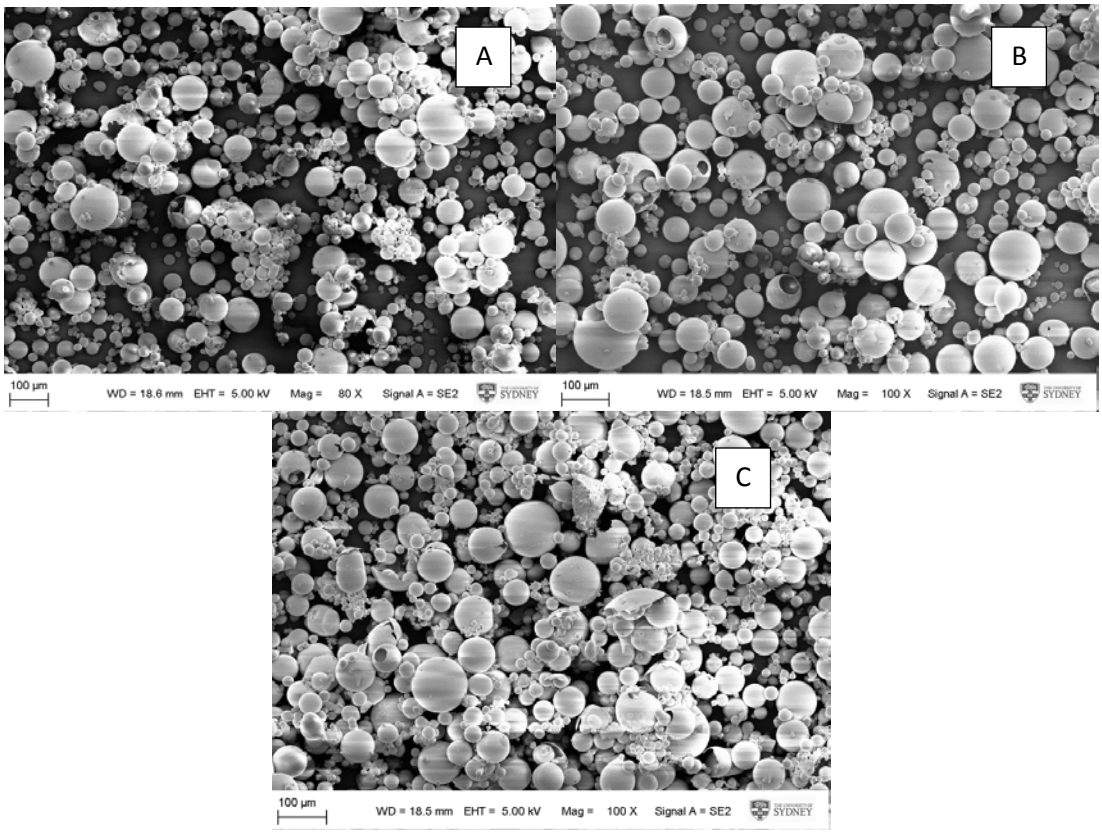

Figure 4-6: SEM images of chemical etched Q-cell microspheres at time points (A) 20 (B) 40 and (C) 60 minutes.

4.4 Discussion

Whole and hollow microspheres were produced using the flame spray process. There was no significant difference in microspheres using the Thermospray and SuperJet flame guns. During the production process, it was noted that collecting microspheres was much easier using the SuperJet gun as opposed to the Thermospray gun. The long narrow barrel and shorter flame length of the SuperJet gun reduced the splash of the water in the collection container. This ensured that microspheres were not being lost and reduced the likelihood and severity of the risks and hazards involved in the process. The use of cooling jets on the Thermospray gun significantly increased splash in the collection container. It was deemed too hazardous to continue using the cooling jets on the Thermospray gun.

Optical and SEM images confirm the presence of whole and hollow microspheres. Attempts to separate the two types of microspheres proved difficult. Initially, it was predicted that hollow microspheres would float in water while whole microspheres would sink. However,

the buoyancy of the hollow microspheres is insufficient for them to float. Having larger microspheres with larger internal diameters would most likely allow these hollow microspheres to float and be separated from whole microspheres.

Red dye encapsulation experiments produced very poor yields of red microspheres. The extremely low yield made it impossible to verify how the red dye was attached to the microsphere whether it is inside, throughout or on the surface of the microsphere. Thus, there is insufficient evidence to support that microsphere design iteration 3 is producible through the alteration of the flame-spray process.

Particle size distribution of the Bioglass 45S5 microspheres and Q-cells are similar. Bioglass 45S5 microspheres produced using both types of flame guns produced microspheres which frequently lies in the 15-20 μm range whilst Q-cells mostly fell in the 10-15 μm range. This result shows minor differences in particle size. This is important for microsphere attachment studies in the following chapter where the size of microspheres would affect the number of microspheres able to be attached to scaffolds and the amount of microsphere surface area that is bonded to the scaffolds.

Chemical etching of Q-cells did not show any observable surface roughening after 60 minutes. It is possible that there was some minor surface texture change on the surface of the Q-cell. However, this cannot be confirmed through the SEM images obtained. Chemical etching of Q-cells should be performed for over 24 hours for observable surface texture roughening. However, it should be noted that Bioglass 45S5 microspheres would react faster with alkaline solutions reducing the time required for chemical etching to have an observable effect on the surface texture.

5 Microsphere Attachment Studies

5.1 Introduction

Adherence of bioglass 45S5 microspheres to the scaffold is achieved through a thermal attachment process. PCL has a transition phase at 60°C where it becomes a transparent mouldable plastic with a sticky surface. By heating the surface of the scaffold until it becomes sticky, microspheres can be attached onto the scaffold surface. When the scaffold cools and hardens, the microspheres remain attached.

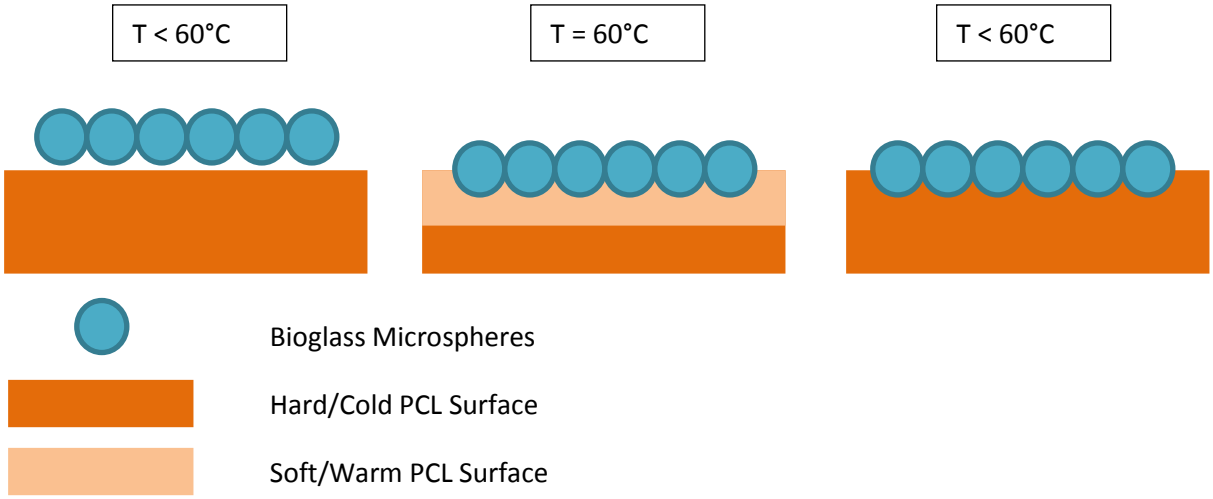

Figure 5-1: Diagram of microsphere attachment to scaffold. As the scaffold is heated to 60°C, the PCL surface begins to melt allowing microspheres to sink in. When the PCL cools and hardens, the microspheres become attached.

Briefly summarizing the relevant manufacturing protocol, bioglass 45S5 powder and scaffold are sealed in a package. The package is agitated to disperse the powder throughout the scaffold evenly. After agitation, the package is heated inside a preheated oven at 60°C for 20 minutes, during which the package is rotated to maximise bioglass 45S5 attachment. After heating, excess bioglass 45S5 powder is removed. The scaffold is agitated again to remove unattached powder.

The major issue encountered with this protocol is heat damage to the scaffold. Excessive heating of the scaffold will cause it to collapse on itself. The fine struts of the scaffold quickly heat up and melt if the temperature is maintained at 60°C for too long. Also, the oven

currently used is known to fluctuate in temperature although the precise magnitude of fluctuation is unknown.

For this chapter, research will be conducted to characterise the oven currently used and evaluate the protocol currently used for bioglass 45S5 attachment to the scaffold. Other powder attachment protocols will also be investigated and evaluated against the current protocol. From this research, the optimum powder-scaffold attachment protocol will be identified and utilised to attach microspheres to the scaffold.

5.2 Methodologies

5.2.1 Materials and Equipment

Scaffolds were produced at the Biomaterials laboratory in the University of Sydney using protocols described in previous research by Elizabeth Boughton [181]. Scaffolds were made from PCL with dimension of 15mm x 15mm x 10mm and porosity of 95%. Sodium borosilicate microspheres were sourced from Barnes (Q-cell 520, Barnes). Medical packaging used in experiments was sourced from Medipack AG. Oven characterization and thermo-attachment studies were conducted using a Pronto oven by Breville. Oven temperature was monitored using a digital thermometer (Thermocouple Thermometer, Digitech). Microsphere attachment studies were conducted using an Iaxsys™ kit (Iaxsys™, Biometic™) capable of actuating scaffolds within 6 well culture plates. Particle counting was conducted using a Leica DMRXE upright microscope and Leica Qwin Image Analysis Software. Scanning Electron Microscopy was carried out at the Australian Centre for Microscopy and Microanalysis (ACMM).

5.2.2 Oven Characterization Studies

Characterization studies of the Pronto oven were conducted using a digital thermometer. The oven was preheated to 60°C for 30 minutes to ensure that the oven is more temperature stable. A K-type thermocouple was sealed in medical packaging and placed in the oven. Temperature change was monitored over 10 minutes.

5.2.3 Thermo-attachment Studies

Thermo-attachment studies were carried out using plain scaffolds and scaffolds with Q-cells. Scaffolds were sealed in medical packaging with or without 1 gram of Q-cells. Packaged scaffolds were placed in the oven that had been pre-heated to 60°C for 30 minutes. Both plain scaffolds and Q-cell coated scaffolds were heated for 1, 2, 3, 4, 5 minutes whilst being rotated. Q-cell coated scaffolds were cleaned using an air jet to remove excess particles. SEM and camera images were taken of both types of scaffolds. Total number of microspheres within a scaffold was calculated by counting the number of microspheres in the SEM images, determining the microsphere per volume count and using that information to estimate the total number of microspheres. The dimensions of the scaffold are on average 15mm x 15mm x 8mm.

5.2.4 Microsphere Attachment Studies

Q-cell coated scaffolds were produced using a similar protocol mentioned in 5.2.3 Thermo-attachment Studies. Q-cell coated scaffolds were cleaned using one of two processes; air jet particle removal or rinsed in ethanol: water (50:50) solution three times. Scaffolds were then placed into a six-well culture plate containing 10mL of ethanol: water (50:50) solution before being loaded onto an Iaxsys™ kit. Iaxsys actuation settings were set at 10mm compression displacement at 1 Hz for 24 hours. After actuation, 1ml of solution from each well was collected. 0.1ml was transferred to a glass slide and the number of microspheres was counted under an optical microscope.

5.3 Results

5.3.1 Oven Characterisation Studies

Temperature fluctuations can have a detrimental effect on the structural integrity of the scaffold during thermo-attachment. Minimal temperature fluctuation is ideal for thermo-attachment of microspheres to the scaffolds leading to more reliable and repeatable production protocols. Large temperature fluctuations can lead to scaffold destruction or non-adhesion of microspheres to the scaffold.

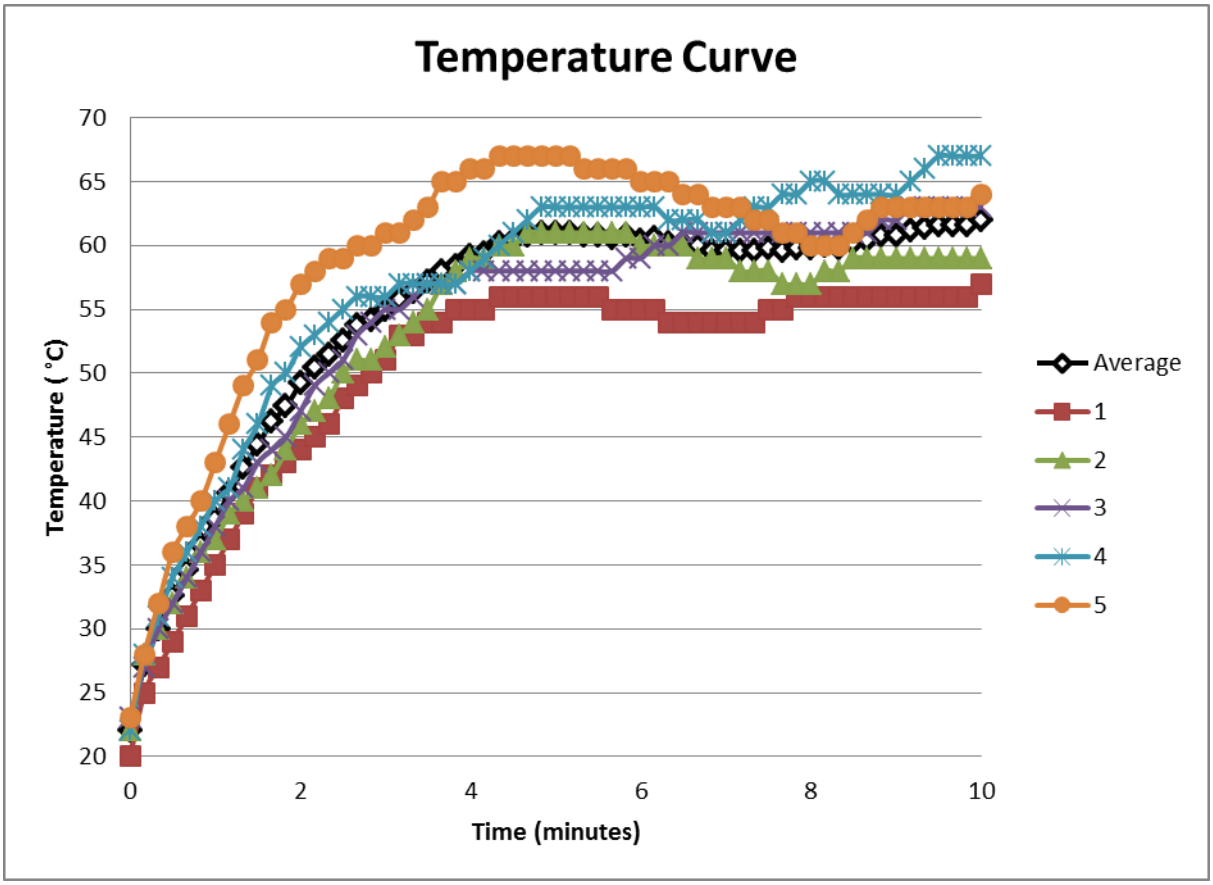

Figure 5-2: Oven temperature graph after preheating for 30 minutes at 60°C. Average temperature is seen in black. Other lines represent individual temperature studies.

Figure 5-2 shows the temperature change after inserting a thermocouple inside the oven. When the oven is opened to place the thermocouple inside, there is a large amount of heat lost as seen in the drop in temperature from 60°C to about 23°C at the zero time point. On average, the oven reaches 60°C after approximately 4 minutes of insertion. However, there is

a large amount of variation in the amount of time it takes for the oven to heat to 60°C and temperature fluctuations. The fastest time the oven reached 60°C was after 1 minute and 50 seconds. Maximum temperature recorded was 68°C and minimum temperature recorded after 4 minutes was 54°C.

5.3.2 Thermo-attachment studies

Maintaining structural integrity of the scaffold is paramount during thermo-attachment of microspheres. Significant reduction in porosity and volume of the scaffold would lead to diminished surface area for microsphere attachment and negatively impact the capacity to encourage vascularisation throughout the scaffold.

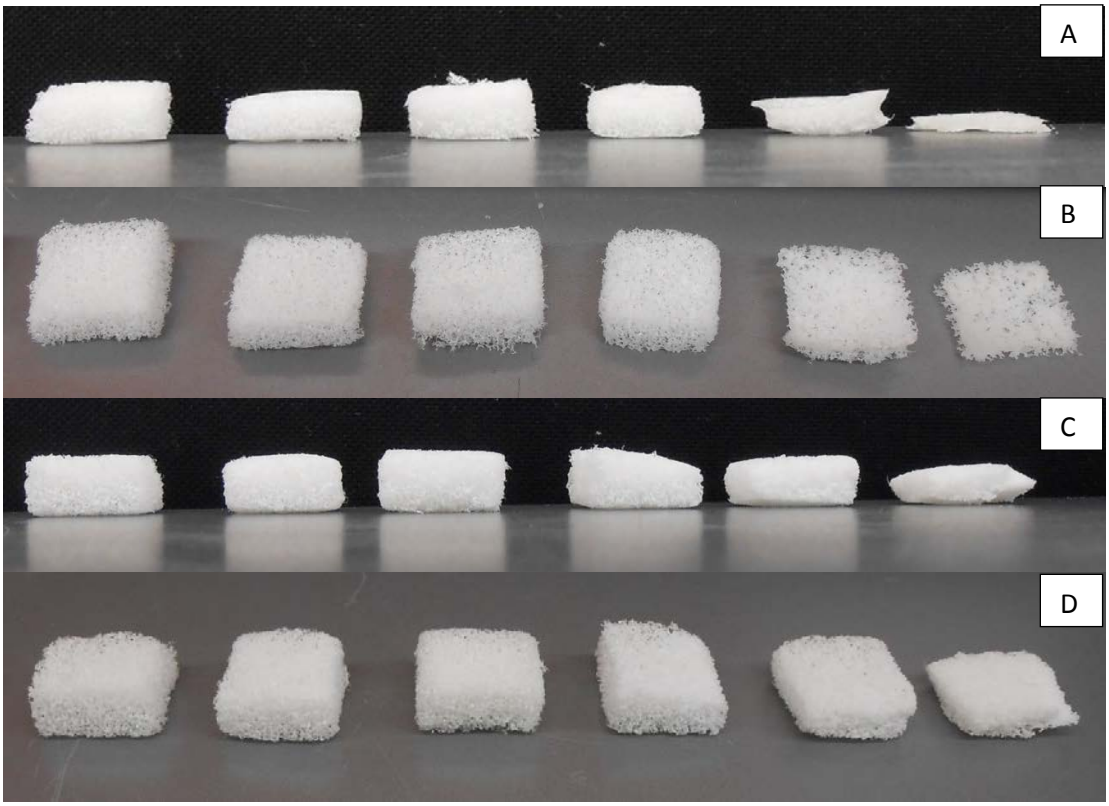

Figure 5-3: Scaffold temperature damage photographs. Images A and B shows plain scaffold temperature damage over 5 minutes and images C and D shows Q-cell coated scaffold thermal damage over 5 minutes. Time points from left to right are 0, 1,2,3,4 and 5 minutes.

Figure 5-3 shows the heat damage to plain scaffolds and Q-cell coated scaffolds over 5 minutes. Plain scaffolds are damaged significantly over 5 minutes as seen in images A and B. By 5 minutes, the height of the scaffold has decreased by approximately 80%. In addition,

the porosity of the plain scaffolds was severely compromised. In comparison, Q-cell coated scaffolds had less thermal damage. By 5 minutes, Q-cells coated scaffolds had a height reduction of approximately 50%. Porosity was not visibly affected.

Figure 5-4 shows SEM images of plain scaffolds with and without thermal damage. Image A shows the SEM of undamaged plain scaffolds where the scaffold has fine struts and high porosity. The struts in these images fall in the range of 20-200 µm. In contrast, image B shows a thermal damaged scaffold. The struts in this image are thicker than the struts in image A lying in the range of 50-600 µm. In addition, the scaffolds are less porous in image B than in image A.

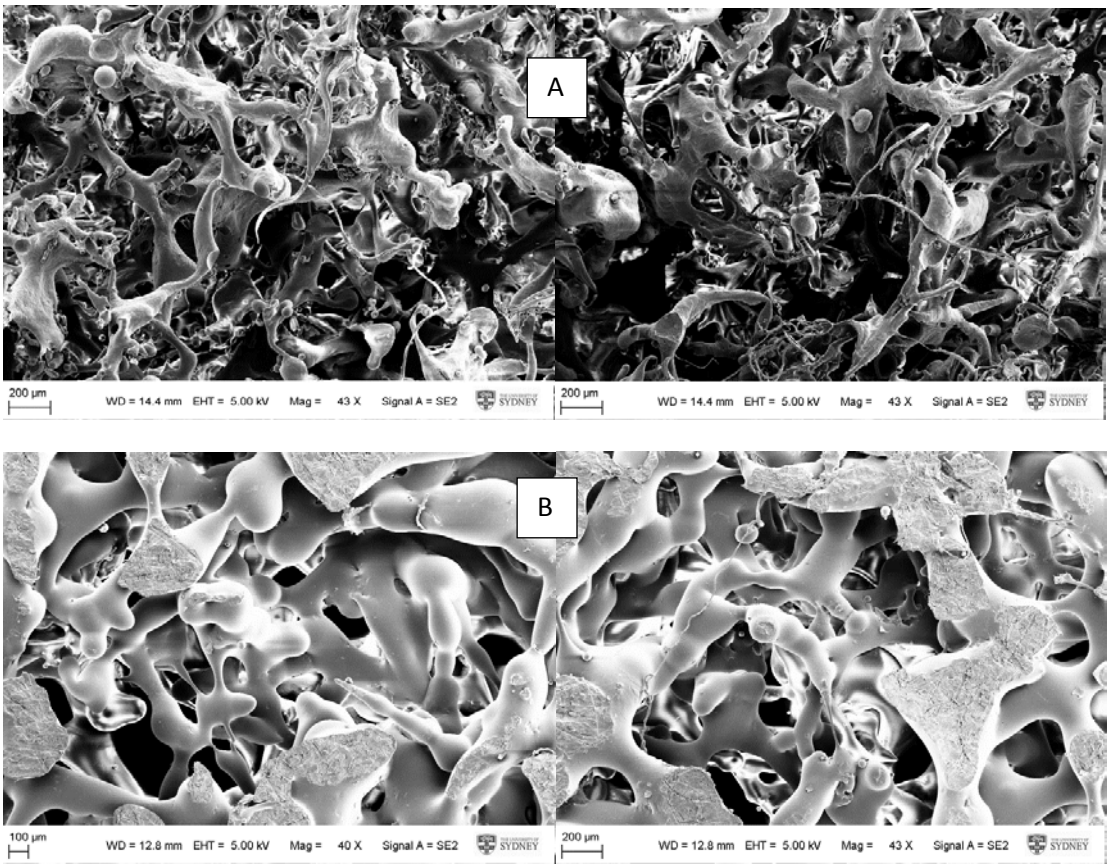

Figure 5-4: SEM images of (A) plain scaffold and (B) heat damaged plain scaffold after 5 minutes

Figure 5-5 shows SEM images of microsphere attachment studies. Image A shows a scaffold with a confluent coating of Q-cells after being heated for 5 minutes. The scaffold is still porous although the extent at which porosity has been compromised is unknown. Image B

shows a scaffold that has been heated for 4 minutes with moderate coating of microspheres. The scaffold surface also contains deformations where microspheres have fallen off during the cleaning process. Image C shows a scaffold that had been heated for 3 minutes. There are a few microspheres attached to the scaffold. In addition, there are no obvious deformations on the scaffold surface to suggest that the scaffold was sufficiently heated to create an adhesive surface for microspheres to attach to. Porosity of this scaffold appears to be unchanged.

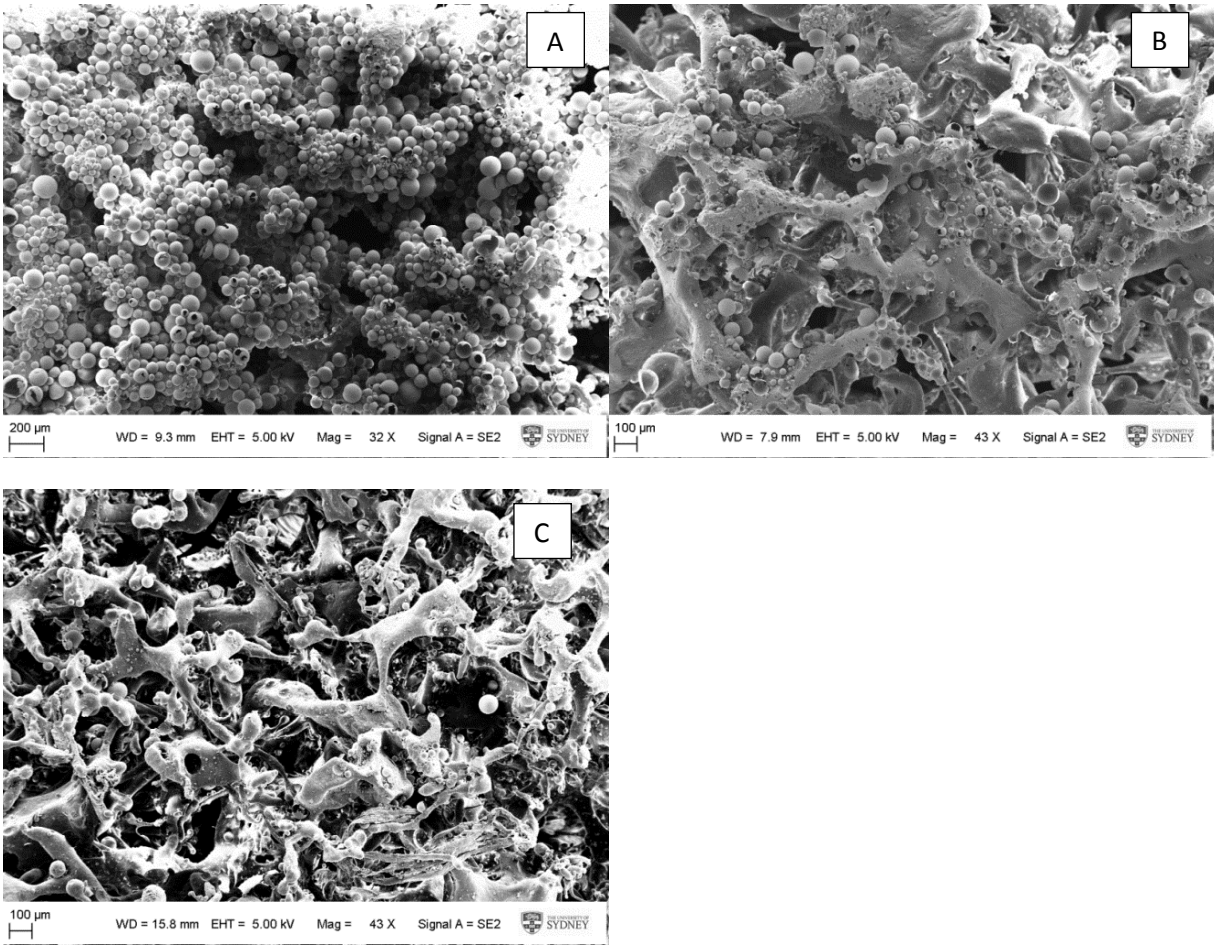

Figure 5-5: Microsphere attachment studies. Scaffolds were heated with Q-cells for (A) 5 minutes, (B) 4 minutes and (C) 3 minutes.

Table 5-1 calculates the total number of microspheres in each scaffold based on the number of microspheres seen in each image and for a standard scaffold with dimensions 15mm x 15mm x 8mm. Estimated total number of microsphere attached to scaffolds differed by orders of magnitude between each heating protocol. The scaffold in SEM image A has an

estimated 1.45 x 10^9 microspheres, SEM image B has an estimated 3.09 x 10^8 microspheres and SEM image C has an estimated 3.66 x 10^7 microspheres.

Table 5-1: Microsphere counts per scaffold based on SEM images as seen in Figure 5-5.

SEM Image Scaffold	Total MS count in SEM image	Field Area (μm^2)	MS count per cm^3 (assuming depth is 200µm)	Estimated number of MS in scaffold (Volume of scaffold = 1912.5cm^3)
A	1030	6.776 x 10^6	7.6 x 10^5	1.45 x 10^9
B	135	4.18 x 10^6	1.61 x 10^5	3.09 x 10^8
C	16	4.18 x 10^6	1.91 x 10^4	3.66 x 10^7

Table 5-2 shows the particle counts for Q-cell coated scaffolds that had been cleaned using an air jet or washed in 50:50 ethanol: water solution and actuated over 24 hours in an Iaxsys kit. An average, Q-cell coated scaffolds cleaned using the air jet had fewer particles released compared to Q-cell coated scaffolds cleaned with ethanol: water solution. On average, air jet cleaned scaffolds released approximately 15,333 microspheres or (1.06 x 10^{-3}) % of total microspheres attached to the scaffold. Scaffold washed with ethanol: water solution released 40,667 microspheres or 2.80 x 10^{-3} % of total attached microspheres.

Table 5-2: Particle count for microsphere attachment study

Scaffold Cleaning method	Total Image Count	Count/mL	Total MS released	% MS released
Air jet 1	230.00	2,300.00	23,000.00	1.59E-03
Air jet 2	100.00	1,000.00	10,000.00	6.90E-04
Air jet 3	130.00	1,300.00	13,000.00	8.97E-04
AIR JET AVERAGE	153.33	1,533.33	15,333.33	1.06E-03
Washed 1	760.00	7,600.00	76,000.00	5.24E-03
Washed 2	160.00	1,600.00	16,000.00	1.10E-03
Washed 3	300.00	3,000.00	30,000.00	2.07E-03
WASHED AVERAGE	406.67	4,066.67	40,666.67	2.80E-03

5.4 Discussion

In this chapter, studies were carried out to determine the optimal method of attaching microspheres to scaffolds.

Results from the oven temperature experiments seen in Figure 5-2 show that some fluctuation in temperature. Temperature fluctuation ranges from 54-67°C. There were also significant differences in the time it took the oven to reach 60°C. Minimum time taken to reach 60°C was 2m 40s. There was a potential to significantly damage and deform the scaffold. Images in Figure 5-3 and Figure 5-4 show how excessive heating can damage plain scaffolds reducing height and porosity, and increasing the thicknesses of struts. The reduction in scaffold volume is not ideal in treating large and deep chronic wounds. In addition, the reduction in scaffold porosity could interfere with the vascularisation of the scaffold.

On the contrary, scaffolds that had been coated with microspheres appeared to be less damaged by excessive heating as seen in Figure 5-3 and Figure 5-5. In order to achieve a confluent coating of microspheres onto the scaffold surface, scaffolds should ideally be heated for 5 minutes. From Table 5-1, the maximum number of microspheres which can be attached to a standard size scaffold (15mm x 15mm x 8mm) is 1.45×10^9. To be able to attach the maximum amount of microspheres whilst minimising scaffold damage is of great benefit. Not only does it reduce heat damage to the scaffold, it also increases the potential drug loading capacity of the scaffold.

Table 5-2 shows the number of microspheres which are lost after the scaffold is actuated for 24 hours with a 10mm compression, and after cleaning using an air jet or ethanol: water solution. Scaffolds cleaning using an air jet released the lowest amount at 15,333 microspheres or 1.06×10^{-3}% of total microspheres attached while scaffolds washed with ethanol: water solution released 40,667 microspheres or 2.8×10^{-3}%. It is hypothesized that less microspheres were released from air jet cleaned scaffolds due to the high shear forces which dislodged weakly bonded microsphere. Minimal microsphere loss is beneficial to maintain localised drug delivery.

Ideal microsphere attachment to scaffolds can be achieved by saturating the scaffold with microspheres, heating the scaffold at 60°C for 5 minutes and removing excess microspheres using an air jet. Microspheres attached using these methods are firmly secured with minimal microsphere loss during cyclical loading.

6 Drug Release Studies

6.1 Introduction

This chapter will investigate the potential of scaffolds and ceramic glass microspheres as delivery vectors for drugs, primarily antibiotics. Experiments in this chapter aim to verify the capability of the two part device to deliver antibiotics and to maintain a sustained drug delivery.

One of the key aspects investigated in this chapter is drug loading efficiency. Drug loading efficiency refers to the percentage of drug mass per unit mass of delivery vector, typically expressed as %w/w. This is different to entrapment efficiency which compares the mass of drug loaded to the total mass of drug available for loading. There are a number of methods which can be used to determine the amount of drug loaded onto delivery vectors. The most common method used is measuring the total amount of drug released using various detection methods. A key limitation of this method is that total amount of drug released is not necessarily similar to the total amount of drug loaded. When using this method, it is important to understand how the drug in entrapped on the delivery vector and the release kinetics most likely associated with the vector. For this chapter, where antibiotics are primarily attached to the immediate surface of the vectors, it is reasonable to deduce that the difference between total drug released and total drug loaded is negligible as there is no other type of bonding between the antibiotic and the delivery vector which would significantly affect the differences.

Another key aspect investigated in this chapter is the drug elution profile. A logarithmic elution profile is expected due to the non-complex method of antibiotic loading. Features of the elution profile which will be analyzed are the rate of release and time length of the burst phase and sustained phase, and total amount of antibiotic released which will be defined at maximum value recorded where neighboring time point values are less than 5% different. These features are important as they affect the capabilities of the device to act as a long-term antimicrobial skin scaffold.

In addition, the concentration of antibiotic released will be calibrated to reflect unit mass of delivery vector used. From this unit of measurement, sample iterations can be compared to reflect drug loading efficiency.

6.2 Methodology

6.2.1 Materials and Equipment

Chloramphenicol antibiotic powder, pure ethanol and potassium hydroxide were sourced from Sigma Aldrich. Chloramphenicol was used as the analogue drug to be loaded onto delivery vectors although any drug would have sufficed. Scaffolds were produced in the Biomaterials laboratory in the University of Sydney according to protocols designed by Elizabeth Boughton to the dimension of 1.5mm x 5mm x 10mm with 95% porosity [181]. Q-cells were sourced from Barnes. Equipment used in the following experiments includes a vibroslicer (752M Vibroslice, Campden Instruments) and a UV-visible spectrophotometer (UV-1601, Shimadzu).

6.2.2 Chloramphenicol Antibiotic Stock Solution

A stock solution of chloramphenicol was produced at a concentration of 100mg/ml. 1g of chloramphenicol powder was dissolved in 10ml of pure ethanol and mixed thoroughly to ensure complete dissolution. Further concentrations of chloramphenicol solutions used in this chapter were produced through dilution of the stock solution in pure ethanol. All solutions of chloramphenicol were stored at 4°C when not in use.

6.2.3 Chloramphenicol Loading onto Vectors

Two methods were used to load chloramphenicol onto the delivery vectors; soaking and infusion. The primary method to be tested is soaking the delivery vector in antibiotic solution. The method of infusing the antibiotic is also experimented as this method is most commonly used in literature.

6.2.3.1 Soaking

Scaffolds (1.5mm x 5mm x 10mm), Q-cell microspheres and chemically etched Q-cell microspheres where soaked in a 10mg/ml chloramphenicol solution for 24 hours. After the

soaking period, scaffolds were removed and air dried on an absorbent cloth in a chemical fume hood. Once dried, the mass of the scaffolds was measured and compared with the pre-loading mass. Microspheres were separated from remaining chloramphenicol solution and attached to unloaded scaffolds using thermal adhesion. Mass before and after loading were recorded and compared.

6.2.3.2 Infusion

Scaffolds were infused with chloramphenicol by adding chloramphenicol powder to the manufacturing process. Briefly summarizing, chloramphenicol powder was added to the polymer solution to a concentration of 10mg/ml. The scaffolds were processed per standard manufacturing protocols. Scaffolds were cut into 1.5mm x 5mm x 10mm slices using a vibroslicer. Mass measurements of scaffolds were taken after loading.

6.2.4 Absorbance Spectrum

The absorbance spectrum of chloramphenicol was determined using the Absorbance program on the spectrophotometer. Briefly summarizing, the program measures the absorbance of the test solution over a range of wavelengths and returns a graph as seen in Figure 6-1. A 50µg/ml solution of chloramphenicol in distilled water was prepared and transferred into a quartz cuvette. The cuvette containing the chloramphenicol solution was placed in the spectrophotometer and analyzed using the Absorbance program. From the graph, an ideal wavelength can be determined for which absorbance spectrum analysis with chloramphenicol solution will be used.

6.2.5 Calibration

Using the best absorbance wavelength determined in 6.2.4 Absorbance Spectrum, a calibration curve can be produced at that wavelength. Chloramphenicol solutions of 100µg/ml, 50µg/ml, 25µg/ml, 12.5µg/ml and 6.25µg/ml were analyzed and their respective absorbance recorded. A graph of absorbance against concentration and trend line through (0, 0) was plotted. From the calibration curve, the absorbance coefficient can be determined using the equation;

$$A = \varepsilon c l$$

Where A is the absorbance, ε is the absorbance coefficient, c is the concentration of the sample and l is the length of cuvette set at 1cm.

6.2.6 Drug Release

The sample iterations used in drug release studies were scaffolds soaked in chloramphenicol solution (positive control), plain scaffolds (negative control), scaffolds with intact microspheres loaded with CAP, scaffolds with chemically etched microspheres loaded with chloramphenicol and scaffolds infused with CAP. Triplicates of each sample iteration were produced to provide a method for measuring reliability through calculation of the standard deviation.

Each sample was placed in 5ml of PBS solution. Before each sampling time point, all the samples and solutions were shaken manually to ensure even distribution of solution and restore any chloramphenicol molecules electrostatically bound to the vial walls to solution. At time points 0, 10 min, 30 min, 1 hour, 2 hours, 3 hours, 4 hours, 24 hours, 3 days and 7 days, 200µl of sample fluid was transferred into 800µl of PBS diluting the original sample by a factor of 5. The absorbance of each diluted sample solution was measured and recorded. Results were calibrated taking into account the dilution factor, amount of antibiotic removed during each sampling and the mass of the delivery vector.

6.3 Results

6.3.1 Absorbance Spectrum

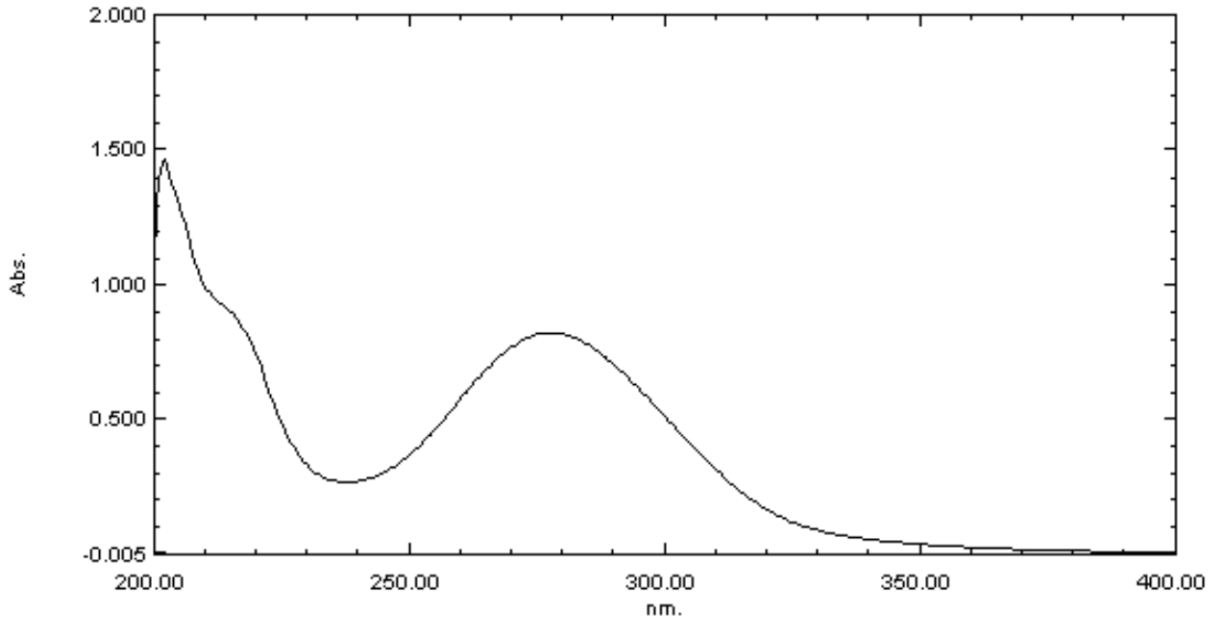

Figure 6-1: Absorbance spectrum of chloramphenicol from 200nm to 400nm wavelengths.

Figure 6-1 shows the absorbance spectrum of chloramphenicol from 200 to 400nm. There are two peaks within this range, one at approximately 205nm and another at 278nm. Whilst the peak at 205nm records a stronger absorbance than the peak at 278nm, it lies on the extremity of the spectrophotometer capabilities thus potentially causing errors. The peak at 278nm records a sufficiently strong absorbance close to 1 and is well defined locally. Further experiments were conducted using an absorbance wavelength of 280nm which corresponds to wavelengths other researchers have used to detect chloramphenicol [190, 191].

6.3.2 Calibration

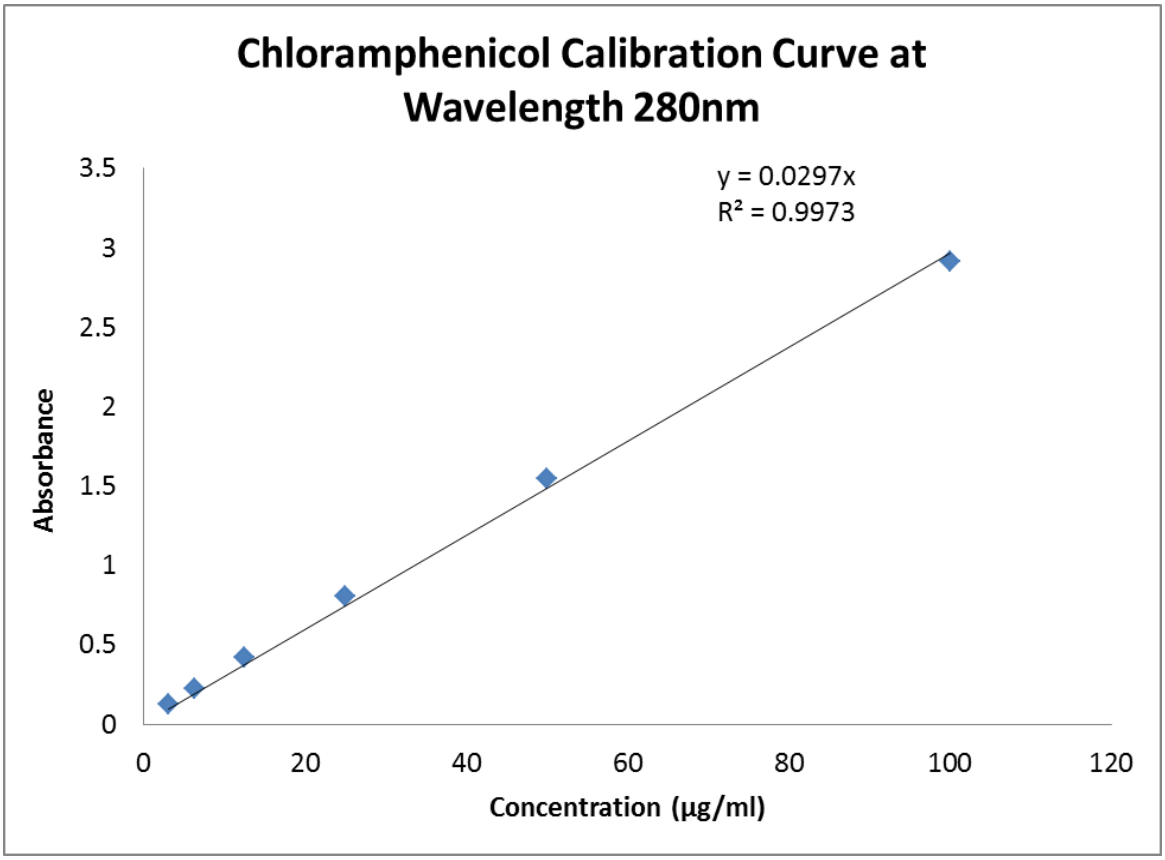

Figure 6-2: Calibration curve of chloramphenicol at 280nm.

The calibration curve shown in Figure 6-2 shows a strong direct linear relationship between absorbance and concentration of chloramphenicol at 280nm. The trend line has a strong correlation coefficient with an R^2 value of 0.9973. From the trend line equation, we can determine that the absorbance coefficient ε is 0.0297. The equation relating absorbance to concentration is as follows;

Equation 2: Absorbance equation

$$Absorbance = 0.0297 \times Concentation\ (\frac{\mu g}{ml})$$

6.3.3 Drug Release

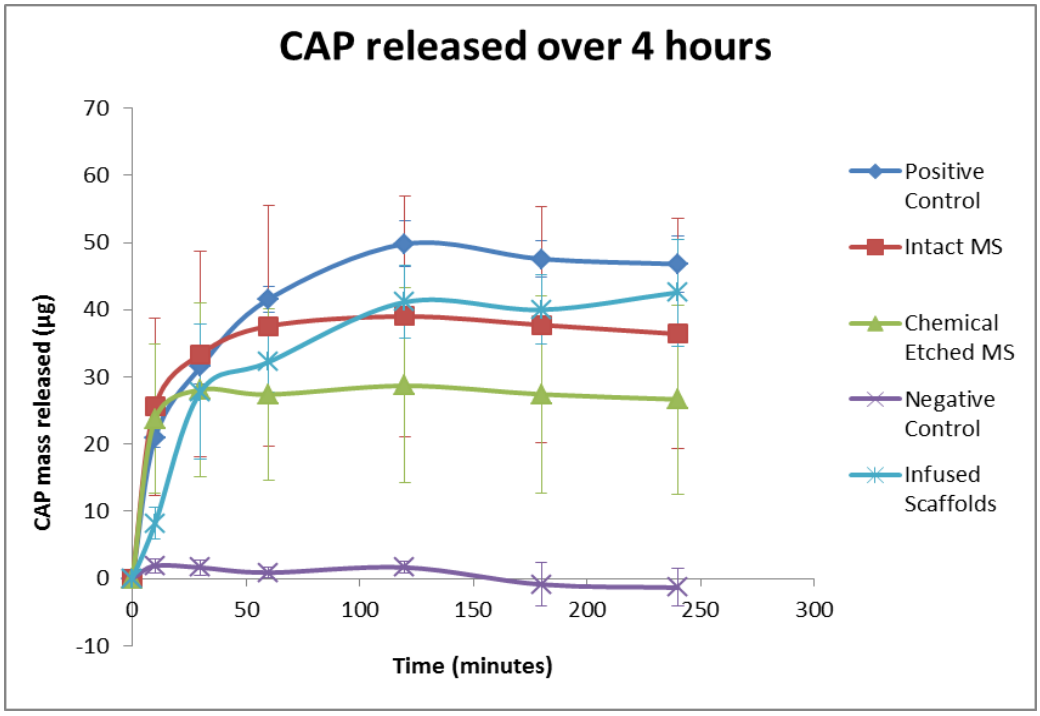

Figure 6-3: Mass of chloramphenicol released in µg over 4 hours.

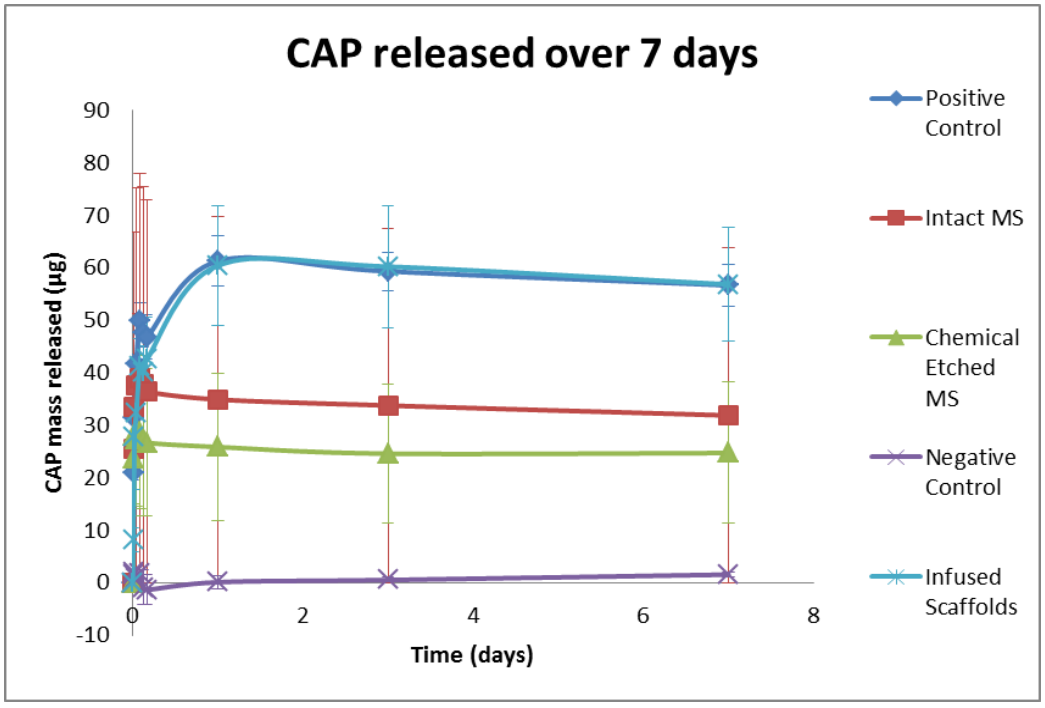

Figure 6-4: Mass of chloramphenicol released in µg over 7 days

Figure 6-3 and Figure 6-4 show the mass of chloramphenicol released over 4 hours and 7 days respectively. Figure 6-3 shows that over a period of 4 hours, the positive control had the largest amount of chloramphenicol released at 49.8 μg. This was followed by infused scaffolds (42.6 μg), intact microspheres (39.0 μg), chemically etched microspheres (28.7 μg) and negative control scaffolds (1.9 μg). The burst phase appears to be over by 2 hours for the positive control and intact microspheres. The burst phase of chemically etched microspheres lasts for 1 hour before the rate of release slows significantly. The burst phase for infused scaffolds does not appear to be over by 4 hours according to Figure 6-3.

Figure 6-4 shows that the burst phase for the positive control and infused scaffolds lasts slightly longer than a day. For each of the scaffold iterations, there is no noticeable increase in chloramphenicol release during the sustained phase. The maximum release recorded belonged to positive control scaffolds with 61.3 μg. This was closely followed by infused scaffolds with a maximum recorded release of 60.4 μg. Intact microspheres had a maximum release of 39.2 μg and chemical etched microspheres had a maximum release of 28.7 μg. Negative control scaffolds showed minor fluctuations in absorbance values averaging close to zero for both figures.

Both graphs show relatively large standard deviations for all sample iterations with exception to negative control scaffolds. The highest standard deviation recorded was 17.9 for intact microspheres at the 2 hour time point. Other maximum standard deviation values recorded include 4.7 for positive control scaffolds, 14.7 for chemical etched microspheres, 11.6 for infused scaffolds and 2.8 for negative control scaffolds.

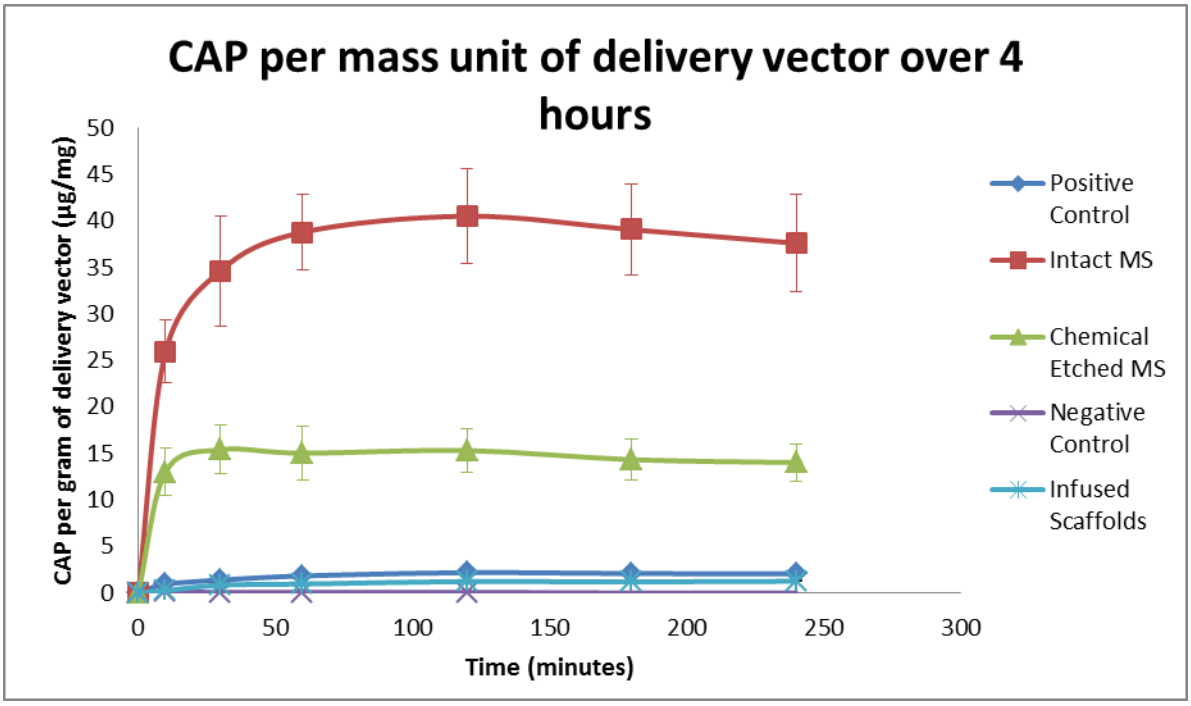

Figure 6-5: Release profile over 4 hours. Burst phase is typically over by 2 hours. Data calibrated to express chloramphenicol concentration release per milligram of delivery vector.

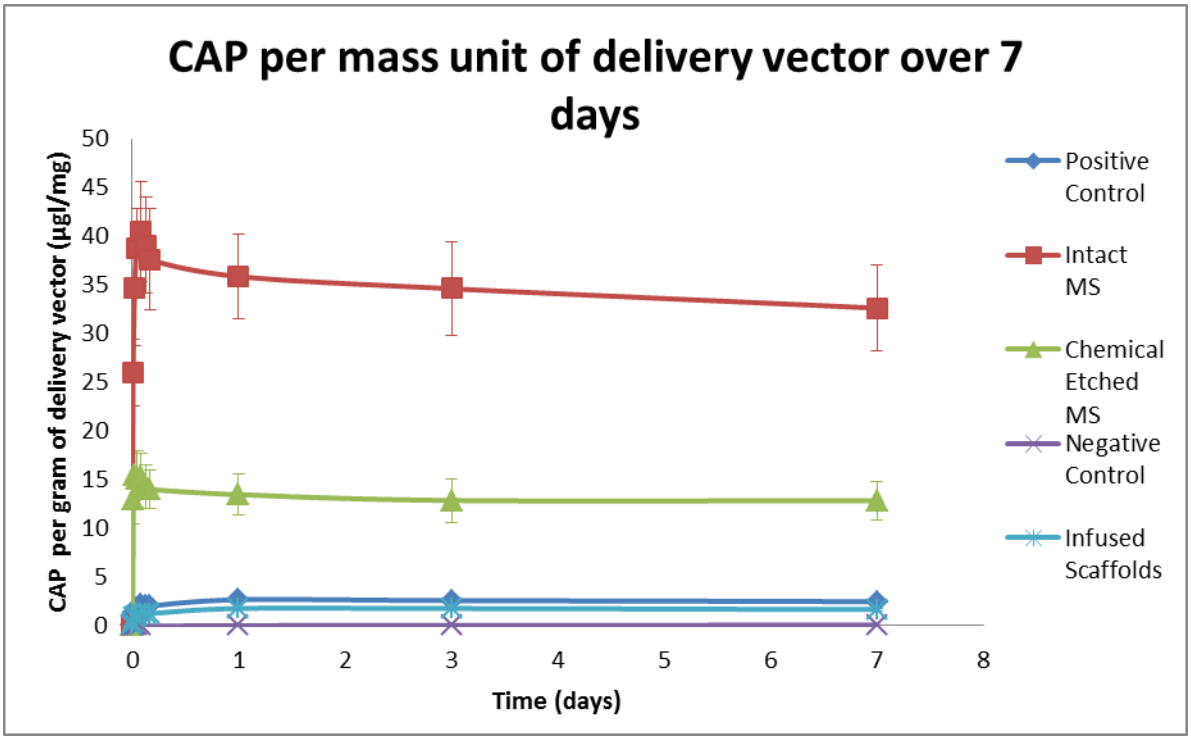

Figure 6-6: Release profile over 7 days. . Data calibrated to express chloramphenicol concentration release per milligram of delivery vector.

Figure 6-5 and Figure 6-6 show the same results as Figure 6-3 and Figure 6-4 but calibrated to show the mass of chloramphenicol released per milligram of delivery vector (μg/mg). Intact microspheres contained the largest amount of chloramphenicol per gram of delivery vector followed by chemically etched microspheres, positive control scaffolds, infused scaffolds and negative control scaffolds. Maximum release per gram of delivery vector for intact microspheres was 40.5 μg/mg followed by chemically etched microspheres (15.4 μg/mg), positive control scaffolds (2.7 μg/mg), infused scaffolds (1.8 μg/mg) and negative control scaffolds (0.07 μg/mg). Burst phase and sustained phase time points remain the same.

Standard deviations are much lower compared to standard deviations in Figure 6-3 and Figure 6-4. Maximum standard deviations for intact microspheres were 5.9 followed by chemically etched microspheres (2.9), infused scaffolds (1.76), positive control scaffolds (0.18) and negative control scaffolds (0.07).

6.4 Discussion

As mentioned in section 6.1 Introduction, drug loading efficiency is one of the key criteria's in assessing viabilities of various drug delivery vectors. Whist direct measurement of drug loading efficiencies was not possible; the efficiency of each delivery vector can be extrapolated from total drug release per unit mass of delivery vector within reasonable values.

Per unit mass of delivery vector, intact microspheres had the highest loading efficiency of the delivery vectors tested. This is expected as there is a high surface area to volume of spheres compared to other 3D structures. This allows for more antibiotics to bind to the microspheres by weak electrostatic bonds. Microspheres which were chemically etched had the second highest drug loading efficiency.

Chemically etched microspheres had a much lower drug loading efficiency compared to intact microspheres. At maximum values, chemically etched microspheres had a 62% lower loading efficiency than intact microspheres. While chemically etched surfaces should ideally have a higher available surface area, results from section 4.3.4

Chemical Etching of Q-cells showed that there was little to no observable change in surface texture. In addition, residual alkaline products may have interacted with antibiotic molecules causing them to degrade even after extensive washing.

Positive control scaffolds and infused scaffolds had the lowest drug loading efficiencies at 2.7 µg/mg and 1.8 µg/mg respectively. Positive control scaffolds would have a higher loading efficiency due to antibiotic molecules binding to the surface of the scaffold. In contrast, while infused scaffolds had antibiotic loaded into the polymer, most of the antibiotic loaded near the surface of the scaffold was removed during the scaffold processing.

Whilst microsphere-centered designs have better drug loading efficiencies, it should be noted that total antibiotic released from scaffolds coated in microspheres are much lower when compared to scaffolds loaded with antibiotics as seen in Figure 6-3 and Figure 6-4. Positive control scaffolds and infused scaffolds had a maximum drug release of 61.3 µg and 60.4 µg respectively. Intact and chemically etched microspheres had a lower maximum drug release of 39.2 µg and 28.7 µg respectively. Microsphere-centred designs had lower maximum drug release as there was much less microspheres attached to the scaffold when compared to antibiotic-loaded scaffolds in terms of mass. In addition, antibiotic-loaded scaffolds had a longer antibiotic burst phase of 1 day compared to microsphere-coated scaffolds which had a burst phase lasting 1 hour or less. A prolonged release of antibiotics is desired to maintain antimicrobial effects.

There is a significant deviation in the release of chloramphenicol for all the delivery vector iterations. The high standard deviations would most likely be issues in manufacturing regarding the reproducibility and reliability of the product. The cause for the high standard deviations in total drug released is most likely due to the non-conformity of the scaffold porosity and subsequently surface area. This would greatly affect the amount of drug and microspheres that can be loaded onto the scaffold. Further repetition of the experiment may yield more concise loading efficiency data which could be extrapolated to estimate the total drug loading.

7 General Discussion

In section 3.4 Experimental Philosophy, Table 3-7 outlined the relevant experiments that would be carried out and the relevant user requirements and design risks associated with each experiment. Table 7-1 shows the completed version with pass/fail/incomplete results filled in.

Table 7-1: Completed experiment table

#	Experiments	Relevant UINs	Pass/Fail/ Incomplete
	Chapter 4 - Production and Characterisation of Microspheres		
4.1	Production of Bioglass 45S5 microspheres	UR3,UR4, UR9, RA4	Pass
4.1a	➢ Whole		Pass
4.1b	➢ Hollow		Pass
4.1c	➢ Porous		Incomplete
4.2	Able to load antibiotics within hollow microspheres	UR3, UR4	Fail
4.3	Standardize particle size	UR3, UR9	Pass
	Chapter 5 - Microsphere Attachment Studies		
5.1	Able to attach microspheres to scaffold	UR2, UR3, RA5	Pass
5.2	Maintain scaffold integrity during attachment process	UR7, RA5, RA6	Pass
5.3	Maintain scaffold integrity during cyclic loading test	UR7, RA9	Pass
	Chapter 6 - Drug Release Studies		
6.1	Able to load antibiotics onto microspheres	UR3, RA7, RA8	Pass
	➢ Able to load antibiotic-loaded microspheres onto scaffolds		Pass
6.2	Release of antibiotic from device	UR4, RA8	Pass
6.2a	➢ 1 day		Fail
6.2b	➢ 1 week		Fail
6.3	Reliable release of antibiotics from device	UR3, UR4	Fail

Chapter 4 investigated the production of whole, hollow and porous microspheres using flame spraying and chemical etching techniques, the potential to load antibiotics inside a hermetic sealed hollowed microsphere and the particle size distribution of microspheres produced. Whole and hollow microspheres were produced in the same batch using a flame spray technique. These microspheres mostly fell within the 15-20 µm size. Production time for the flame spray technique did not exceed one hour including set-up time. Attempts were made to separate the whole and hollow microspheres using buoyancy differences but were unsuccessful due to the negligible differences.

Attempts at creating a hollow microsphere filled with fluid were not successful. Red dye, which was used as an analogue for antibiotic solutions, was detected in very minute amounts often on irregularly shaped particles. While it may be impossible to load antibiotic solutions inside hermetically sealed microspheres using flame spray techniques, the production of hollow microspheres allow for alternative drug loading avenues to be considered.

Creation of porous microspheres was conducted on sodium borosilicate microspheres instead of bioglass 45S5 microspheres due to supply constraints of bioglass 45S5. Over a one hour period, no observable etching of the microsphere surface was found on SEM imaging. It should be noted that Bioglass 45S5 would react faster to alkaline solutions reducing the time required for chemical etching to have an observable effect on surface texture [192].

Whilst outcomes 4.1c and 4.2 were not achieved, all other outcomes set for the chapter passed. The outcomes which were not achieved do not prevent the development of a two part synthetic skin scaffold with antimicrobial properties.

Experiments conducted in chapter 5 investigated the attachment of microspheres to scaffolds whilst maintaining scaffold integrity. In addition, the mechanical stability of the device was tested under a cyclic loading test with parameters of 50% compression, 1 Hz cycle for 24 hours.

Microspheres were able to be attached to the scaffold with minimal damage. Scaffolds were heated together with microspheres at 60° for 5 minutes whilst being constantly rotated to

maximize microsphere attachment. This protocol takes advantage of the low glass transition phase of PCL and the structural support confluent coatings of microspheres which prevent complete scaffold collapse. Using this protocol, approximately 1.45×10^{9} microspheres were attached to the scaffold. During cyclic loading tests, 15,333 microspheres or 1.06×10^{-3}% of microspheres were displaced from the scaffold.

These results satisfy the user requirements and design risks linked to the experiments. Results from this chapter validate the capability for two separate products to be successfully combined to act as a single device.

Loading of antibiotics and their subsequent release form microspheres attached to scaffolds were explored in Chapter 6. Chloramphenicol antibiotic was successfully loaded onto microspheres. Microspheres coated scaffolds had a higher drug loading efficiency compared to scaffolds infused with chloramphenicol. However, total chloramphenicol release was higher for infused scaffolds compared to microsphere coated scaffolds. This is due to the greater volume and surface area of the scaffold compared to microspheres. Burst phase of microsphere coated scaffolds lasted for 1 hour compared to infused scaffolds which lasted 1 day.

Overall, while the device was able to load and release antibiotics, more design modifications may be required to create a sustained antimicrobial device. Nevertheless, the device can be used as a wound healing device with local delivery of antibiotics directly to the infection site.

8 Conclusions

The core aim of this thesis was the development of a two-part synthetic skin scaffold consisting of bioactive glass microspheres and a biocompatible biodegradable 3D porous scaffold. The thesis looked at three parts of the development; production of hollow Bioglass 45S5 microspheres, attachment of microspheres to 3D porous scaffolds using non-destructive methods and loading and release of drugs such as antibiotics from the device. Main finidings of this thesis are summarized below.

- Bioglass 45S5 microspheres can be produced from Bioglass 45S5 powder using a flame spray technique. Microspheres produced this way were whole or hollow.
- Liquid solutions were unable to be loaded inside hermetically sealed microspheres during the flame spray process.
- Resultant microspheres were mostly 10-15 μm in size which is ideal for attachment to scaffolds.
- Microspheres could be attached to PCL scaffolds using a thermal attachment process.
- Scaffold integrity was not compromised during microsphere attachment.
- Minimal loss of microspheres occurred during cyclic mechanical actuation.
- Antibiotics could be loaded onto the surface of microspheres.
- Subsequent release of antibiotics from microsphere coated scaffolds lasted for 1 hour.
- Release of antibiotics from scaffolds infused with antibiotic lasted for 1 day.
- There was a wide variation in total antibiotic release due to variables in microspheres attached and surface area of scaffolds.
- A two part chronic skin wound healing device with antimicrobial activity could be constructed from polyester scaffolds and bioactive glass microspheres. Antibiotics could be delivered locally to the wound site using this device.

9 Future Recommendations

This thesis was able to develop hollow Bioglass 45S5 microspheres, thermoattach microspheres to a 3D porous scaffold and load and deliver antibiotics from the two part device. Further areas for future investigations are listed below.

- Modifications to hollow microspheres to include a hollow porous design to increase surface area and bonding sites for antibiotics. Continuing on, these modified microspheres could be coated in a biocompatible polymer to help delay and create a sustained antibiotic release. This could form the basis of a follow-up Masters or PhD project.

- There is a potential for antibiotic loaded microspheres to be used in conjunction with biological skin grafts provided that there is sufficient penetration of the microsphere within the graft to provide an antimicrobial environment through the graft. This would require a method of inserting microspheres evenly through a graft. Burst and sustained release of antibiotics would be a major requirement. If successful, other drugs or biologically active proteins could be loaded to encourage vascularization throughout the graft.

- Microbiological and animal studies should be carried out once a solution has been created for sustained antimicrobial activity. Microbiological tests should be carried out against a range of microorganisms such as *staphylococcus aureus, pseudomonas aeruginosa* and other bacterial and fungal strains.

10 References

1. Ousey K, McIntosh C (2008) Physiology of Wound Healing. Low Extrem Wounds 25–46. doi: 10.1002/9780470697870.ch2

2. Demidova-Rice TN, Hamblin MR, Herman IM (2012) Normal and chronic wounds: biology, causes and approaches to care.(Acute and Impaired Wound Healing: Pathophysiology and Current Methods for Drug Delivery). Adv Skin Wound Care 25:304.

3. Dealey C (2008) The Management of Patients with Chronic Wounds. Care Wounds. Blackwell Publishing Ltd, pp 121–178

4. Siddiqui AR, Bernstein JM (2010) Chronic wound infection: facts and controversies. Clin Dermatol 28:519–26. doi: 10.1016/j.clindermatol.2010.03.009

5. Bowler PG, Davies BJ (1999) The microbiology of acute and chronic wounds. WOUNDS-A Compend Clin Res Pract 11:72–78.

6. Howell-Jones RS, Wilson MJ, Hill KE, et al. (2005) A review of the microbiology, antibiotic usage and resistance in chronic skin wounds. J Antimicrob Chemother 55:143–149. doi: 10.1093/jac/dkh513

7. M.B.Minnis A (2008) A Substantive Theory to explain the Impact of Living with a Chronic Wound whilst receiving Conflicting or Inappropriate Advice and Care. Sch Heal Sci Sci Eng Technol Master of :175.

8. Böttcher-Haberzeth S, Biedermann T, Reichmann E (2010) Tissue engineering of skin. Burns 36:450–460. doi: 10.1016/j.burns.2009.08.016

9. Robert J S Treatment of nonhealing ulcers with allografts. Clin Dermatol 23:388–395.

10. A.J.A H (2005) Treatment of partial-thickness burns: a prospective, randomized trial using transcyte: Kumar RJ, Kimble RM, Boots R, et al. Aust N Z J Surg 2004 (August);74:622-626. J Pediatr Surg 40:600–601.

11. Holder IA, Boyce ST (1996) Formulation of “idealized” topical antimicrobial mixtures for use with cultured skin grafts. J Antimicrob Chemother 38:457–463. doi: 10.1093/jac/38.3.457

12. Zilberman M, Elsner JJ (2008) Antibiotic-eluting medical devices for various applications. J Control Release 130:202–215.

13. Halim AS, Khoo TL, Shah JMY (2010) Biologic and synthetic skin substitutes: An overview. Indian J. Plast. Surg. 43:

14. Chow B, Baume A, Lok P, et al. (2012) Development of 3D Antibiotic-Eluting Bioresorbable Scaffold with Attenuating Envelopes. J Biomim Biomater Tissue Eng 15:55–62. doi: 10.4028/www.scientific.net/JBBTE.15.55

15. Madhavan R V, Rosemary MJ, Nandkumar MA, et al. (2011) Silver Nanoparticle Impregnated Poly (ε-Caprolactone) Scaffolds: Optimization of Antimicrobial and Noncytotoxic Concentrations. Tissue Eng Part A 17:439–449. doi: 10.1089/ten.tea.2009.0791

16. Percival SL, Emanuel C, Cutting KF, Williams DW (2012) Microbiology of the skin and the role of biofilms in infection. Int Wound J 9:14–32. doi: 10.1111/j.1742-481X.2011.00836.x

17. Seeley RR, Tate P, Stephens TD (2011) Seeley's anatomy & physiology, 8th ed. McGraw-Hill, New York

18. Dealey C (2008) The Physiology of Wound Healing. Care Wounds. Blackwell Publishing Ltd, pp 1–12

19. Powell J (2007) Skin physiology. Found Years 3:193–196. doi: 10.1016/j.mpfou.2007.07.008

20. Venus M, Waterman J, McNab I (2011) Basic physiology of the skin. Surg 29:471–474. doi: 10.1016/j.mpsur.2011.06.010

21. Zeng Q, Macri LK, Prasad A, et al. (2011) 5.534 - Skin Tissue Engineering. In: Editor-in-Chief: Paul D (ed) Compr. Biomater. Elsevier, Oxford, pp 467–499

22. Gaboriau HP, Murakami CS (2001) Skin anatomy and flap physiology. Otolaryngol Clin North Am 34:555–569. doi: 10.1016/s0030-6665(05)70005-0

23. Gantwerker EA, Hom DB (2011) Skin: Histology and Physiology of Wound Healing. Facial Plast Surg Clin North Am 19:441–453.

24. Ovaere P, Lippens S, Vandenabeele P, Declercq W (2009) The emerging roles of serine protease cascades in the epidermis. Trends Biochem Sci 34:453–463. doi: 10.1016/j.tibs.2009.08.001

25. Candi E, Schmidt R, Melino G (2005) The cornified envelope: a model of cell death in the skin. Nat Rev Mol Cell Biol 6:328–340.

26. Riley PA (1997) Melanin. Int J Biochem & Cell Biol 29:1235–1239. doi: 10.1016/s1357-2725(97)00013-7

27. Schmidt RF, Willis WD (2007) Langerhans Cells. Encycl Pain 1038.

28. Boulais N, Misery L (2007) Merkel cells. J Am Acad Dermatol 57:147–165. doi: 10.1016/j.jaad.2007.02.009

29. McDougall S, Dallon J, Sherratt J, Maini P (2006) Fibroblast migration and collagen deposition during dermal wound healing: mathematical modelling and clinical implications. Philos Trans R Soc A Math Phys Eng Sci 364:1385–1405. doi: 10.1098/rsta.2006.1773

30. Mahjour SB, Ghaffarpasand F, Wang H (2012) Hair Follicle Regeneration in Skin Grafts: Current Concepts and Future Perspectives. Tissue Eng Part B Rev 18:15–23. doi: 10.1089/ten.teb.2011.0064

31. Seeley RR, Tate P, Stephens TD (2008) Integumentary System. Anat. Physiol. McGraw-Hill, pp 149–172

32. Unal S, Ersoz G, Demirkan F, et al. (2005) Analysis of skin-graft loss due to infection - Infection-related graft loss. Ann Plast Surg 55:102–106. doi: 10.1097/01.sap.0000164531.23770.60

33. Tahir A, Titley OG (2005) Reducing infections in cutaneous oncology defects reconstructed using skin grafts. Eur J Plast Surg 28:27–31. doi: 10.1007/s00238-004-0706-y

34. Rothman S, Lorincz AL (1963) Defense Mechanisms of the Skin. Annu Rev Med 14:215–242. doi: 10.1146/annurev.me.14.020163.001243

35. Nizet V, Gallo RL, Ohtake T, et al. (2001) Innate antimicrobial peptide protects the skin from invasive bacterial infection. Nature 414:454–457. doi: 10.1038/35106587

36. Cogen AL, Nizet V, Gallo RL (2008) Skin microbiota: a source of disease or defence? Br J Dermatol 158:442–455. doi: 10.1111/j.1365-2133.2008.08437.x

37. Gallo RL, Hooper L V (2012) Epithelial antimicrobial defence of the skin and intestine. Nat Rev Immunol 12:503–516. doi: 10.1038/nri3228

38. Urbancic-Rovan V, Gubina M (1997) Infection in Superficial Diabetic Foot Ulcers. Clin Infect Dis 25:S184–S185. doi: 10.1086/516184

39. Hansson C, Hoborn J, Moller A, Swanbeck G (1995) The Microbial Florain Venous Leg Ulcers without Clinical Signs of Infection - Repeated Culture using a Validated Standardized Microbiological Technique. Acta Dermoato-Venereologica 75:24–30.

40. Young A, McNaught C-E (2011) The physiology of wound healing. Surg 29:475–479. doi: 10.1016/j.mpsur.2011.06.011

41. Strodtbeck F (2001) Physiology of wound healing. Newborn Infant Nurs Rev 1:43–52. doi: 10.1053/nbin.2001.23176

42. Metz M, Maurer M (2009) Innate immunity and allergy in the skin. Curr Opin Immunol 21:687–693. doi: 10.1016/j.coi.2009.09.009

43. Enoch S, Leaper DJ (2005) Basic science of wound healing. Surg 23:37–42. doi: 10.1383/surg.23.2.37.60352

44. Cooper DM (1999) Wound healing: New understandings. NURSE Pract FORUM-CURRENT Top Commun 10:74–86.

45. Thomas K, Hunt TK, Hopf H, Hussain Z (2000) Physiology of wound healing. Adv Skin Wound Care 13:6.

46. Menke NB, Ward KR, Witten TM, et al. (2007) Impaired wound healing. Clin Dermatol 25:19–25. doi: 10.1016/j.clindermatol.2006.12.005

47. Green KA, Almholt K, Ploug M, et al. (2008) Profibrinolytic Effects of Metalloproteinases during Skin Wound Healing in the Absence of Plasminogen. J Invest Dermatol 128:2092–2101. doi: 10.1038/jid.2008.54

48. Barrientos S, Stojadinovic O, Golinko MS, et al. (2008) Growth factors and cytokines in wound healing. Wound Repair Regen 16:585–601. doi: 10.1111/j.1524-475X.2008.00410.x

49. Kobayashi Y (2006) Neutrophil infiltration and chemokines. Crit Rev Immunol 26:307–315.

50. Segal AW (2005) How neutrophils kill microbes. Annu Rev Immunol 23:197–223. doi: 10.1146/annurev.immunol.23.021704.115653

51. Hellberg L, Roth S, Behnen M, et al. (2012) Phagocytosis of apoptotic neutrophils by neutrophil granulocytes. Eur J Clin Invest 42:31.

52. Koh TJ, DiPietro LA (2011) Inflammation and wound healing: the role of the macrophage. Expert Rev Mol Med 13:e23–e23. doi: 10.1017/S1462399411001943

53. Knapik A, Hegland N, Calcagni M, et al. (2012) Metalloproteinases facilitate connection of wound bed vessels to pre-existing skin graft vasculature. Microvasc Res 84:16–23. doi: 10.1016/j.mvr.2012.04.001

54. Zhu P, Yang C, Chen L-H, et al. (2010) Impairment of human keratinocyte mobility and proliferation by advanced glycation end products-modified BSA. Arch Dermatol Res 1–12. doi: 10.1007/s00403-010-1102-z

55. Tonnesen MG, Feng X, Clark RAF (2000) Angiogenesis in Wound Healing. J Investig Dermatology Symp Proc 5:40–46. doi: 10.1046/j.1087-0024.2000.00014.x

56. Simon JM (2007) Hypoxia and angiogenesis. Bull Cancer 94:S160–S165.

57. Ferrara N (2001) Role of vascular endothelial growth factor in regulation of physiological angiogenesis. Am J Physiol - Cell Physiol 280:C1358–C1366.

58. Bao P, Kodra A, Tomic-Canic M, et al. (2009) The Role of Vascular Endothelial Growth Factor in Wound Healing. J Surg Res 153:347–358.

59. Meyr AJ, Saffran B (2008) The Pathophysiology of the Chronic Pain Cycle. Clin Podiatr Med Surg 25:327–346.

60. Guo S, Dipietro LA (2010) Factors affecting wound healing. J Dent Res 89:219–229. doi: 10.1177/0022034509359125

61. Ben-Porath I, Weinberg RA (2005) The signals and pathways activating cellular senescence. Int J Biochem Cell Biol 37:961–976. doi: http://dx.doi.org/10.1016/j.biocel.2004.10.013

62. Eming SA, Krieg T, Davidson JM (2007) Inflammation in Wound Repair: Molecular and Cellular Mechanisms. J Invest Dermatol 127:514–525. doi: http://dx.doi.org/10.1038/sj.jid.5700701

63. Gottrup F (2004) A specialized wound-healing center concept: importance of a multidisciplinary department structure and surgical treatment facilities in the treatment of chronic wounds. Am J Surg 187:S38–S43. doi: 10.1016/S0002-9610(03)00303-9

64. Santamaria N, Austin D, Clayton L (2002) A Multi-site Clinical Evaluation Trial of the Alfred/Medseed Wound Imaging System Prototype. Prim Intent Aust J Wound Manag 10:120–125.

65. Vaska VL, Nimmo GR, Jones M, et al. (2012) Increases in Australian cutaneous abscess hospitalisations: 1999–2008. Eur J Clin Microbiol Infect Dis 31:93–96. doi: 10.1007/s10096-011-1281-3

66. Broadbent J, Walsh T, Upton Z (2010) Proteomics in chronic wound research: Potentials in healing and health. PROTEOMICS – Clin Appl 4:204–214. doi: 10.1002/prca.200900152

67. Robins M, Warmington S, Duncan G, et al. (2001) A Patient-centred Wound Management Clinic: Theory Put into Practice. Prim Intent Aust J Wound Manag 9:68–72.

68. McGuiness W, Rice J (2009) The management of chronic wounds. Aust Nurs J 16:37–39.

69. Health R, Centre A, Health AA, et al. (2010) Rural Health in Australia. Rural Soc 20:2–9.

70. Allan J, Ball P, Alston M, Community TL (2010) What Is Health Anyway?: Perceptions and Experiences of Health and Health Care from Socio-economically Disadvantaged Rural Residents. Rural Soc 20:85–97. doi: 10.5172/rsj.20.1.85

71. Leung PC (2007) Diabetic foot ulcers -- a comprehensive review. Surg 5:219–231. doi: Doi: 10.1016/s1479-666x(07)80007-2

72. Wong M, Haswell-Elkins M, Tamwoy E, et al. (2005) Perspectives on clinic attendance, medication and foot-care among people with diabetes in the Torres Strait Islands and Northern Peninsula Area. Aust J Rural Health 13:172–177. doi: 10.1111/j.1440-1854.2005.00678.x

73. Black CE, Costerton JW (2010) Current Concepts Regarding the Effect of Wound Microbial Ecology and Biofilms on Wound Healing. Surg Clin North Am 90:1147–1160. doi: 10.1016/j.suc.2010.08.009

74. Prescott LM, Harley JP, Klein DA (2005) Microbiology. McGraw-Hill, Boston

75. Douglas LJ (2003) Candida biofilms and their role in infection. Trends Microbiol 11:30–36. doi: 10.1016/s0966-842x(02)00002-1

76. Gjødsbøl K, Christensen JJ, Karlsmark T, et al. (2006) Multiple bacterial species reside in chronic wounds: a longitudinal study. Int Wound J 3:225–231. doi: 10.1111/j.1742-481X.2006.00159.x

77. Davies CE, Hill KE, Newcombe RG, et al. (2007) A prospective study of the microbiology of chronic venous leg ulcers to reevaluate the clinical predictive value of tissue biopsies and swabs. Wound Repair Regen 15:17–22. doi: 10.1111/j.1524-475X.2006.00180.x

78. Mainous Arch G 3rd, Hueston WJ, Everett CJ, Diaz VA (2006) Nasal carriage of Staphylococcus aureus and methicillin-resistant S aureus in the United States, 2001-2002. Ann Fam Med 4:132–137. doi: 10.1370/afm.526

79. Thomson CH (2011) Biofilms: do they affect wound healing? Int Wound J 8:63–67. doi: 10.1111/j.1742-481X.2010.00749.x

80. Percival SL, Thomas JG, Williams DW (2010) Biofilms and bacterial imbalances in chronic wounds: anti-Koch. Int Wound J 7:169–175. doi: 10.1111/j.1742-481X.2010.00668.x

81. Wilson M (2001) Bacterial biofilms and human disease. Sci Prog 84:235–254.

82. Dufour D, Leung V, Lévesque CM (2010) Bacterial biofilm: structure, function, and antimicrobial resistance. Endod Top 22:2–16. doi: 10.1111/j.1601-1546.2012.00277.x

83. Anthony W S (2005) Biofilms and antibiotic therapy: Is there a role for combating bacterial resistance by the use of novel drug delivery systems? Adv Drug Deliv Rev 57:1539–1550.

84. Schierle CF, De la Garza M, Mustoe TA, Galiano RD (2009) Staphylococcal biofilms impair wound healing by delaying reepithelialization in a murine cutaneous wound model. Wound Repair Regen 17:354–359. doi: 10.1111/j.1524-475X.2009.00489.x

85. Götz F (2002) Staphylococcus and biofilms. Mol Microbiol 43:1367–1378. doi: 10.1046/j.1365-2958.2002.02827.x

86. 2009_Cutting_Biofilms possible strategies for suppression in chronic wounds.pdf.

87. Kokare CR, Chakraborty S, Khopade AN, Mahadik KR (2009) Biofilm: Importance and applications. INDIAN J Biotechnol 8:159–168.

88. Cosgrove SE, Carmeli Y (2003) The impact of antimicrobial resistance on health and economic outcomes. Clin Infect Dis 36:1433–1437. doi: 10.1086/375081

89. Colsky AS, Kirsner RS, Kerdel FA (1998) Analysis of antibiotic susceptibilities of skin wound flora in hospitalized dermatology patients. The crisis of antibiotic resistance has come to the surface. Arch Dermatol 134:1006–1009. doi: 10.1001/archderm.134.8.1006

90. Kuehn BM (2008) Community-Acquired MRSA. JAMA J Am Med Assoc 299:890. doi: 10.1001/jama.299.8.890-a

91. Wegener HC (2003) Antibiotics in animal feed and their role in resistance development. Curr Opin Microbiol 6:439–445. doi: http://dx.doi.org/10.1016/j.mib.2003.09.009

92. Campoccia D, Montanaro L, Speziale P, Arciola CR (2010) Antibiotic-loaded biomaterials and the risks for the spread of antibiotic resistance following their prophylactic and therapeutic clinical use. Biomaterials 31:6363–6377. doi: DOI: 10.1016/j.biomaterials.2010.05.005

93. Dealey C (2008) Wound Management Products. Care Wounds. Blackwell Publishing Ltd, pp 83–120

94. Lionelli GT, Lawrence WT (2003) Wound dressings. Surg Clin North Am 83:617–638. doi: 10.1016/S0039-6109(02)00192-5

95. Boateng JS, Matthews KH, Stevens HNE, Eccleston GM (2008) Wound healing dressings and drug delivery systems: A review. J Pharm Sci 97:2892–2923. doi: 10.1002/jps.21210

96. Jung SBMRCMU of S, Technology Rolla M, Day DEMRCMU of S (2011) WOUND CARE. US2011/020:

97. Lebrun E, Tomic-Canic M, Kirsner RS (2010) The role of surgical debridement in healing of diabetic foot ulcers. Wound Repair Regen 18:433–438. doi: 10.1111/j.1524-475X.2010.00619.x

98. Jones V, Grey JE, Harding KG (2006) Wound dressings. BMJ 332:777–780. doi: 10.1136/bmj.332.7544.777

99. Lipsky BA, Hoey C (2009) Topical Antimicrobial Therapy for Treating Chronic Wounds. Clin Infect Dis 49 :1541–1549. doi: 10.1086/644732

100. Field FK, Kerstein MD (1994) Overview of wound healing in a moist environment. Am J Surg 167:2S–S6. doi: 10.1016/0002-9610(94)90002-7

101. JANITZ R (1983) Comparison of synthetic adhesive moisture vapor permeable and fine mesh gauze dressings for splitthickness skin graft donor sites Barnett A, Berkowitz RL, Mills R, et al. Am J Surg 145:379, 1983. J Oral Maxillofac Surg 41:753–754. doi: 10.1016/0278-2391(83)90200-8

102. Toy LW, Macera L (2011) Evidence-based review of silver dressing use on chronic wounds. J Am Acad Nurse Pract 23:183–192. doi: 10.1111/j.1745-7599.2011.00600.x

103. Poon VKM, Burd A (2004) In vitro cytotoxity of silver: implication for clinical wound care. Burns 30:140–147. doi: 10.1016/j.burns.2003.09.030

104. Innes ME, Umraw N, Fish JS, et al. (2001) The use of silver coated dressings on donor site wounds: a prospective, controlled matched pair study. Burns 27:621–627. doi: 10.1016/S0305-4179(01)00015-8

105. Huang Y, Li X, Liao Z, et al. (2007) A randomized comparative trial between Acticoat and SD-Ag in the treatment of residual burn wounds, including safety analysis. Burns 33:161–166. doi: 10.1016/j.burns.2006.06.020

106. Houang ET, Gilmore OJ, Reid C, Shaw EJ (1976) Absence of bacterial resistance to povidone iodine. J Clin Pathol 29:752–755. doi: 10.1136/jcp.29.8.752

107. Landis SJ (2008) Chronic wound infection and antimicrobial use. Adv Skin Wound Care 21:531–540. doi: 10.1097/01.ASW.0000323578.87700.a5

108. Howell-Jones RS, Price PE, Howard AJ, Thomas DW (2006) Antibiotic prescribing for chronic skin wounds in primary care. Wound Repair Regen 14:387–393. doi: 10.1111/j.1743-6109.2006.00144.x

109. Lazic T, Falanga V (2011) Bioengineered Skin Constructs and Their Use in Wound Healing. Plast Reconstr Surg 127:75S–90S 10.1097/PRS.0b013e3182009d9f.

110. Macneil S, Sheila M (2008) Biomaterials for tissue engineering of skin. Mater Today 11:26–35. doi: 10.1016/s1369-7021(08)70087-7

111. Gravante G, Di Fede MC, Araco A, et al. (2007) A randomized trial comparing ReCell® system of epidermal cells delivery versus classic skin grafts for the treatment of deep partial thickness burns. Burns 33:966–972. doi: 10.1016/j.burns.2007.04.011

112. Horch RE, Kopp J, Kneser U, et al. (2005) Tissue engineering of cultured skin substitutes. J Cell Mol Med 9:592–608. doi: 10.1111/j.1582-4934.2005.tb00491.x

113. Yim H, Cho YS, Seo CH, et al. (2010) The use of AlloDerm on major burn patients: AlloDerm prevents post-burn joint contracture. Burns 36:322–328.

114. Zhong SP, Zhang YZ, Lim CT (2010) Tissue scaffolds for skin wound healing and dermal reconstruction. Wiley Interdiscip Rev Nanomed Nanobiotechnol 2:510–525. doi: 10.1002/wnan.100

115. Eaglstein WH, Falanga V Tissue engineering and the development of Apligraf®, a human skin equivalent. Clin Ther 19:894–905. doi: 10.1016/s0149-2918(97)80043-4

116. Holland AJA (2011) Tissue engineering in burns: II. 24.

117. Bo S, Biedermann T, Reichmann E, Böttcher-Haberzeth S (2010) Tissue engineering of skin. Burns 36:450–460. doi: 10.1016/j.burns.2009.08.016

118. MacNeil S (2007) Progress and opportunities for tissue-engineered skin. Nature 445:874–880. doi: 10.1038/nature05664

119. Andreassi A, Bilenchi R, Biagioli M, D'Aniello C (2005) Classification and pathophysiology of skin grafts. Clin Dermatol 23:332–337. doi: 10.1016/j.clindermatol.2004.07.024

120. Concentrations N (2011) Silver Nanoparticle Impregnated Poly (e-Caprolactone) Scaffolds: Optimization of Antimicrobial and Noncytotoxic Concentrations. doi: 10.1089/ten.tea.2009.0791

121. Hollister SJ, Maddox RD, Taboas JM (2002) Optimal design and fabrication of scaffolds to mimic tissue properties and satisfy biological constraints. Biomaterials 23:4095–4103.

122. Liu C, Xia Z, Czernuszka JT (2007) Design and Development of Three-Dimensional Scaffolds for Tissue Engineering. Chem Eng Res Des 85:1051–1064.

123. Raghavendra GM, Jayaramudu T, Varaprasad K, et al. (2013) Cellulose-polymer-Ag nanocomposite fibers for antibacterial fabrics/skin scaffolds. Carbohydr Polym 93:553–560. doi: 10.1016/j.carbpol.2012.12.035

124. Veleirinho B, Coelho DS, Dias PF, et al. (2012) Nanofibrous poly(3-hydroxybutyrate-co-3-hydroxyvalerate)/chitosan scaffolds for skin regeneration. Int J Biol Macromol 51:343–350. doi: 10.1016/j.ijbiomac.2012.05.023

125. Unnithan AR, Pichiah PBT, Gnanasekaran G, et al. (2012) Emu oil-based electrospun nanofibrous scaffolds for wound skin tissue engineering. COLLOIDS SURFACES A-PHYSICOCHEMICAL Eng Asp 415:454–460. doi: 10.1016/j.colsurfa.2012.09.029

126. Garric X, Guillaume O, Dabboue H, et al. (2012) Potential of a PLA-PEO-PLA-Based Scaffold for Skin Tissue Engineering: In Vitro Evaluation. J Biomater Sci Ed 23:1687–1700. doi: 10.1163/092050611X590912

127. Rnjak-Kovacina J, Wise SG, Li Z, et al. (2011) Tailoring the porosity and pore size of electrospun synthetic human elastin scaffolds for dermal tissue engineering. Biomaterials 32:6729–6736. doi: 10.1016/j.biomaterials.2011.05.065

128. Franco RA, Min Y-K, Yang H-M, Lee B-T (2013) Fabrication and biocompatibility of novel bilayer scaffold for skin tissue engineering applications. J Biomater Appl 27:605–615. doi: 10.1177/0885328211416527

129. Ahn S, Yoon H, Kim G, et al. (2010) Designed three-dimensional collagen scaffolds for skin tissue regeneration. Tissue Eng Part C Methods 16:813–820. doi: 10.1089/ten.tec.2009.0511

130. Chang HI, Lau YC, Yan C, Coombes AGA (2008) Controlled release of an antibiotic, gentamicin sulphate, from gravity spun polycaprolactone fibers. J Biomed Mater Res Part A 84A:230–237. doi: 10.1002/jbm.a.31476

131. Zhu X, Cui W, Li X, Jin Y (2008) Electrospun fibrous mats with high porosity as potential scaffolds for skin tissue engineering. Biomacromolecules 9:1795–1801. doi: 10.1021/bm800476u

132. Zhang Y, Lim CT, Ramakrishna S, Huang Z-M (2005) Recent development of polymer nanofibers for biomedical and biotechnological applications. J Mater Sci Mater Med 16:933–946. doi: 10.1007/s10856-005-4428-x

133. Vieira AC, Vieira JC, Ferra JM, et al. (2011) Mechanical study of PLA–PCL fibers during in vitro degradation. J Mech Behav Biomed Mater 4:451–460.

134. Sun H, Mei L, Song C, et al. (2006) The in vivo degradation, absorption and excretion of PCL-based implant. Biomaterials 27:1735–1740.

135. Chong EJ, Phan TT, Lim IJ, et al. (2007) Evaluation of electrospun PCL/gelatin nanofibrous scaffold for wound healing and layered dermal reconstitution. Acta Biomater 3:321–330.

136. Sripriya R, Kumar MS, Sehgal PK (2004) Improved collagen bilayer dressing for the controlled release of drugs. J Biomed Mater Res Part B Appl Biomater 70B:389–396. doi: 10.1002/jbm.b.30051

137. Lee CH, Singla A, Lee Y (2001) Biomedical applications of collagen. Int J Pharm 221:1–22. doi: 10.1016/s0378-5173(01)00691-3

138. Ji C, Annabi N, Khademhosseini A, Dehghani F (2011) Fabrication of porous chitosan scaffolds for soft tissue engineering using dense gas CO2. Acta Biomater 7:1653–1664. doi: 10.1016/j.actbio.2010.11.043

139. Katti DS, Robinson KW, Ko FK, Laurencin CT (2004) Bioresorbable nanofiber-based systems for wound healing and drug delivery: optimization of fabrication parameters. J Biomed Mater Res B Appl Biomater 70:286–296. doi: 10.1002/jbm.b.30041

140. Timko BP, Dvir T, Kohane DS (2010) Remotely triggerable drug delivery systems. Adv Mater 22:4925–4943. doi: 10.1002/adma.201002072

141. Mathiowitz E (2008) Drug delivery systems. Toxicol Pathol 36:16–20. doi: 10.1177/0192623307311411

142. Hiralal SC, Mahadev SL, Amol SA, et al. (2011) PULSATILE DRUG DELIVERY SYSTEM. Int J Pharm Sci Rev Res 8:160.

143. Barbe C, Bartlett J, Kong LG, et al. (2004) Silica particles: A novel drug-delivery system. Adv Mater 16:1959–1966. doi: 10.1002/adma.200400771

144. Jifu Hao Yanfang Zhou, Jianzhu Wang, Fengguang Guo, Fei Li, and Xinsheng Peng3 XF (2011) Development and optimization of solid lipid nanoparticle formulation for ophthalmic delivery of chloramphenicol using a Box-Behnken design. Int J Nanomedicine 6:683–692. doi: 10.2147/IJN.S17386

145. Schnieders J, Gbureck U, Thull R, Kissel T (2006) Controlled release of gentamicin from calcium phosphate—poly(lactic acid-co-glycolic acid) composite bone cement. Biomaterials 27:4239–4249. doi: http://dx.doi.org/10.1016/j.biomaterials.2006.03.032

146. Hetrick EM, Schoenfisch MH (2006) Reducing implant-related infections: active release strategies. Chem Soc Rev 35:780–789.

147. Wu P, Grainger DW (2006) Drug/device combinations for local drug therapies and infection prophylaxis. Biomaterials 27:2450–2467.

148. Elsner JJ, Berdicevsky I, Zilberman M (2011) In vitro microbial inhibition and cellular response to novel biodegradable composite wound dressings with controlled release of antibiotics. Acta Biomater 7:325–336. doi: DOI: 10.1016/j.actbio.2010.07.013

149. Hench LL (2006) The story of Bioglass. J Mater Sci Mater Med 17:967–978. doi: 10.1007/s10856-006-0432-z

150. Bretcanu O, Chatzistavrou X, Paraskevopoulos K, et al. (2009) Sintering and crystallisation of 45S5 Bioglass® powder. J Eur Ceram Soc 29:3299–3306. doi: 10.1016/j.jeurceramsoc.2009.06.035

151. Tilocca A (2010) Models of structure, dynamics and reactivity of bioglasses: a review. J Mater Chem 2:6848–6858. doi: 10.1039/c0jm01081b

152. Wilson J, Pigott GH, Schoen FJ, Hench LL (1981) Toxicology and biocompatibility of bioglasses. J Biomed Mater Res 15:805–817. doi: 10.1002/jbm.820150605

153. Gillette RL, Swaim SF, Sartin EA, et al. (2001) Effects of a bioactive glass on healing of closed skin wounds in dogs. Am J Vet Res 62:1149–1153. doi: doi:10.2460/ajvr.2001.62.1149

154. Gorustovich AA, Roether JA, Boccaccini AR (2010) Effect of Bioactive Glasses on Angiogenesis: A Review of In Vitro and In Vivo Evidences. Tissue Eng Part B Rev 16:199–207. doi: 10.1089/ten.teb.2009.0416

155. Rahaman MN, Day DE, Sonny Bal B, et al. (2011) Bioactive glass in tissue engineering. Acta Biomater 7:2355–2373. doi: 10.1016/j.actbio.2011.03.016

156. Verrier S, Blaker JJ, Maquet V, et al. (2004) PDLLA/Bioglass® composites for soft-tissue and hard-tissue engineering: an in vitro cell biology assessment. Biomaterials 25:3013–3021.

157. Cannillo V, Chiellini F, Fabbri P, Sola A (2010) Production of Bioglass® 45S5 - Polycaprolactone composite scaffolds via salt-leaching. Compos Struct 92:1823–1832. doi: 10.1016/j.compstruct.2010.01.017

158. Hu S, Chang J, Liu M, Ning C (2009) Study on antibacterial effect of 45S5 Bioglass. J Mater Sci Mater Med 20:281–286. doi: 10.1007/s10856-008-3564-5

159. Allan I, Newman H, Wilson M (2002) Particulate Bioglass reduces the viability of bacterial biofilms formed on its surface in an in vitro model. Clin Oral Implants Res 13:53–58. doi: 10.1034/j.1600-0501.2002.130106.x

160. Allan I, Newman H, Wilson M (2001) Antibacterial activity of particulate Bioglass ® against supra- and subgingival bacteria. Biomaterials 22:1683–1687. doi: 10.1016/s0142-9612(00)00330-6

161. Xie Z-P, Zhang C-Q, Yi C-Q, et al. (2008) Failure of particulate bioglass to prevent experimental staphylococcal infection of open tibial fractures. J Antimicrob Chemother 62:1162–1163. doi: 10.1093/jac/dkn336

162. Pratten J, Nazhat SN, Blaker JJ, Boccaccini AR (2004) In Vitro Attachment of Staphylococcus Epidermidis to Surgical Sutures with and without Ag-Containing Bioactive Glass Coating. J Biomater Appl 19:47–57. doi: 10.1177/0885328204043200

163. Hum J, Boccaccini AR (2012) Bioactive glasses as carriers for bioactive molecules and therapeutic drugs: a review. J Mater Sci Mater Med 23:2317–2333. doi: 10.1007/s10856-012-4580-z

164. Stoor P, Soderling E, Salonen JI (1998) Antibacterial effects of a bioactive glass paste on oral microorganisms. Acta Odontol Scand 56:161. doi: 10.1080/000163598422901

165. Munukka E, Leppäranta O, Korkeamäki M, et al. (2008) Bactericidal effects of bioactive glasses on clinically important aerobic bacteria. J Mater Sci Mater Med 19:27–32. doi: 10.1007/s10856-007-3143-1

166. Radin S, Ducheyne P, Kamplain T, Tan BH (2001) Silica sol-gel for the controlled release of antibiotics. I. Synthesis, characterization, and in vitro release. J Biomed Mater Res 57:313–320.

167. López-Noriega A, Arcos D, Vallet-Regí M (2010) Functionalizing mesoporous bioglasses for long-term anti-osteoporotic drug delivery. Chemistry 16:10879–10886. doi: 10.1002/chem.201000137

168. Xia W, Chang J (2006) Well-ordered mesoporous bioactive glasses (MBG): A promising bioactive drug delivery system. J Control Release 110:522–530. doi: http://dx.doi.org/10.1016/j.jconrel.2005.11.002

169. Fu H, Rahaman MN, Day DE, Brown RF (2011) Hollow hydroxyapatite microspheres as a device for controlled delivery of proteins. J Mater Sci Mater Med 22:579–591. doi: 10.1007/s10856-011-4250-6

170. Gatti J, Brinker A, Avigan M (2013) Spontaneous Reports of Seizure in Association With Leuprolide (Lupron Depot), Goserelin (Zoladex Implant), and Naferelin (Synarel Nasal Spray). Obstet Gynecol 121:1107. doi: 10.1097/AOG.0b013e31828c9cb3

171. Muneyyirei-Delale O, Jiang XC, Dalloul M, et al. (2010) F11R/JAM and SM Levels in Women with Endometriosis on Treatment with Lupron-Depot vs. Norethindrone Acetate. Reprod Sci 17:94A–94A.

172. Kemp SF, Saenger P, Fielder PJ, et al. (2004) Pharmacokinetic and pharmacodynamic characteristics of a long-acting growth hormone (GH) preparation (nutropin depot) in GH-deficient children. J Clin Endocrinol Metab 89:3234–3240. doi: 10.1210/jc.2003-030825

173. Cook DM, Attie KM, Dao LN, et al. (2002) The pharmacokinetic and pharmacodynamic characteristics of a long-acting growth hormone (GH) preparation (Nutropin Depot) in GH-deficient adults. J Clin Endocrinol Metab 87:4508–4514. doi: 10.1210/jc.2002-020480

174. (2004) Alkermes, Inc.; Companies agree to discontinue commercialization of Nutropin Depot. Biotech Week 33.

175. Sivakumar SM, Safhi MM, Kannadasan M, Sukumaran N (2011) Vaccine adjuvants - Current status and prospects on controlled release adjuvancity. SAUDI Pharm J 19:197–206. doi: 10.1016/j.jsps.2011.06.003

176. Writers BE& M (2000) Geron and Modex Announce License Agreement for Encapsulated Cell- based Therapeutic Protein Delivery Products. Bus Wire U6 - ctx_ver=Z3988-2004&ctx_enc=info%3Aofi%2Fenc%3AUTF-

8&rfr_id=infosid/summon.serialssolutions.com&rft_val_fmt=infoofi/fmtkevmtxjournal&rft.genre=article&rft.atitle=Geron+and+Modex+Announce+License+Agreement+for+Encapsulated+Cell-+ba 1.

177. Nishimura Y, Shishido T, Ishii J, et al. (2012) Protein-encapsulated bio-nanocapsules production with ER membrane localization sequences. J Biotechnol 157:124–129. doi: 10.1016/j.jbiotec.2011.09.015

178. Wang DQ, Robinson DR, Kwon GS, Samuel J (1999) Encapsulation of plasmid DNA in biodegradable poly(D,L-lactic-co-glycolic acid) microspheres as a novel approach for immunogene delivery. J Control RELEASE 57:9–18.

179. Ahmad Z, Zahoor a, Sharma S, Khuller GK (2005) Inhalable alginate nanoparticles as antitubercular drug carriers against experimental tuberculosis. Int J Antimicrob Agents 26:298–303. doi: 10.1016/j.ijantimicag.2005.07.012

180. Goldberg M, Gomez-Orellana I (2003) Challenges for the oral delivery of macromolecules. Nat Rev DRUG Discov 2:289–295. doi: 10.1038/nrd1067

181. Boughton EA, University of Sydney. School of Aerospace M &amp, Engineering M (2011) Development of bioactive soft tissue scaffold systems.

182. Wong L, Boughton DP (2010) Design of a Sustained Antibiotic Releasing Scaffold for Wound Application. Mechnical Eng Bachelor o:91.

183. Lei B, Chen X, Wang Y, Zhao N (2009) Synthesis and in vitro bioactivity of novel mesoporous hollow bioactive glass microspheres. Mater Lett 63:1719–1721. doi: http://dx.doi.org/10.1016/j.matlet.2009.04.041

184. Livage J, Sanchez C (1992) Sol-gel chemistry. J Non Cryst Solids 145:11–19. doi: 10.1016/S0022-3093(05)80422-3

185. Brunner TJ, Grass RN, Stark WJ (2006) Glass and bioglass nanopowders by flame synthesis. Chem Commun 0:1384–1386. doi: 10.1039/B517501A

186. Itälä A, Nordström EG, Ylänen H, et al. (2001) Creation of microrough surface on sintered bioactive glass microspheres. J Biomed Mater Res 56:282–288. doi: 10.1002/1097-4636(200108)56:2<282::aid-jbm1096>3.0.co;2-5

187. Wegner K, Schimmoeller B, Thiebaut B, et al. (2011) Pilot Plants for Industrial Nanoparticle Production by Flame Spray Pyrolysis. KONA POWDER Part J 29:251–265.

188. Management SW Collagen-based dressings as therapeutic agents.

189. Gruchalla RS, Pirmohamed M (2006) Clinical practice. Antibiotic allergy. N Engl J Med 354:601–609.

190. Bartlett JG (2010) Chloramphenicol.

191. ECONOCHLOR® (2009) Chloramphenicol.

192. El Badry KM, Moustafa FA, Azooz MA, El Batal FH (2002) Corrosion behaviour of some selected bioglasses by different aqueous solutions. Glas Technol 43:162–170.

11 Appendix

11.1 Appendix A – Protocols

11.1.1 Chapter 4 Production and Characterisation of Microspheres

Flame Spray Protocol

Aim

Production of Bioglass 45S5 microspheres

Equipment

- Bioglass 45S5 powder (<40µm)
- Flame guns: Thermospray Type 5P (Metco), SuperJet S (Eutalloy)
- Paint spray gun (Metabo)
- Red dye
- Steel collection container
- Filter paper (>50cm diameter)
- Funnel

Safety

- Tinted glassed
- Flame guns to be operated by trained personnel

Method

1. Load bioglass 45S5 powder into dispensing container and attach to flame gun. Fill steel collection container with 1-2cm of water.

2. Ignite flame gun and set acetylene/oxygen pressures to 34/34 psi. Following this set air jet pressure to 500kPa if needed. If red dye is required, set paint sprays gun pressure to 40kPa.

3. Aim flame path towards to steel collection container whilst maintaining approximately 20-40cm distance to bottom of container. Be aware of splash back and compensate accordingly. If paint spray gun is also being used, point towards the bottom of container whilst crossing flame spray gun. Be careful of steam generation.

4. Engage powder dispenser and collect bioglass 45S5 microspheres in container.

5. Disengage powder dispenser and turn of acetylene/oxygen fuel.

6. Filter the microsphere containing water and dry the filter paper. Store filter paper in plastic bag for analysis.

Chemical Etching of Q-cells (Sodium Borosilicate microspheres)

Aim

This experiment protocol aims to produce porous hollow microspheres through chemical etching techniques using Potassium Hydroxide (KOH) solutions.

Equipment

- Q-Cell
- KOH pellets (85% ACS)
- Distilled water/demineralized water or pure ethanol
- Heating stove with magnetic stirring
- Filter paper.
- Glass funnel
- Fume hood
- 10 ml containers (preferably plastic).

Safety Precautions

- Fume hood
- Safety goggles
- Gloves
- Lab coat

Hazards

KOH solution is corrosive. Avoid physical contact and inhalation of fumes. Always wear the personal protective equipment and use the fume hood to conduct the experiment.

Methodology/Protocol

1. Make a stock solution of 0.5M KOH and store in plastic container. The molar mass of KOH is 56.1056 g/mol. Therefore 28.0528g of KOH in 1L for a 0.5M solution. Use ethanol if we have enough. If not, use demineralized water or ratio as determined by your previous results.

a. NOTE: THERE IS ONLY 26g of 85% KOH LEFT
    i. Effective KOH left = 22.1g
        1. Therefore 0.3939 moles left
            a. Therefore a 0.5M solution needs 26g of KOH in 787.8ml of solvent
            b. 16.5g of KOH in 500mL of solvent
            c. MAKE SURE YOU SLOWLY ADD PELLETS TO WATER, NOT THE OTHER WAY ROUND!!!!!!!!!!

2. Before adding stock solution to Q-cells, heat solution to 90°C in a fume hood (Allow 30mins or so. Use a water bath setup.
    a. If you are using ethanol, reduce heat to 50°C or the ethanol will boil.
3. In six separate containers, add 0.1g of q-cell. In each container, add 5ml of KOH stock solution.
4. Maintain temperature at 90°C and stir or agitate slowly.
5. Samples should be taken at relevant intervals.
6. Filter microspheres out using filter paper and immediately wash with de-mineralized water.
    a. If filter paper breaks, add 90ml of water to reduce the strength of the base and filter again. Repeat if necessary.
7. Dry filter paper in 60°C oven in S197 lab. Do not forget to label them.
8. Take microscope shots. Leave some for scanning electron microscopy.

11.1.2 Chapter 5 Microsphere Attachment Studies

Oven Characterisation

Aim

Observe the temperature fluctuations of the Pronto Oven

Equipment

- Pronto Oven + Package attachment
- Digital Thermometer and K-Type sensor (Digitech)
- Medipack Packaging
- Heat Sealer

Method

1. Insert the K-Type sensor in the medipack packaging and seal using the heat sealer.
2. Pre heat the oven to 60°C.
3. Attach the package to the package attachment and insert inside the oven
4. Record temperature every 10s for 5-10 minutes.

Thermo-attachment studies

Aim

Determine if thermoattachment process damages the scaffold.

Equipment

- Polycaprolactone scaffolds
- Pronto oven
- Medipack packaging
- Q-cell/Sodium Borosilicate microspheres

Method

1. Place scaffold in medipack packaging with Q-cells. Seal the package
2. Preheat the oven to 60°C.
3. Insert package in oven and set rotating option on.
4. Heat the package for 1,2,3,4 or 5 minutes.
5. Remove package and retrieve scaffolds. Remove excess q-cells using air jet blasts.
6. Repeat for plain scaffolds.
7. Take optical and SEM images.

Microsphere attachment studies

Aim

Determine microsphere loss during cyclic loading

Equipment

- Scaffolds coated with Q-cells
- Iaxsys kit and well inserts
- 6 well culture plate
- Ethanol: water solution (50:50)

Method

1. Attach scaffolds to well inserts using adhesive glue and place in culture plate
2. Fill wells with 10 ml of ethanol: water solution. Close culture plate.
3. Place culture plate onto Iaxsys kit.
4. Set settings to 10mm compression displacement, 1Hz frequency and 24 hour duration.
5. Start machine.
6. Once finished, agitate solutions in wells to ensure even distribution of unattached Q-cells.
7. Pipette 1ml of solution into Eppendorf tubes and label accordingly. Use 0.1ml of solution when preparing glass slide for optical counts.

11.1.3 Chapter 6 Drug Release Studies

Spectrophotometry protocol

Introduction

As part of research and development into synthetic polyester skin scaffolds, we are investigating the potential of sustained controlled drug delivery using bioactive glass microsphere vehicles loaded using novel methods.

Equipment required

Chloramphenicol stock solution (100mg/ml)

Spectrophotometer

Quartz cuvette

Phosphate Buffered Solution (PBS)

Drug-loaded microspheres

Protocol

The experiment protocol will be divided into 3 broad aspects

Determine Absorbance and Calibration curve

The wavelength where maximum absorption occurs is required to ensure the highest sensitivity of the spectrophotometer. Chloramphenicol has a max absorption peak at 280nm. In order to create our own absorbance spectrum graph, a 100 µl/ml sample will be used to test absorbance from 200 to 350nm at 10nm intervals.

Given an antibiotic stock solution, a concentration curve is required for determining drug loading and release from the carriers. From the stock solution (100mg/ml), 1ml samples of concentrations 5, 10, 20, 50, 100 µl/ml will be prepared. The absorbance at the max absorption wavelength of each sample will be recorded and used to create a graph with a linear correlation which should fit the equation:

$$A = \varepsilon c l$$

Where A = Absorbance

ε = calibration factor

c = concentration of sample

l = length of cuvette (normally 1cm)

Determine Loading Efficiency

Drug loading efficiency will be determined by measuring the antibiotic concentration in the soaking solution before and after drug loading over microspheres. Microsphere samples will be soaked in 10mg/ml antibiotic solution over 24 hours to load antibiotics. Loading efficiency is determined by:

$$Drug\ Loading\ Efficiency\ \% = \frac{Initial\ Concentration - After\ Concentration}{Initial\ Concentration}$$

Mass of antibiotic loaded onto microspheres per gram of microspheres will also be calculated.

$$Loaded\ antibiotic\ per\ gram\ of\ microspheres = \frac{Mass\ of\ antibiotics\ before - Mass\ of\ antibiotics\ after}{mass\ of\ microspheres}$$

This will be used to determine how much drug loaded microspheres is required to produce absorbance readings for drug elution tests.

Determine Drug Elution

After antibiotic loading, the loaded microspheres will be rinsed in water to remove excess antibiotic not bound to the microspheres. The rinsed water will be collected and tested for antibiotics to determine potential loss in loading efficiency.

Loaded microspheres will be tested for drug releasing kinetics over a period of 24 hours. A standard amount of microspheres will be placed in 5 ml of PBS and continuously shaken for the duration of the experiment. The amount of microspheres to be placed in each testing jar is determined as follows:

$$Mass\ of\ microspheres = \frac{loaded\ antibiotic\ per\ gram\ of\ microspheres}{5\ ml} \times calibration\ factor$$

This equation is designed to give a max absorbance reading of 1.

Samples from each testing jar will be taken at time points 0, 10 min, 30 min, 1 hr, 1.5 hr, 2 hr, 4hr, 8 hr and 24 hrs. Tests will be conducted in triplicates.

11.2 Results

11.2.1 Chapter 4 Microspheres Results

Bioglass 45S5 microspheres and Q-cell Particle size analysis

Thermospray

Bin	Length (µm)		Count	Count (%)	Bin	Length (µm)		Count	Count (%)	Bin	Length (µm)		Count	Count (%)
1	0-5		0	0	1	0-5		6	8.7	1	0-5		6	4.35
2	5-10		26	23.85	2	5-10		4	5.8	2	5-10		18	13.04
3	10-15		24	22.02	3	10-15		12	17.39	3	10-15		24	17.39
4	15-20		24	22.02	4	15-20		14	20.29	4	15-20		29	21.01
5	20-25		13	11.93	5	20-25		13	18.84	5	20-25		26	18.84
6	25-30		9	8.26	6	25-30		13	18.84	6	25-30		17	12.32
7	30-35		5	4.59	7	30-35		2	2.9	7	30-35		9	6.52
8	35-40		5	4.59	8	35-40		4	5.8	8	35-40		5	3.62
9	40-45		2	1.83	9	40-45		1	1.45	9	40-45		3	2.17
10	45-50		1	0.92	10	45-50		0	0	10	45-50		1	0.72
TOTAL														

Bin	Length (µm)	Count	Count (%)
1	0-5	12	3.80
2	5-10	48	15.19
3	10-15	60	18.99
4	15-20	67	21.20
5	20-25	52	16.46
6	25-30	39	12.34
7	30-35	16	5.06
8	35-40	14	4.43
9	40-45	6	1.90
10	45-50	2	0.63
	Total Count	316	

Eutajet

Bin	Length (µm)		Count	Count (%)	Bin	Length (µm)		Count	Count (%)	Bin	Length (µm)		Count	Count (%)
1	0-5		22	8.98	1	0-5		5	2.36	1	0-5		0	0
2	5-10		27	11.02	2	5-10		66	31.13	2	5-10		38	12.03
3	10-15		43	17.55	3	10-15		44	20.75	3	10-15		107	33.86
4	15-20		57	23.27	4	15-20		51	24.06	4	15-20		89	28.16
5	20-25		48	19.59	5	20-25		26	12.26	5	20-25		63	19.94
6	25-30		29	11.84	6	25-30		10	4.72	6	25-30		15	4.75
7	30-35		9	3.67	7	30-35		4	1.89	7	30-35		4	1.27
8	35-40		7	2.86	8	35-40		2	0.94	8	35-40		0	0
9	40-45		1	0.41	9	40-45		3	1.42	9	40-45		0	0
10	45-50		2	0.82	10	45-50		1	0.47	10	45-50		0	0
TOTAL														
Bin	Length (µm)	Count	Count (%)											
1	0-5	27	3.49											
2	5-10	131	16.95											
3	10-15	194	25.10											
4	15-20	197	25.49											
5	20-25	137	17.72											
6	25-30	54	6.99											
7	30-35	17	2.20											
8	35-40	9	1.16											
9	40-45	4	0.52											
10	45-50	3	0.39											
	Total Count	773												

Q-cell

Bin	Length		Count	Count	Bin	Length		Count	Count	Bin	Length		Count	Count
	(µm)			(%)		(µm)			(%)		(µm)			(%)
1	0-5		1	1.27	1	0-5		8	8.51	1	0-5		1	63.54
2	5-10		4	5.06	2	5-10		16	17.02	2	5-10		9	9.38
3	10-15		15	18.99	3	10-15		30	31.91	3	10-15		11	11.46
4	15-20		18	22.78	4	15-20		20	21.28	4	15-20		2	2.08
5	20-25		18	22.78	5	20-25		11	11.7	5	20-25		3	3.13
6	25-30		16	20.25	6	25-30		5	5.32	6	25-30		2	2.08
7	30-35		5	6.33	7	30-35		3	3.19	7	30-35		2	2.08
8	35-40		2	2.53	8	35-40		1	1.06	8	35-40		3	3.13
9	40-45		0	0	9	40-45		0	0	9	40-45		2	2.08
10	45-50		0	0	10	45-50		0	0	10	45-50		1	1.04
TOTAL														
Bin	Length	Count	Count											
	(µm)		(%)											
1	0-5	10	4.78											
2	5-10	29	13.88											
3	10-15	56	26.79											
4	15-20	40	19.14											
5	20-25	32	15.31											
6	25-30	23	11.00											
7	30-35	10	4.78											
8	35-40	6	2.87											
9	40-45	2	0.96											
10	45-50	1	0.48											
	Total Count	209												

11.2.2 Chapter 5 Microsphere Attachment Studies Results

Oven Temperature Characterisation Study Results

Time (min)	Time (s)	1	2	3	4	5	Average	STD
0	0	20	22	23	22	23	22	1.224745
0.17	10	25	28	27	28	28	27.2	1.30384
0.33	20	27	30	30	31	32	30	1.870829
0.5	30	29	32	32	34	36	32.6	2.607681
0.67	40	31	34	34	36	38	34.6	2.607681
0.83	50	33	36	36	38	40	36.6	2.607681
1	60	35	37	38	40	43	38.6	3.04959
1.17	70	37	39	40	41	46	40.6	3.361547
1.33	80	39	40	41	44	49	42.6	4.037326
1.5	90	41	41	43	46	51	44.4	4.219005
1.67	100	42	42	44	49	54	46.2	5.215362
1.83	110	43	44	45	50	55	47.4	5.029911
2	120	44	46	47	52	57	49.2	5.263079
2.17	130	45	47	49	53	58	50.4	5.176872
2.33	140	46	48	50	54	59	51.4	5.176872
2.5	150	48	50	51	55	59	52.6	4.393177
2.67	160	49	51	53	56	60	53.8	4.32435
2.83	170	50	51	54	56	60	54.2	4.024922
3	180	51	52	55	56	61	55	3.937004
3.17	190	53	53	55	57	61	55.8	3.34664
3.33	200	53	54	56	57	62	56.4	3.507136
3.5	210	54	55	57	57	63	57.2	3.49285
3.67	220	54	57	57	57	65	58	4.123106
3.83	230	55	58	57	57	65	58.4	3.847077
4	240	55	59	58	58	66	59.2	4.086563
4.17	250	55	59	58	59	66	59.4	4.037326
4.33	260	56	60	58	60	67	60.2	4.147288
4.5	270	56	60	58	61	67	60.4	4.159327
4.67	280	56	61	58	62	67	60.8	4.207137
4.83	290	56	61	58	63	67	61	4.301163
5	300	56	61	58	63	67	61	4.301163
5.17	310	56	61	58	63	67	61	4.301163
5.33	320	56	61	58	63	66	60.8	3.962323
5.5	330	56	61	58	63	66	60.8	3.962323
5.67	340	55	61	58	63	66	60.6	4.27785
5.83	350	55	61	59	63	66	60.8	4.147288
6	360	55	60	59	63	65	60.4	3.847077

6.17	370	55	60	60	63	65	60.6	3.781534
6.33	380	54	60	60	62	65	60.2	4.024922
6.5	390	54	60	61	62	64	60.2	3.768289
6.67	400	54	59	61	62	64	60	3.807887
6.83	410	54	59	61	61	63	59.6	3.435113
7	420	54	59	61	61	63	59.6	3.435113
7.17	430	54	58	61	62	63	59.6	3.646917
7.33	440	54	58	61	63	62	59.6	3.646917
7.5	450	55	58	61	63	62	59.8	3.271085
7.67	460	55	57	61	64	61	59.6	3.577709
7.83	470	56	57	61	64	61	59.8	3.271085
8	480	56	57	61	65	60	59.8	3.563706
8.17	490	56	58	61	65	60	60	3.391165
8.33	500	56	58	61	64	60	59.8	3.03315
8.5	510	56	59	61	64	61	60.2	2.949576
8.67	520	56	59	61	64	62	60.4	3.04959
8.83	530	56	59	62	64	63	60.8	3.271085
9	540	56	59	62	64	63	60.8	3.271085
9.17	550	56	59	63	65	63	61.2	3.63318
9.33	560	56	59	63	66	63	61.4	3.911521
9.5	570	56	59	63	67	63	61.6	4.219005
9.67	580	56	59	63	67	63	61.6	4.219005
9.83	590	56	59	63	67	63	61.6	4.219005
10	600	57	59	63	67	64	62	4

Microsphere Attachment Studies Results

A1		**A2**		**A3**	
Field #	**Count**	**Field #**	**Count**	**Field #**	**Count**
1	150	*1*	60	*1*	50
2	50	*2*	20	*2*	70
3	30	*3*	20	*3*	10
Total	230	**Total**	100	**Total**	130
Mean	76.67	**Mean**	33.33	**Mean**	43.33
Std Dev	52.49	**Std Dev**	18.86	**Std Dev**	24.94
Std Error	30.31	**Std Error**	10.89	**Std Error**	14.4
W1		**W2**		**W3**	
Field #	**Count**	**Field #**	**Count**	**Field #**	**Count**
1	230	*1*	40	*1*	130
2	310	*2*	40	*2*	60
3	220	*3*	80	*3*	110
Total	760	**Total**	160	**Total**	300
Mean	253.33	**Mean**	53.33	**Mean**	100
Std Dev	40.28	**Std Dev**	18.88	**Std Dev**	29.44
Std Error	23.25	**Std Error**	10.89	**Std Error**	17

11.2.3 Chapter 6 Drug Release Studies Results

Chloramphenicol Calibration Data

Calibration curve		
Concentration (µg/mL)	Absorbance	ε
100	2.914	0.02914
50	1.546	0.03092
25	0.805	0.0322
12.5	0.419	0.03352
6.25	0.225	0.036
3.125	0.125	0.04

Calibration Co-efficient	0.0297	µg/ml

Images

From top left to bottom right: chemically etched microspheres on scaffold, CAP infused scaffolds, Intact microspheres on scaffolds, Negative control, and Positive control.

Mass of Drug Vector

	Initial Mass (g)	After Loading (g)	Mass Difference (g)	Mass Difference (mg)	Effective Mass of Drug Vector (mg)
Positive control 1	0.02358	0.02303	-0.00055	-0.55	23.03
Positive control 2	0.02353	0.0227	-0.00083	-0.83	22.7
Positive control 3	0.02385	0.0232	-0.00065	-0.65	23.2
Intact Microspheres 1	0.02467	0.0252	0.00053	0.53	0.53
Intact Microspheres 2	0.02362	0.02524	0.00162	1.62	1.62
Intact Microspheres 3	0.02476	0.0256	0.00084	0.84	0.84
Chemical Etched Microspheres 1	0.02328	0.02624	0.00296	2.96	2.96
Chemical Etched Microspheres 2	0.02368	0.0258	0.00212	2.12	2.12
Chemical Etched Microspheres 3	0.0242	0.02495	0.00075	0.75	0.75
Negative Control 1	0.03219	0.03228	9E-05	0.09	32.28
Negative Control 2	0.02251	0.02254	3E-05	0.03	22.54
Negative Control 3	0.02729	0.02732	3E-05	0.03	27.32
Infused Scaffolds 1	0.03656	0.03476	-0.0018	-1.8	34.76
Infused Scaffolds 2	0.0478	0.03994	-0.00786	-7.86	39.94
Infused Scaffolds 3	0.0396	0.0281	-0.0115	-11.5	28.1

Raw Absorption Data

Time (days)	**0**	**0.006944**	**0.020833**	**0.041667**	**0.083333**	**0.125**	**0.166667**	**1**	**3**	**7**
Time (minutes)	**0**	**10**	**30**	**60**	**120**	**180**	**240**	**1440**	**4320**	**10080**
Positive control 1	0	0.119	0.174	0.257	0.321	0.33	0.336	0.492	0.474	0.474
Positive control 2	0	0.135	0.189	0.25	0.303	0.299	0.298	0.422	0.43	0.429
Positive control 3	0	0.12	0.206	0.273	0.348	0.332	0.358	0.468	0.484	0.495
Average	**0**	**0.124667**	**0.189667**	**0.26**	**0.324**	**0.320333**	**0.330667**	**0.460667**	**0.462667**	**0.466**
Intact Microspheres 1	0	0.075	0.105	0.128	0.139	0.138	0.136	0.136	0.135	0.134
Intact Microspheres 2	0	0.232	0.288	0.35	0.37	0.375	0.378	0.387	0.392	0.392
Intact Microspheres 3	0	0.149	0.208	0.223	0.248	0.25	0.257	0.253	0.263	0.26
Average	**0**	**0.152**	**0.200333**	**0.233667**	**0.252333**	**0.254333**	**0.257**	**0.258667**	**0.263333**	**0.262**
Chemical Etched Microspheres 1	0	0.178	0.222	0.213	0.243	0.245	0.251	0.255	0.25	0.274
Chemical Etched Microspheres 2	0	0.18	0.203	0.217	0.237	0.239	0.24	0.248	0.252	0.262
Chemical Etched Microspheres 3	0	0.065	0.079	0.078	0.077	0.07	0.074	0.072	0.073	0.076
Average	**0**	**0.141**	**0.168**	**0.169333**	**0.185667**	**0.184667**	**0.188333**	**0.191667**	**0.191667**	**0.204**
Negative Control 1	0	0.018	0.017	0.01	0.017	-0.033	-0.032	0.004	0.008	0.015
Negative Control 2	0	0.005	0.003	0.005	0.006	0.011	0.005	-0.01	0.001	0.01
Negative Control 3	0	0.011	0.009	0.0012	0.01	0.002	-0.002	0.01	0.004	0.015
Average	**0**	**0.011333**	**0.009667**	**0.0054**	**0.011**	**-0.00667**	**-0.00967**	**0.001333**	**0.004333**	**0.013333**
Infused Scaffolds 1	0	0.033	0.106	0.198	0.284	0.286	0.324	0.504	0.519	0.51
Infused Scaffolds 2	0	0.053	0.23	0.23	0.293	0.293	0.345	0.507	0.527	0.526
Infused Scaffolds 3	0	0.06	0.174	0.174	0.228	0.23	0.237	0.356	0.366	0.366
Average	**0**	**0.048667**	**0.17**	**0.200667**	**0.268333**	**0.269667**	**0.302**	**0.455667**	**0.470667**	**0.467333**

Calibrated Data (µg)	0	0.006944	0.020833	0.041667	0.083333	0.125	0.166667	1	3	7
A/e*V +previous m/ml*0.1	0	10	30	60	120	180	240	1440	4320	10080
Positive control 1	0	20.03367	29.10774	42.12939	51.67568	52.21059	52.0441	74.04542	70.30911	68.6654
Positive control 2	0	22.72727	31.63636	41.04968	48.8047	47.34816	46.18082	63.54476	63.70009	62.14806
Positive control 3	0	20.20202	34.39057	44.82306	56.00452	52.61246	55.38617	70.56414	71.6778	71.66693
Average	**0**	**20.98765**	**31.71156**	**42.66738**	**52.16163**	**50.72374**	**51.2037**	**69.38477**	**68.56234**	**67.49346**
Standard Deviation	**0**	**1.508903**	**2.642217**	**1.943366**	**3.624428**	**2.930233**	**4.659863**	**5.348754**	**4.266075**	**4.866442**
Intact Microspheres 1	0	12.62626	17.57576	21.04556	22.43508	21.85108	21.08108	20.61662	20.01401	19.41494
Intact Microspheres 2	0	39.05724	48.2963	57.5513	59.75117	59.35211	58.56299	58.63473	58.08682	56.7852
Intact Microspheres 3	0	25.08418	34.81818	36.75098	40.01144	39.57185	39.79965	38.36592	38.94939	37.67348
Average	**0**	**25.58923**	**33.56341**	**38.44928**	**40.73256**	**40.25835**	**39.81458**	**39.20576**	**39.01674**	**37.95787**
Standard Deviation	**0**	**13.22272**	**15.39866**	**18.31203**	**18.66849**	**18.75994**	**18.74096**	**19.02297**	**19.03649**	**18.68675**
Chemical Etched Microspheres 1	0	29.96633	37.22559	35.18395	39.18754	38.77991	38.87334	38.64163	37.07351	39.60965
Chemical Etched Microspheres 2	0	30.30303	34.09764	35.76658	38.25019	37.83067	37.18604	37.5671	37.33865	37.91885
Chemical Etched Microspheres 3	0	10.94276	13.25253	12.87652	12.45345	11.10672	11.45357	10.92119	10.81723	10.99904
Average	**0**	**23.73737**	**28.19192**	**27.94235**	**29.96373**	**29.2391**	**29.17099**	**29.04331**	**28.40979**	**29.50918**
Standard Deviation	**0**	**11.08174**	**13.03208**	**13.05064**	**15.17159**	**15.71027**	**15.36691**	**15.70341**	**15.23618**	**16.05253**
Negative Control 1	0	3.030303	2.86532	1.674638	2.725124	-5.05313	-4.95834	0.482407	1.169213	2.148403
Negative Control 2	0	0.841751	0.511785	0.818525	0.966548	1.724269	0.79506	-1.46381	0.111513	1.416735
Negative Control 3	0	1.851852	1.521886	0.224998	1.587179	0.343534	-0.29556	1.474913	0.612645	2.13546
Average	**0**	**1.907969**	**1.632997**	**0.906054**	**1.759617**	**-0.99511**	**-1.48628**	**0.164502**	**0.631124**	**1.900199**
Standard Deviation	**0**	**1.095355**	**1.180695**	**0.728773**	**0.891879**	**3.581516**	**3.055936**	**1.494934**	**0.529092**	**0.418743**
Infused Scaffolds 1	0	5.555556	17.59933	32.35917	45.61691	45.26687	50.07497	75.77944	76.86367	73.90874
Infused Scaffolds 2	0	8.922559	38.12458	37.94977	47.15762	46.38383	53.28107	76.29513	78.03364	76.19857
Infused Scaffolds 3	0	10.10101	28.90909	28.71119	36.67896	36.4033	36.70047	53.55631	54.20709	53.01821
Average	**0**	**8.193042**	**28.211**	**33.00671**	**43.15116**	**42.68466**	**46.6855**	**68.54363**	**69.70147**	**67.70851**
Standard Deviation	**0**	**2.358906**	**10.28042**	**4.653204**	**5.657786**	**5.468415**	**8.794628**	**12.98196**	**13.43127**	**12.77359**

Calibrated Data (µg/mg)	0	0.006944	0.020833	0.041667	0.083333	0.125	0.166667	1	3	7
	0	10	30	60	120	180	240	1440	4320	10080
Positive control 1	0	0.869894	1.263906	1.829326	2.243842	2.267069	2.25984	3.215173	3.052936	2.981563
Positive control 2	0	1.001201	1.393672	1.808356	2.149987	2.085822	2.034397	2.799329	2.806171	2.7378
Positive control 3	0	0.870777	1.482352	1.932028	2.413988	2.267778	2.387335	3.041558	3.089561	3.089092
Average	**0**	**0.913958**	**1.379977**	**1.85657**	**2.269272**	**2.20689**	**2.227191**	**3.018686**	**2.982889**	**2.936152**
Standard Deviation	**0**	**0.075557**	**0.109865**	**0.066185**	**0.133825**	**0.104848**	**0.17872**	**0.208863**	**0.154134**	**0.179995**
Intact Microspheres 1	0	23.82314	33.16181	39.7086	42.33034	41.22845	39.77563	38.89928	37.76229	36.63196
Intact Microspheres 2	0	24.10941	29.81253	35.52549	36.88344	36.6371	36.14999	36.19428	35.85606	35.05259
Intact Microspheres 3	0	29.86211	41.45022	43.75117	47.63266	47.10934	47.38054	45.67371	46.36833	44.84938
Average	**0**	**25.93155**	**34.80818**	**39.66175**	**42.28215**	**41.6583**	**41.10205**	**40.25576**	**39.99556**	**38.84464**
Standard Deviation	**0**	**3.406974**	**5.990982**	**4.113037**	**5.374773**	**5.249334**	**5.731564**	**4.883128**	**5.600674**	**5.25987**
Chemical Etched Microspheres 1	0	10.12376	12.57621	11.88647	13.23904	13.10132	13.13289	13.0546	12.52483	13.38164
Chemical Etched Microspheres 2	0	14.29388	16.08379	16.87103	18.04254	17.84466	17.54059	17.72033	17.61257	17.88625
Chemical Etched Microspheres 3	0	14.59035	17.67003	17.16869	16.60459	14.80896	15.27143	14.56159	14.42298	14.66538
Average	**0**	**13.00266**	**15.44335**	**15.30873**	**15.96206**	**15.25164**	**15.31497**	**15.11217**	**14.85346**	**15.31109**
Standard Deviation	**0**	**2.497606**	**2.606604**	**2.9675**	**2.465372**	**2.402454**	**2.204172**	**2.381093**	**2.571041**	**2.320685**
Negative Control 1	0	0.093876	0.088765	0.051878	0.084421	-0.15654	-0.1536	0.014944	0.036221	0.066555
Negative Control 2	0	0.037345	0.022706	0.036314	0.042881	0.076498	0.035273	-0.06494	0.004947	0.062854
Negative Control 3	0	0.067784	0.055706	0.008236	0.058096	0.012574	-0.01082	0.053987	0.022425	0.078165
Average	**0**	**0.066335**	**0.055725**	**0.032143**	**0.0618**	**-0.02249**	**-0.04305**	**0.001329**	**0.021198**	**0.069191**
Standard Deviation	**0**	**0.028293**	**0.033029**	**0.022118**	**0.021016**	**0.120411**	**0.098477**	**0.060622**	**0.015673**	**0.007988**
Infused Scaffolds 1	0	0.159826	0.50631	0.930931	1.312339	1.302269	1.440592	2.180076	2.211268	2.126258
Infused Scaffolds 2	0	0.223399	0.954546	0.950169	1.180712	1.161338	1.334028	1.910244	1.953772	1.907826
Infused Scaffolds 3	0	0.359467	1.028793	1.021751	1.305301	1.295491	1.306066	1.905918	1.929078	1.886769
Average	**0**	**0.247564**	**0.829883**	**0.967617**	**1.266117**	**1.253033**	**1.360229**	**1.998746**	**2.031373**	**1.973618**
Standard Deviation	**0**	**0.10199**	**0.282671**	**0.047858**	**0.074047**	**0.079482**	**0.070987**	**0.157051**	**0.156283**	**0.132609**